ABSTRACT

Title of Document: AN ANALYSIS OF THE EFFICACY OF LOW-SCALE CONCENTRATED PHOTOVOLTAICS

Thomas Brooks, Sean Collins, Alexander Edgerton, Blaine Ford, Preetha Gautam, Matthew Goldfinger, Ian Hall, Billy Huang, Michael Lanzo, Melissa McGowan, Taylor Myers, Christopher Salata, Andy Zheng

Directed By: Dr. Ray Adomaitis

The plausibility of low-concentrating flat-plate photovoltaics as a viable small-scale energy generation system was explored. A flat-plate photovoltaic panel utilizing an inexpensive parabolic reflector to increase the solar radiation incident on the panel was constructed. This concentration system's performance was compared to a solitary flat-plate photovoltaic panel with no concentration. The concentrating panel experienced a maximum of seven times and averaged three to four times the power output of the flat system. It is projected that similar systems could provide a less costly alternative to consumer scale solar panels that use expensive efficiency-increasing tracking systems.

AN ANALYSIS OF THE EFFICACY OF LOW-SCALE CONCENTRATED PHOTOVOLTAICS

By

Gemstone Team LEAF (Light Energy Acquisition of the Future):

Thomas Brooks, Sean Collins, Alexander Edgerton, Blaine Ford, Preetha Gautam, Matthew Goldfinger, Ian Hall, Billy Huang, Michael Lanzo, Melissa McGowan, Taylor Myers, Christopher Salata, Andy Zheng

Thesis submitted to the Faculty of the Gemstone Program of the

University of Maryland, College Park, in partial fulfillment

of the requirements for the Gemstone Citation.

Submitted for Approval:

March 2012

Advisory Committee:

Professor Ray Adomaitis, Chair

Dr. Vivek Dwivedi

Dr. Sheryl Erhman

Dr. Greg Jackson

Mr. Peter Lowenthal

Dr. Chunseng Wang

Acknowledgements

The members of the team would like to thank the following individuals: Dr. Ray Adomaitis, for coming up with the concept for the ray tracing program, developing the initial version, and most of all for his enthusiasm and generosity in providing excellent advice and guidance for the team as a mentor over the past four years; Drs. Vivek Dwivedi, Sheryl Erhman, Greg Jackson, and Chunseng Wang, and Mr. Peter Lowenthal, for participating as discussants for the thesis defense; Ms. Nedelina Tchangalova, for serving as the team librarian; and Drs. Rebecca Thomas and James Wallace, Ms. Courtenay Barrett, and the remainder of the Gemstone staff who have made the entire experience possible.

Table of Contents

List of Tables

List of Figures

Introduction

The Problem and Proposed Solutions

The forces of economic recession and global climate change have produced an energy environment in need of affordable, alternative, and renewable energy sources. Some of the most promising candidates to fill this need are solar, wind, and geothermal energy, but, even with the volatility of oil prices, fossil fuels have remained the world's favored energy source. However, despite the barrier to new energy systems that fossil fuels present, in the near future sustainable sources of energy will become a necessity rather than a luxury. This fundamental change in the way the world perceives renewable energy will occur due to rising prices and dwindling supplies of fossil fuels, and drastic climate changes. Team LEAF looks to address this future need by assessing the feasibility and effectiveness of a low cost solar energy system.

The focus of this research is on solar power because the team views it as the most promising of the proposed renewable energy sources. Each new energy source has aspects that are better and worse than fossil fuels and although solar is not currently the most competitive renewable energy source, it has the potential to be. The other main renewable energy sources were considered, but were eventually decided against due to the team's research interests and goals. There are a number of benefits to using solar energy, the most evident of which is that solar energy can be collected anywhere. While day-to-day and hour-to-hour availability cannot be guaranteed, the vast majority of the Earth's surface can expect to regularly receive a nontrivial amount of sunlight over the course of a year (Antony, Dürschner, & Remmers, 2007).

There are two major subsets of solar collection technology, solar thermal systems and photovoltaic (PV) systems. Solar thermal converts sunlight into heat energy, and is generally

used to heat water, provide cooling[1], and produce high temperaturegas that drives turbines for electricity. Photovoltaic systems convert sunlight directly into electricity (Antony, Dürschner, & Remmers, 2007). Although solar thermal systems are more common than photovoltaic cells, there are a number of advantages to photovoltaic systems. Among these advantages is that generating electricity directly from sunlight bypasses the typical chain of conversions and energy losses that are associated with conventional power generation. Another benefit is that the direct electrical output of photovoltaic systems makes them applicable on a small, individual scale; practical options to suit diverse household needs, instead of simply heating water or providing cooling.

As much potential as photovoltaic systems have, however, they also have limitations. One such limitation is the overhead cost. Currently, the most efficient photovoltaic systems include tracking systems that follow the sun in order to maximize the incident light on the PV panel throughout the day. While tracking systems do add to the overall efficiency, they have the disadvantage of significantly increasing the cost of the system, making them unattractive in small-scale applications, as it takes far too long to recoup the costs of installation. Another drawback to photovoltaic systems is that the creation of some types of photovoltaic cells requires hazardous materials, such as arsenic and cadmium, which if improperly regulated can be harmful to both people and the environment (Union of Concerned Scientists, 2002).

It was determined that if the more expensive elements of these structures could be removed or replaced by cheaper materials, methods or both, PV systems would become more

1 Although cooling seems to be counter intuitive to thermal energy generation, running water through closed energy systems will heat the water while simultaneously cooling the rest of the system.

viable for the average consumer. An option to increase efficiency while decreasing cost is to introduce the concept of a concentrator, to redirect the rays of the sun that would otherwise miss the cells so that their energy can be harvested. Furthermore, maximizing the efficiency of a relatively small number of cells lowers the total demand for cells, cutting down on the downsides inherent in creating photovoltaic cells as well. Until very recently, there has been little development in concentration for photovoltaic solar systems because, historically, concentrating photovoltaic systems have been viewed as large-scale operations, forcing them to compete with comparatively low-cost fossil fuel plants in an era that had remarkably low oil prices, whereas flat-plate systems were used in remote, isolated regions and only required to perform on a small scale (Swanson, 2000). However, as the price of oil rises, and solar technology matures, the cost of concentrated photovoltaic systems has become a more viable option.

The Objective

The overarching question is how can the cost efficiency of photovoltaic systems be improved? More specifically, to what extent can low scale concentrating, photovoltaic systems compare to the conventional, flat-plate, photovoltaic designs in terms of power output and cost? This study proposes the use of a parabolic reflecting surface in order to improve the efficiency of a flat-plate photovoltaic collection system. This reflector will increase the power output of the photovoltaic cells by focusing more light onto the solar collector. The higher energy generation and lower cost of installation would maintain a higher level of returns while minimizing the initial investment.

The question of maximizing the solar collection capabilities of a photovoltaic system with a reflector led the team to a secondary issue. Because the expensive tracking components of the photovoltaic system were to be removed to decrease costs, the reflector and cells could not

be adjusted to the relative position of the Sun in the sky throughout the year. Therefore, it was necessary to determine the optimum arrangement of the cells and reflector to maximize the amount of solar energy collected over a given period. It was discovered that there were no tools available that were capable of making such calculations, and so it was resolved to create a tool capable of just that, building from Dr. Ray Adomaitis' preexisting program, which calculates, given the angle and intensity of the Sun's rays, the optimum design of a reflector in an ideal world.

The Experiment

It was decided to pursue the team objectives using a two-pronged approach. The majority of Team LEAF would create a proof-of-concept design of a low cost, low concentrating photovoltaic system, optimized for an arbitrary season. The performance of the concentrated system then would be compared to that of a flat-plate photovoltaic solar collection system acting as a control. This experiment would study the idea that concentrated photovoltaic technology can be implemented on a consumer level. If the concentrating system, constructed of low-cost materials and lacking a tracking system was able to produce significantly more electricity than the flat-plate system, even when not optimized for the period of time that it was to be collecting for, then it would serve as proof of the concept of the viability of small-scale concentrating photovoltaic systems.

The second, sub-team would be responsible for developing a program, based on Dr. Adomaitis's original work that would be capable of predicting the optimum configuration of the reflector and cells of the concentrating photovoltaic system over a period of time. This program would take in several variables that would better account for the actual performance of the prototype system, instead of the ideal presented by the original program, and then would

simulate the operation of that system. With this tool, it would be possible to simulate several different orientations for the concentrating photovoltaic system, and determine which provides the most energy over a specific period of time.

Literature Review

There exists a large body of research on solar energy. In this section we will discuss current findings related to economics, photovoltaics, concentration, weathering, and photovoltaic implementation.

Economics

The nature of electric power is such that economics are often the deciding factor when it comes to selecting how to power a system. The scale at which the world consumes power is tremendous, and it is difficult to meet the ever growing demand. Solar power is noted as an environmentally friendly option for meeting some of the energy need, but the economics of such a system are just as frequently called into question. As a result, a large amount of research has been done on the topic. Our focus is on the economics of photovoltaics, and specifically, concentrated photovoltaic systems. That said, the economics of solar thermal energy systems, as well as any "green" system, are also relevant when placed in the proper context.

In 1998, only a small percentage of the world's electricity was generated by renewable and sustainable sources: 17.9% hydropower and 1.6% biomass, geothermal, solar, and wind combined (Keoleian & Lewis, 2003). Instead, non-renewable and non-sustainable energy sources like coal, natural gas, fuel oil, and nuclear fuel, made up and continue to make up the majority of our energy sources (Keoleian & Lewis, 2003). These fuel sources have been documented as incredibly detrimental to the environment. The byproducts of the usage of these energy sources include the release of greenhouse gases, the acidification of local air and water, the generation of radioactive waste, the emitting of air pollutants such as mercury, and the formation of smog (Keoleian & Lewis, 2003).

The same problems found on global and national levels are also encountered on the local scale of energy generation. In Maryland, electricity generation is the source of 39% of the state's CO_2 emissions (Ridlington & Heavner, 2005). This energy comes primarily from the seven oldest coal-fired power plants in the state (Ridlington & Heavner, 2005). In 2004, these power plants accounted for "59 percent of the power generated in the state but 80 percent of the carbon dioxide" (Ridlington & Heavner, 2005). Additionally, many of the coal power plants in Maryland are in violation of the Environmental Protection Agency (EPA) emission standards (Ridlington & Heavner, 2005).

In addition to the environmental drivers, there exist concerns about the longevity of non-renewable energy (Bradford, 2006). The estimates for fossil fuel peaking vary from the not so distant future to the near past. The once abundant supply of these cheap resources is dwindling quickly. In other words, the days of readily available fossil fuels are nearing their end, and renewable sources of energy must be implemented to sustain the growing energy demand. It is therefore necessary, and desirable, to move away from the use of these fuels as a main source of energy.

There are several alternative, environmentally friendly energy sources that can serve as replacements for outdated energy producing technologies. Among these are bio-fuels, geothermal, hydroelectric, solar, and wind energy generation. Due to scale and location restrictions, solar and wind energy are often turned to in order to serve as the primary generators of energy (Bradford, 2006). Solar energy stands out from wind power because of its ability to supply electricity by distributed means (Bradford, 2006). Both power sources can be installed on a local level to minimize distribution losses. Wind power, however, is often restricted by zoning, and is seemingly impossible to implement within an urban environment. As a result, large

centralized generation plants must be used, leading to power loss in an inefficient distribution system. This severely limits the application of wind energy.

Solar energy is often presented as a natural solution to distributed power problem (Bradford, 2006). Although solar technology can be used to generate energy in large centralized power plants, it is most promising in its capacity to be installed on an as needed basis at any desired location. Sunlight falls everywhere and solar panels are small and thin enough to be implemented in all but the most limited of spaces. It is very easy for small portions of land or existing surfaces to be converted to solar energy generation particularly in suburban and rural locales.

The limits of solar energy generation are then neither environmental nor spatial, but instead economic. According to Bradford, photovoltaics are not immediately economically feasible. Solar cells are relatively expensive compared to other traditional means of supplying energy and their use is not yet widespread in the United States (Brogren, 2004). As a result, while the United States possesses the resources necessary to make efficient use of solar energy, it is currently lagging behind many other countries, such as Germany, Japan, and China in this area (Wiser, Barbose, Peterman, & Darghouth, 2009). Large flat panel photovoltaic arrays are simply not competitive with traditional energy generation systems (Matthews, Cicas, & Aguirre, 2004).

One barrier to cost-effectiveness is the inconsistency in power generation. Solar energy generation is dependent on incident solar flux (Bradford, 2006). Incident solar flux is not steady through all 365 days of the year, much less through all 24 hours of the day. Additionally, incident solar flux is not evenly distributed throughout the United States. States in the southwest region receive dramatically more solar radiation than states in the northeast region (Bradford, 2006). The resultant inconsistencies drive much of the United States away from solar power.

A second problem lies in the high upfront costs associated with installing photovoltaic systems. Although the cost is made up over the lifetime of an efficient system, it is difficult to justify such a large initial investment. That noted, if current trends in cost reduction hold large scale solar energy will be cost-competitive with conventional power sources by the year 2020 (Antony, Dürschner, & Remmers, 2007, p.25). In more highly insolated areas, such as rural southwest, it may be competitive even earlier. It should be noted, despite these barriers, there has been a large growth in photovoltaic systems over the last decade (Englander & Kann, 2009). Global photovoltaic demand grew at an average rate of 51% per year from 2000 to 2008 (Englander & Kann, 2009). Within the United States, during the same time frame, installed photovoltaics grew from 4 MW to 290 MW, an average growth rate of 71% per year (Englander & Kann, 2009).

A number of means exist to improve cost competitiveness of solar energy. The first, and most obvious, is through improvement of energy generation efficiency itself. Many advances in photovoltaics have been reached over the past decade. The highest reported PV module efficiency as of 2008 was 22% (Cheng, Sanchez-Jimenez, & Lee, 2009). In early 2012, a U.S. based solar company, Semprius, reported a module efficiency of over 33% (Snieckus, 2012). Though panels of this efficiency will not be commercially available until the end of 2012 we can expect strong increases as time continues. (Bradford, 2006).

The cost competitiveness of solar energy is also improved by offered government financial incentives, provided for homeowners who install PV systems (N.C. Solar Center & the Interstate Renewable Energy Council, 2009). A number of financial incentives are offered throughout the United States and Maryland in particular (Ridlington & Heavner, 2005). The U.S. is not, however, in the lead when it comes to developing these solar technologies. Presently the

United States falls behind many nations, although current growth trends suggest that by mid-2012 there is the potential to trail only Germany in production (Englander & Kann, 2009). This is a consequence of stronger policies supporting the solar industry outside of the United States. The U.S. does have federal and state policies in place that encourage the installation and manufacture of photovoltaics (N.C. Solar Center and the Interstate Renewable Energy Council, 2009). These policies, however, are severely overrun by those in other western nations, such as Spain and Germany (Englander & Kann, 2009) and by highly industrialized nations, such as China (Bradsher, 2011). The large subsidies offered by these nations draw business away from the United States, towards a cheaper manufacturing environment. Further growth within the U.S. is additionally hindered by the established energy substructure. Less developed nations, like those in Eastern Europe, have more of an obvious need for solar power (Dusonchet & Telaretti, 2010).

Additional government incentives have been made available for building-integrated photovoltaics. Building integrated photovoltaics (BIPV) are defined as photovoltaic systems that are incorporated into a building's exterior structure, replacing traditional materials and blending harmoniously with the building's façade while generating electricity. In order for BIPV to become more commercially available and marketable worldwide, many governments have set in place incentives for homeowners and building owners alike.

Germany leads the world market in BIPV due to its focus on supportive legislation (Sivanandan, 2009). In 1999 the German government began its 100,000 roofs program, granting homeowners feed-in tariffs (FiTs) and interest free loans (Sivanandan, 2009). In 2000 the German Renewable Energy Act or EEG was established, later guaranteeing high FiTs for BIPV, especially for façade-integrated applications, because of the high initial cost (Sivanandan, 2009).

In 2002, the British government initiated the Renewables Obligation in which certificates (ROCs) could be granted to consumers for every MWh of electricity generated which could then be sold back to local electricity suppliers (James, Jentsch, & Bahaj, 2009). In 2006 the French government initiated FiTs similar to the German government, granting higher FiTs for BIPV than non-integrated PV (Henemann, 2008; Sivanandan, 2009). With supplemental subsidies available as tax credits, France reached the position of the second largest BIPV market by 2007 (Henemann, 2008; Sivanandan, 2009). In 2007, the Italian government caught on and amended the Conto Energia laws to include high FiTs for BIPV as well as offering several payment options (Sivanandan, 2009). In 2009, Spain realized the importance of BIPV and thus began to grant higher tariffs for BIPV and fewer tariffs for open-field PV (Sivanandan, 2009).

Overall, the European market for BIPV grew to an astounding installed capacity of 25.7 MW worth 143 million by 2007 (Sivanandan, 2009). In the US there is a need for BIPV federal legislation like that of Germany (Henson, 2005). While the US government has initiatives in place for general PV, it lacks BIPV-specific policy.

The established electric grid structure is both a blessing and a curse in solar implementation. Although the established system reduces the incentive for solar adoption, a grid provides an avenue for solar adopters to profit after the initial upfront costs. In addition to government-financed solar incentives, people with grid-tied photovoltaic systems can sell the power they generate if they do not use it themselves (Bradford, 2006). Solar energy linked to the preexisting power grid in this manner are referred to as grid-tied systems. In Maryland, any homeowner who produces excess electricity through solar panels is allowed to sell it back to the grid.

While the cost for PVs has declined drastically since 1975 and their usage has climbed, PVs remain comparatively expensive (Azzopardi, Mutale, & Kirschen, 2008). The chief downfall of photovoltaics then, is that such a large amount of solar cells are needed to generate the energy demanded. The high upfront costs of photovoltaic cells are the limiting factor. An additional cost cutting solution that has been adopted is concentration of photovoltaics (Bradford, 2006). Through concentration, additional energy can be generated in each individual cell. As a result, concentrated photovoltaics (CPV) has seen a boom in the last decade ("Concentrating photovoltaic installations in the USA set to grow at a CAGR of 75% in the next five years," 2011).

Reduction of the cost of photovoltaic energy presents the opportunity for cheap, reliable, and distributed power. The ideal solar system is one which produces a large amount of power at a low cost, a system that does not require extensive or complicated maintenance, and a system that can be set up in any location where there is sufficient sunlight.

Photovoltaics

Photovoltaic (PV) cells are devices that utilize the photovoltaic effect to convert sunlight to electricity to power some external load. The photovoltaic effect refers to the phenomenon in which sunlight striking semiconductors in a certain arrangement produces a voltage difference (Sandia National Laboratories, 2001). This voltage difference results in differences in the electrical conductivity of the different layers of the cell. Silicon during solar cell production undergoes a process called doping where atoms of boron and phosphorus are added uniformly throughout the silicon semiconductor lattice. As a result, these atoms are more likely to donate and accept electrons, respectively, due to their valence shells. When a photon hits the boron doped, or ‘p-type,’ semiconductor layer within the cell, an electron is excited up through a

junction between the two layers and into the phosphorus doped ‘n-type’ semiconductor layer and then out of the cell through the circuit (Wenham, Green, Watt, & Corkish, 2006, p. 31-38).

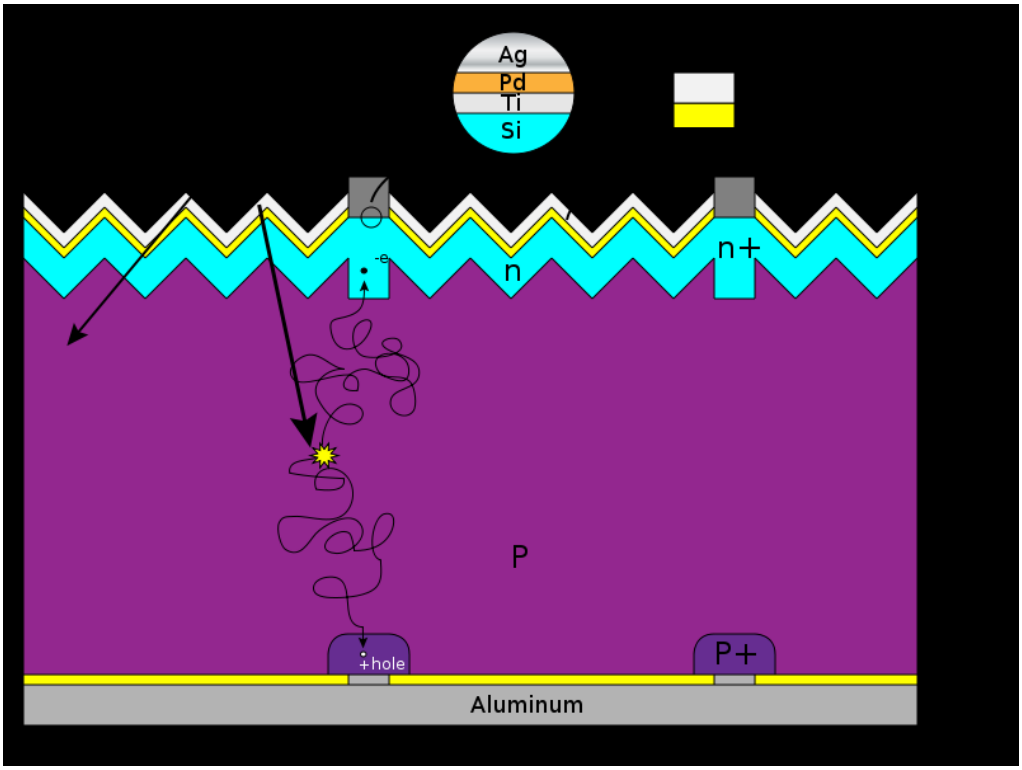

Figure 1: Diagram of the photovoltaic effect mechanism in a silicon PV cell. Source: en.wikipedia.org

PV cells are usually on the order of square centimeters, so they are arranged into groups called PV modules or more colloquially, solar panels. A group of solar panels is referred to as a solar array (Antony, et al., 2007, p. 46). Note that “solar panels” can also refer to solar thermal technology, which utilizes heat from the sun rather than the photovoltaic effect, so it is usually important to distinguish between the two usages. In this paper, “solar” refers to PV and not solar thermal technology unless stated otherwise.

The energy output of a PV cell is dependent on a number of factors. One of the most obvious is the amount of solar irradiation on the cell. If it is cloudy or raining, or if the cell is in the shade, there will be less irradiation. This is obviously a problem in cloudy areas. However, PV can be effective even in non-sunny regions as long as the yearly insolation is reasonably

constant (Antony, et al., 2007, p. 21-22). In other words, the disadvantage of a cloudy winter season can be offset by a sunny summer season. This is especially true if the owner of a solar array is connected to the regular power grid, as is usually the case, and is not wholly reliant on their array during the cloudier parts of the year.

Another factor in the energy output of a PV system is the conversion efficiency of the solar cells. Not all solar energy gets converted into electric power. The conversion efficiency varies with the type of solar cell, which will be discussed in a later section. The efficiency of a whole solar panel is different from the efficiencies of the individual cells that comprise it. Since the cells in a panel are usually part of the same circuit, they influence each other to determine the panel's efficiency. Unfortunately, this means that if one cell is shaded or defective, the output of the whole panel will drop significantly (Antony, et al., 2007, p. 126-127). The wiring and electrical connections between cells and modules also influences on the power output of a solar array.

One last consideration is that the electricity produced by a photovoltaic cell is direct current, whereas devices and the power grid in the United States are designed to run on alternating current. A device known as an inverter is needed to convert direct current to alternating current so it can be used for normal devices or safely fed into the power grid (Antony, et al., 2007, p. 83).

Photovoltaic technologies have advanced rapidly in recent years. This is reflected in the differences between the different "generations" of PV cells. There are three main "generations" of PV cells, of which the first two are already widely used and the applications of the third are still emerging (Azzopardi, et al., 2008). Crystalline silicon cells are usually regarded as the first generation, while "thin film" materials such as amorphous silicon, cadmium telluride, and

copper-indium-gallium-selenide (CIGS) are regarded as second generation technologies. Third generation technologies still have limited applications for domestic use and a high price point.

Monocrystalline and polycrystalline are the dominant PV technology for they provide the highest conversion efficiency at the lowest price (Cheng, et al., 2009; Henemann, 2008; James, et al., 2009; Marsh, 2008). There is an increasing shortage of crystalline silicon wafers, but other types of PV have risen to challenge the dominant form (Henemann, 2008; Marsh, 2008).

Thin film collectors, which include amorphous, non-crystalline, or micromorphous silicon products, are becoming more popular (Henemann, 2008; Marsh, 2008). While they produce less electricity per square foot (conversion efficiencies are about 10-20% for crystalline products and less than 10% for thin film products) and need about double the amount of area as crystalline products for the same power output ("BIPV: Solar-friendly versus architectural aesthetic," 2003; Marsh, 2008), thin films maximize the surface area exposed to the sun for a given volume of silicon (Henemann, 2008; Marsh, 2008). Thin films use less than 2% of the silicon required for crystalline products (Marsh, 2008). German company Schott Solar can coat a substrate with thin film PV in a layer less than a micron thick, while crystalline wafers are at least 180 microns thick (Marsh, 2008). Because of this, thin films are widely applied to glass. Energy can be generated while still retaining semi-transparency (Henemann, 2008; Marsh, 2008). Used in skylights, atria, canopies, and parking lots, these transparent systems typically allow about 50 percent of visible light through ("BIPV: Solar-friendly versus architectural aesthetic," 2003). Thin films used in this manner serve a dual purpose: as a source of shade and thermal insulation that not only creates an ambient temperature inside all-year-round, but also reduces cooling loads as well as energy generation (Henemann, 2008; Henson, 2005).

Despite increasing use of thin-film technologies, crystalline silicon remains the most available and most widely used photovoltaic cell technology (Parida, Iniyan, & Goic, 2011). Conventional crystalline silicon cells have a considerably longer lifetime than thin-film cells (Azzopardi, et al., 2008). Additionally, crystalline silicon is cheaper than thin-film technologies. Researchers at the Lawrence Berkeley National Laboratory who studied PV cost trends found that in systems below 10-kW size, crystalline silicon generally had lower installed costs than thin-film modules (Wiser, et al., 2009).

As mentioned previously, photovoltaic systems can be used to generate electricity even in the absence of an existing power grid. All that is needed to produce power is sunlight. This makes them ideal in isolated areas. PV systems that are tied into a power grid offer many of their own benefits. First, a grid-tied system enables the user to not be wholly reliant on their PV array. If it is not large enough to provide sufficient energy for the owner's needs, the owner can draw power from the utility grid to make up the difference. Grid-tying also helps to smooth over the inconsistencies of energy generated. Excess power generated during specific times can be sold to the grid, and when shortages arise, for example at night, power can be pulled back from the grid. Grid-tying also eliminates the necessity for local energy storage. Batteries are often large, expensive, and cumbersome. Eliminating the need for batteries reduces the overall cost of a system installation.

Concentration

Concentrated solar power (CSP) is a growing field. Generically, concentrated solar power refers to systems that "focus the light of the sun to generate power" (Roselund, 2010). CSP, as it is used today, is limited by the amount of sunlight a geographical location gets, and is thus limited to regions of the world that get more sunlight over the course of the year. It is

generally implemented on a large-scale in places such as the southwest United States and Spain. The state of Maryland and nearby areas do not get enough direct radiation and solar flux to warrant a large-scale CSP implementation. Regions that receive the most direct sunlight throughout the year are best suited for CSP adoption, and diffuse sunlight does not work as effectively. In regions that receive more than 1800 kWh m^-2 per year of radiation, an area of 4-12 m^2 of land would be able to generate 1 MWh of solar electricity (Müller-Steinhagen, 2004).

Concentrated solar power is a fast growing energy source. It is typically used in solar thermal applications. The types of reflectors used include solar power towers with heliostats, Fresnel reflectors, integrated solar combined cycle (ISCC), dish Stirling, and parabolic troughs. Each of these types have been proven to be effective solar power concentrators through their implementation in the United States, Europe, and the Middle East. As of 2010, 509 MW of power in the United States was from concentrated solar power and 25 new locations for solar concentrator farms announced for construction (Sawin & Martinot, 2011).

The use of parabolic reflectors and mirrors in solar thermal applications are used for high-temperature collectors. Concentrated solar power generally utilizes glass mirrors. Large parabolic reflectors concentrate light and heat onto pipes with fluids running through them. These heated fluids then generate electricity in conventional turbines, as would happen in a heat engine by bringing the heated fluids from their very high temperatures to a low temperature using a heat sink. This process generates the mechanical work required to drive the engine. These reflectors are typically 3m by 100m and use a tracking system to keep the sunlight concentrated on the pipe throughout the day.

Typically, concentrating parabolic reflectors have a cylindrical shape defined by the equation $Z = x^2/4f$ where f defines the position of focal point of parabola from the vertex, x horizontal position, and Z vertical height (Price et al., 2002). Reflectors that utilize this equation to derive the size and shape of the concentrator use tracking systems. To eliminate the tracking system, the team instead used a MATLAB script to keep sunlight focused on a specific line.

Parabolic trough concentrators have a 10-200 MW power generation capacity (Müller-Steinhagen, 2004). They concentrate sunlight between 70-80 times, and run at an average of 10-15% solar efficiency, with the highest reported efficiencies at 21% (Müller-Steinhagen, 2004). They lose further efficiency during the thermal power conversion cycle (Müller-Steinhagen, 2004). The thermal cycle efficiency is between 30-40% (Müller-Steinhagen, 2004). The tubes filled with the working fluid reach temperatures of 350 – 500 degrees Celcius (Müller-Steinhagen, 2004). They have also been proven to be the lowest cost CSP system (U.S. Department of Energy, 2003).

Commercial solar concentrating systems currently in use in the Mojave Desert, Spain, Egypt and other locations use metal supports for the frame. Since the concentrators are being produced on a mass scale by corporations, they have the ability to manufacture as many of these large support structures as is required. The material used for reflecting and concentrating the sunlight varies by the manufacturer (Müller-Steinhagen, 2004).

Advances in the research and design of concentrators are being made, primarily by European companies. One of the concentrators that has recently been developed is EuroTrough through the joint efforts of eight companies from Germany, Spain, and Israel. They sought to combine the best features of two popular structural systems for concentrators known as the LS-

2 and LS-3 in addition to any design improvements they deemed necessary. This effort produced a more effective solar concentrator for thermal systems (Müller-Steinhagen, 2004).

CSP systems that utilize solar towers have large arrays, of about one to two square miles, of heliostats with tracking systems focusing concentrated sunlight on the tower. Due to this structure, the reflectors focusing light onto them require tracking systems that rotate and follow the sun to accurately reflect sunlight on one target all day. Without tracking, the setup would be useless for most parts of the day as the focus would not be on the solar thermal tube or heating tower.

These towers, like the tubes in parabolic reflector solar thermal systems, have a working fluid that heats up during the day and cools down in a heat sink and at night to generate mechanical power and electricity. This working fluid is generally saltpeter, composed of sodium nitrate and potassium nitrate, or salt water. These are referred to as central receiver systems, or solar towers.

Solar power towers and reflector systems are capable of power generation of 10-150 MW per year. The solar radiation concentration by heliostats can be from 300 times up to 1000 times. The data from 2004 shows annual solar efficiencies of 8-10%, with a projected efficiency of up to 25% as technology and research advances. The highest demonstrated efficiency is 29%. Steam turbines, which use water as the working fluid, have a thermal cycle efficiency of 30-40%, and combined cycle power towers have efficiencies ranging from 45% to 55% (Müller-Steinhagen, 2004).

Dish Stirling CSP systems also use mirrors to reflect light onto a focal point. They use small parabolic mirrors set up in dish-shaped reflectors to focus light onto Stirling engines, a type of internal combustion engine (Brakmann, Aringhoff, Geyer, & Teske, 2005). These

engines use heat to create rotational motion between pistons in two cylinders, one at a high temperature and one at a lower temperature, both with a working fluid. The pressure difference between them drives the motion and creates mechanical work and this is converted to electricity (Walker, 1980). The solar tracking system in these systems rotates the support structure and mechanism to optimize solar flux and concentration throughout the day. This system is ideal for generating electricity in more isolated regions (Müller-Steinhagen, 2004).

Dish Stirling systems have the lowest annual capacity of the most widely adopted CSP systems at 0.01-0.4 MW of power, but the highest concentration of 1000-3000 times of solar radiation being focused on the Stirling engine. The demonstrated peak solar efficiency is 29%, with demonstated annual solar efficiency of 16-18%, and projected efficiency of up to 23%. The Stirling engine has an efficiency of 30-40%. Some systems use a gas turbine instead, which has an efficiency of 20-30% (Müller-Steinhagen, 2004).

Linear Fresnel reflector systems use mirrors to focus light and heat onto linearly set up pipes that heat up and generate electricity the same way as they did for parabolic trough solar thermal CSP systems. Linear Fresnel systems have the capacity to produce 10-200 MW of power annually, with 25-100 times solar radiation concentration. The projected peak efficiency for these systems is 20%, and the projected annual solar efficiency is capped at 11%. The steam turbine that would be used to convert the heat to mechanical power has an efficiency of 30-40% (Müller-Steinhagen, 2004).

Fresnel lenses are “a chain of prisms” that refract and focus light (Xie, Dai, Wang, & Sumathy, 2011). Chen & Su (2010) attempted to use a Fresnel design as has been done in the past, and added optical elements of differing shapes to refract the light and spread it out more evenly. For their control, they simply tested a Fresnel lens, and in order to keep from

concentrating on a very small spot on the solar cell, which would decrease efficiency and harm the cell by overheating it, they placed the cell 10mm in front of the focal point of the light.

This project attempts to adapt lowly-concentrated solar thermal concentration methods to a small scale photovoltaic system in the style of micro-CSP systems. Solar company Sopogy located in Honolulu, Hawaii, has developed a micro-CSP system that utilizes technology similar to parabolic trough systems on a smaller scale. Sopogy's SopaNova system has a capacity of 3kW for electricity and hot water production, and is advertised for both on-grid and off-grid applications. In December of 2009, a 2MW plant using Sopogy micro-CSP units opened in Hawaii (Roselund, 2010).

Solar thermal systems lend themselves more easily to concentration than photovoltaic systems. The heat generated by focused sunlight is the desired effect in the system, whereas in photovoltaic systems, excessive heat increases the resistance of the PV cells and decreases their efficiency and effectiveness. Directly modifying and adapting a solar thermal system would be harmful to photovoltaic cells.

Weathering

Concerns over durability issues arise in regards to the reflective surface, the base, and the photovoltaics. These concerns come from various types of weather, along with natural wear and tear associated with materials being placed outdoors for a prolonged period of time. Such concerns regarding durability and weathering have been seen in previous studies that involve the usage of photovoltaics.

Typical photovoltaic systems utilize materials designed to last at least as long as the projected 20-year life-span of the solar system (Bradford, 2006). These materials must withstand chemical degradation, corrosion, static loads on the structural members, and dynamic loads due

to wind. Large-scale PV and CSP systems utilize steel, aluminum, steel alloys, or steel reinforced with carbon for construction. Aluminum alloys are also widely chosen for their lower weight and density than steel, ease of fabrication, variety, high strength-to-weight ratio, and low corrosion.

The photovoltaic panel is meant to capture sunlight and generate power. These panels are positioned nearly horizontal to absorb the optimal amount of light from the sun. Such a low panel angle is prone to having sand or dust accumulate on the surface of the photovoltaics, thus blocking out the sunlight. A study in 2005 aimed to compare the sand dust accumulation on the panels with the panels efficiency (Al-Hassan, 2005, p. 187). The authors of this study installed two panels on top of a roof in Kuwait. They made sure to continuously clean one of the panels, while leaving the other to accumulate dust (Al-Hassan, 2005, p. 190). From their results they found that the maximum output power decreased as the amount of sand dust particles accumulated on the surface of the panel (Al-Hassan, 2005, p. 196). This study concludes that dust on the panel significantly decreases the panel's efficiency.

Another study performed in 2001 focused on the effect of dust accumulation of panels tilted at different angles. Located in Egypt, the study states that nine glass plates were placed at differing angles, and each was observed after certain time limits to measure the dust accumulation (Hegazy, 2001, p. 531). From this study the author concluded that a horizontal panel accumulated nearly double the amount of dust as a panel that was placed at 45 degrees (Hegazy, 2001, p. 529). This study establishes that the more horizontal a panel is placed at, the more dust it will accumulate, which greatly impacts the panel's output. As a result it is often more advantageous to tilt the panels.

From the two previous studies we can generalize that clean photovoltaic panels will generally be more efficient than those that are not clean. However, many panels are left unclean

due to human neglect or an inability to clean such panels. In 2004 a survey in Chile reported that 91% of people who were instructed to clean their panels, after the solar system was implemented, did not clean them despite the instructions (Nieuwenhout, et al., 2004, p. 11). The study believes the cause of this to be due to two major reasons. The first is that many elderly members were unable to clean the panels because of certain physical limitations. The second reason is that of human neglect, as some people did not understand the purpose of cleaning the panels (Nieuwenhout, et al., 2004, p. 11).

Solar systems require regular maintenance to maintain high function and effectiveness. The maintenance must be continuously updated to meet the demands of the system. Beyond simple maintenance, the system must be treated in the manner in which it was designed for. The manufacturer must clearly explain all of these aspects to the end user to maximize the system's performance. However, currently a considerable amount of photovoltaic systems implemented in rural communities, the implementation occurs by groups who are visiting for a short amount of time, only to vacate the area (Mapako, 2005). This leaves many of the users of the new systems without a clear understanding of the services and maintenance needs of the system.

The implementation of solar systems can prove to be very complex by nature. This inherent feature makes these systems increasingly vulnerable to many factors possibly affecting the functionality of these systems. One of these major factors is temperature, which has been briefly discussed earlier; it can have dramatic effects on the panel, reflective surface, and base of the system. A previous study acknowledged this fact by applying a wide range of temperatures to a solar home system. From their results they were able to establish a “deterioration degree” based on the health of the solar system. This deterioration degree allows one to factor varying temperatures on the average life of the system (Tsujikawa, 2009). The most decisive results

occur when the temperatures reach extremes, and thus the "deterioration degree" calculation becomes more critical (Tsujikawa, 2009).

The voltage output of photovoltaic systems is an important indicator of the health of the entire solar system. The manufacturer usually designates normal voltage ranges for the solar panels, and any batteries that are associated with the system. In a healthy solar system, the recorded voltages for the panels will be in the range of the manufacturer designated voltage range. If the new system is not within these ranges, then the photovoltaic system may be malfunctioning.

One study used the battery voltage value to diagnose the health of the entire solar system. In this study the research group encountered problems such as a dirty panel, and a lack of a charge controller. The researchers created a method of early detection, based on comparing expected voltage, with the actual voltage. If there is a discrepancy between the expected voltage and actual voltage, the problem was detected by a model the team used to estimate the voltage (Lorenzo & Labed, 2005). In the article the authors suggest that rather than using expected voltages, one could use voltages from a newly implemented system to collect the data (Lorenzo & Labed, 2005). The authors of this research only proposed a detection system, and no method was created. Thus, creating and implementing of a system which not only determines whether the system is healthy or not, but also acts as a potential tool for detection.

PV Implementation

An important consideration in designing any energy generation system is considering how it will be implemented. Traditionally, PV systems are utilized residentially and commercially as fixed frames on rooftops, which are added on post construction (Marsh, 2008). Some states even pole-mount PV arrays and attach them to roads signs or cell phone towers

(Aristizábal & Gordillo, 2008). On a wider scale, PV plants are constructed in rural areas (Aristizábal & Gordillo, 2008). While any PV use is beneficial to our environment, these systems are conventionally limited by high costs for additional land and structural support (Aristizábal & Gordillo, 2008). Therefore, there is a pull towards building integrated photovoltaics (BIPV), or systems that do not need additional land or structural support because they actually replace a traditional part of a structure.

A typical photovoltaic system is made up of the collector (the photovoltaic array of cells that converts sunlight into electricity), the conductor (the conductive material that carries electricity from the collector to the converter), and the combiner or converter (the system that either combines DC current for direct distribution or the system that converts DC current to AC current for electricity storage, respectively) ("BIPV: Solar-friendly versus architectural aesthetic," 2003). BIPV systems have a fourth component: the building element or the part of the building the BIPV system is being integrated and ultimately replacing ("BIPV: Solar-friendly versus architectural aesthetic," 2003). There are many benefits to BIPV over traditional PV systems. First and foremost, because PV cells are integrated into the building structure, there are no additional costs for land or structural support (Cheng, et al., 2009; Garris, 2009; Keoleian & Lewis, 2003; Yoon, Song, & Lee, 2011). There is no additional weight added to the building and no additional penetration needed for structuring, reducing vulnerability to high winds (Garris, 2009; Henemann, 2008; Marsh, 2008). BIPV can be integrated anywhere, on both existing and new buildings and unrestricted in urban areas (Garris, 2009; Marsh, 2008). Additionally, BIPV systems are often cheaper than the traditional building materials they replace (Keoleian & Lewis, 2003). For example, BIPV systems act as electrical resistors that protect against lightning and repel electromagnetic interference, especially important in hospitals and airports (Henemann,

2008). This can greatly reduce overall cost. Furthermore, BIPV systems are seamlessly integrated into the building structure, providing a modern, futuristic aesthetic (Garris, 2009; Henemann, 2008; James, et al., 2009; Marsh, 2008). This can increase resale value (Henemann, 2008). Finally, because electricity is generated at the point of use, transmission and distribution losses are eliminated (Cheng, et al., 2009; Garris, 2009; James, et al., 2009; Marsh, 2008; Yoon, et al., 2011).

BIPV systems can either be grid-tied or simply stand-alone systems (Cheng, et al., 2009; Henemann, 2008; Henson, 2005). If they are grid-tied systems, then there is the opportunity for the system to have a net zero energy consumption and provide income by selling electricity back to the grid (Cheng, et al., 2009; Henemann, 2008; Henson, 2005). If they are stand-alone systems, then there is the opportunity for the building to be located in remote areas away from the grid or simply be self-reliant in areas where the cost of electricity is high (Garris, 2009).

BIPV can be integrated in numerous innovative ways. One common practice is to integrate PV cells into roofing systems. For example, Kyocera Solar introduced their product MyGen Meridian as a replacement of conventional concrete roofing tiles (Henson, 2005). MyGen is made up of a metal cassette system that holds the PV modules in place while interlocking with adjacent concrete roofing tiles (Henson, 2005). Similarly, Open Energy Corporation introduced SolarSave as a replacement roofing tile that comes in three colors; black, red/brown, and blue/grey (Marsh, 2008).

Thin film or other second and third generation PV cells allow for even more creative implementation. Thin-film PV cells can be flexible. This allows BIPV to be readily applied to less than optimal positions, including flat roofs, east/west facing roofs, and facades (Henemann, 2008; Marsh, 2008). Many times, a combination of PV types is utilized on a single building to

reach maximum electricity generation. For example, IBC Solar constructed the “Zero Energy Office” in Pusat Tenega, Malaysia (Henemann, 2008). This self-sufficient building utilizes polycrystalline modules on one roof, amorphous silicon modules on another roof, semi-transparent modules on atrium glass, and monocrystalline modules on the parking roof (Henemann, 2008).

Location is also an important consideration in PV implementation. Different areas have different incident solar radiation or insolation (Keoleian & Lewis, 2003; Lu & Yang, 2010), as well as cloudiness and shadows that could reduce a system’s conversion efficiency (Cheng, et al., 2009; Yoon et al., 2011). Optimal tilt angles also vary according to location. Because optimal tilt angles and a location’s latitude are directly correlated one can average a location’s yearly optimal angle without additional calculations to find the optimal tilt angle for a fixed system (Cheng et al., 2009).

When working with BIPV systems, the architecture of the building must also be considered on deciding how PV can be integrated optimally ("BIPV: Solar-friendly versus architectural aesthetic," 2003). The type and area of available surface decide which type of PV is used. The type of PV determines the conversion efficiency of the system as well as the amount of power that can be generated. Another characteristic of the building that will determine efficiency is the building’s orientation ("BIPV: Solar-friendly versus architectural aesthetic," 2003; Cheng, et al., 2009; Lu & Yang, 2010). In the northern hemisphere, southern orientation is optimal (Cheng, et al., 2009; Lu & Yang, 2010). Additionally, cooling options must be accounted for (Garris, 2009; Muller, Rodriguez, & Marion, 2009).

For a roofing application, there are three ways in which solar roofing tiles can be integrated; direct, batten, or counter-batten (Muller, et al., 2009). A direct configuration requires

that solar tiles are directly screwed to roof sheeting (Muller, et al., 2009). While this is the least expensive, there is no airflow or convective cooling (Muller, et al., 2009). A batten configuration requires that equally-spaced horizontal furring strips are directly attached to roof sheeting and solar tiles are attached on top of the furring strips (Muller, et al., 2009). This provides some convective cooling (Muller, et al., 2009). A counter-batten configuration requires that equally-spaced vertical furring strips are directly attached to roof sheeting, equally-spaced horizontal furring strips are attached on top of the vertical furring strips, and solar tiles are attached on top of the horizontal furring strips (Muller, et al., 2009). While this is more costly, it provides the most convective cooling and water drainage (Muller, et al., 2009). Research has found that there are differences as high as 10 degrees Celsius at midday between direct and counter batten systems (Muller, et al., 2009). Because voltage and power output decrease with increasing temperature, counter batten systems that improve system cooling are preferred (Muller, et al., 2009).

Methodology

Introduction

The process of designing, building, and testing a working low cost concentrating photovoltaic system involved three generations of solar panels and extensive experimentation with different solar cells, reflector designs, structural materials, protective coverings, wiring schemes, and data acquisition methods. The experimental study resulted in detailed analyses of reflector geometry, thermal properties of solar concentrating systems, and the power output response of PV cells under concentrated light, all of which will contribute to future renewable energy research. In the end, a working prototype was completed and tested that produced a greater power output than a similarly sized control panel.

Due to a tight budget and unique shape requirements, each panel was assembled by hand from solar cells and other purchased materials. The first generation used a wood backing and a Plexiglas cover with caulk sealant. To prevent warping of the backing, the second generation used a PVC based wood substitute and a better-sealed Plexiglas cover. Due to thermal and environmental issues, the third generation eschewed weatherproofing in favor of a simple metal structure with pre-assembled PV cells. The solar panel supports and reflectors were constructed wood to lower costs. The panels were each between six and eight feet long and were carried back and forth from the test site on the roof of Glenn L. Martin Hall to a storage location between tests and for inclement weather. The reflectors, however, were much larger and had to be assembled and left on site. The reflectors and panel supports were covered with a tarp and tied to the ground during severe weather, but they were still damaged on multiple occasions, requiring one complete rebuilding.

For each generation, two PV cell panels were built. The "flat panel" was left on the ground and pointed at the sun at a predetermined angle. This provided control data while the other, "bifacial panel" was mounted in front of the reflector. Data loggers were used to record the voltage produced by each panel over a certain period of time. The sampling rate of the loggers was variable and could be set as high as one measurement per second. The data loggers included batteries and could record data for up to several days at a time. Although the loggers only recorded voltage, power is the most important metric when evaluating the overall performance of a solar panel. Therefore, a resistive load was added to each panel, so a voltage measurement could be used to find the power output. After each panel was assembled, a test was performed to determine the resistance that would produce the peak power output, since this would likely be the resistance used in a real-world application.

Even though the testing of the solar panels rarely went according to plan, the results indicate a great potential for the technology, and the knowledge gained in the process will help pave the way for future developments.

Concentration Modeling

The starting point for this project was a ray-tracing program written by Dr. Adomaitis, the team's mentor. This program was designed to determine the optimal shape of a reflector to focus light across a line segment defining the location of the PV cells. As opposed to a standard parabolic reflector, which would focus light to a point, the reflector shapes generated by this program concentrated light in an even distribution across a flat surface, lending itself to photovoltaic applications. The program generates shapes based the angle of the sun, the length of a line segment (the width of a solar panel), and the vertical displacement of the line segment (or solar panel) above the ground.

The program works by assuming an even distribution of light across the surface of the PV panel. It then determines the optimal reflector curve to recreate the uniform reflection of parallel light rays that would be coming from the sun. The program then graphs the reflector curves and provides a visual representation of the calculated curves.

The reflector was optimized to perform best during the summer months, as there are more clear days and greater solar flux in the summer, and thus a better opportunity for solar power. The sunlight angle was determined to be roughly 66° from the horizontal using the subsequently described method. Note that for the calculation, all the angle measurements are in degrees. Additionally, these calculations are for conditions in College Park, Maryland.

The reflector was optimized for summer, and so it was necessary to normalize θ, the angle of the sun, across a certain period of time to get the average angle of the sun. In this case, that period of time consisted of the summer months only, where θ changes from 51° to 74° and back to 51° again. Because the graph of θ would be symmetric about 74° no matter what equation was fit to it, the calculation only considered the lower and upper limits of 51° and 74°, respectively. The angle of the sun is normalized based on a sinusoidal function. The function should vary from 0 to 1 as θ varies from 51° to 74°, so the normalization equation becomes equation 1, below.

$$\cos\left(\frac{74-\theta}{23}*90\right) \tag{1}$$

The terms in the parenthesis are an average of the angle, with 23 being the difference between the maximum and minimum summer angles. This means that the function has a value of 0 at θ=51°, and a value of 1 at θ=74°. To normalize θ, the definition of normalization in equation 2 is used. The actual evaluation of this definite integral is trivial and was simply solved in MATLAB. Solving equation 2 returns the average angle θ=65.54°.

$$\theta = \frac{\int_{51}^{74} \theta \cos\left(\frac{74-\theta}{23} * 90\right) d\theta}{\int_{51}^{74} \cos\left(\frac{74-\theta}{23} * 90\right) d\theta} \quad (2)$$

The next input needed by the program was the cell length. The individual solar cells that would be used for the project were six by three inches, so the smaller of the two lengths (3 inches, or 0.0762 meters) was chosen for the program in order to return a higher concentration ratio without unnecessarily increasing the size of the reflectors. The height above the ground was chosen to be 0.25 meters or 9.8 inches based on what would give a meaningful output in the program. The resulting graph, shown in Figure 2, below, was used as the basis for the reflector construction. Note that the panel height changed later on, due to testing delays that cause much of the testing to be completed during non-optimum months.

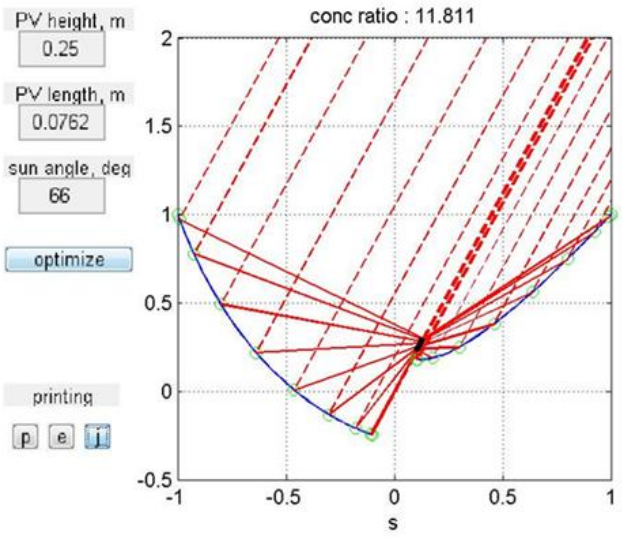

Figure 2: Reflector Shape Output used for Prototype

The program was based on the assumption that the solar panel was bifacial and of the length specified. This meant that custom panels had to be built to accommodate the reflectors. Market-ready solar panels could not be used because bifacial panels are typically very expensive and most premade solar panels are far too large for the applications of this project. Constructing

custom solar panels from individual PV cells was a much cheaper option, which was important given the small budget of the project. Additionally, while the program could have been run for a larger panel, this would have made the reflectors extremely large, thus defeating the purpose of small scale CPV and making the construction more difficult and the system less consumer friendly.

With the output of the MATLAB program and perfectly precise construction, an ideal reflector can be constructed. However, imperfections in the construction of the reflector meant that a mechanism for evaluating the performance of the constructed reflector was needed. This resulted in the creation of a Python program to evaluate such performance. This program takes in the location of the reflector, the location of the PV element, and the angle of the sun to model the reflection of rays of sunlight.

The Python program employs Snell's Law of Reflection to model the reflection of rays of sunlight as it hits a reflective surface. Snell's Law of Reflection states that the angle of incidence is equal to the angle of reflection with respect to the surface of reflection. Currently, the assumption is that there is no energy lost when the rays are reflected, but the algorithm can be modified to factor in percentage losses.

There are two types of surfaces in the context of the program, reflective and absorbing. A reflector is composed of two types of surfaces, a reflective and an absorbing side, while a PV element is solely absorbing. Every physical construct is then approximated with linear elements, so that normals to surfaces can be easily determined. As the number of linear elements constituting the reflector is increased, the precision is increased, but the processing time is increased as well.

The sunlight can be represented in the form of parallel lines incident on a reflecting or absorbing surface. Less spacing between lines represents more intense sunlight, while more spacing represents less intense sunlight. For each ray of sun, the first incidence on a construct is computed. If this occurs on a reflecting surface, the line is plotted until first incidence, the new reflected ray is computed, and the first incidence is computed again. If this occurs on an absorbing surface, the line is plotted until first incidence and nothing further occurs. If no incidence occurs, the line is plotted in its entirety and nothing further occurs.

Reflector Construction

The shapes of the two reflector's surfaces were optimized to evenly distribute the reflected light across the surface of the solar panels, as discussed in the concentration modeling section, above. Turning the simulation's output into a functioning prototype involved several steps. First, a mockup of the reflector was created using a CAD (computer-aided-design) program, as seen in Figure 3, below. Then, the materials were chosen based on cost and durability. Next, the materials were tested to confirm that they could withstand extended periods outside under various weather conditions. Finally, following the testing, the two reflectors were constructed and integrated into the CPV system. Additionally, further along in the project, one of the reflectors was removed to increase the efficiency of the solar panels. Note that the single reflector used in the final prototype is the one displayed in Figure 3.

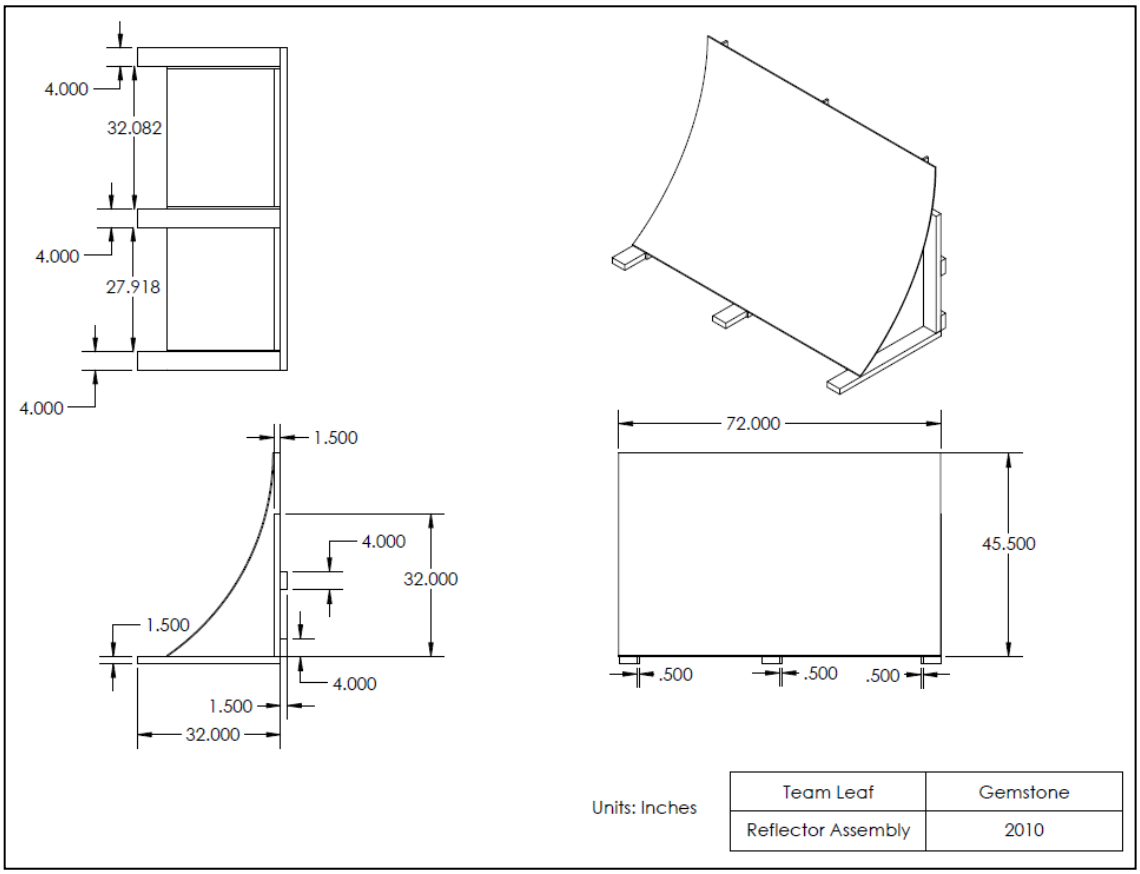

Figure 3: Reflector CAD Drawing

The reflectors were composed of four main components: a wooden frame, three particle board ribs, a curved Masonite backing, and a Mylar reflective surface. These components were combined to create two separate reflectors, one facing directly towards the sun, and one facing the opposite direction. The particle board ribs supported the shape of the reflector as determined by the ray-tracing program, and were in turn supported by the wooden frame. The Masonite backing was attached to the ribs, taking the shape of the reflector, and the Mylar was adhered to the Masonite to give it a reflective surface. This set-up provided the durability needed to maintain the shape of the reflective surface over the course of the testing process. Originally, the reflector was designed to be eight feet long, matching the length of the first set of solar panels (Generation 1), but was later shrunk down to six feet for reasons discussed in the Generation 2 section of Solar Panels Construction and Testing. Before beginning construction on the

prototype reflectors, the materials were carefully chosen and tested to ensure that the reflectors would last for the two years that they would be in use.

The material selection process took place in two stages. First, the team researched potential materials based on the needs and constraints of the project. Then, a short testing phase was conducted to ensure that the materials performed as required. The testing phase involved creating a scale model of the reflector, to determine if the chosen materials could retain the correct shape and withstand the weather for an extended period of time. Before going more into the testing process, it is first necessary to review the factors that influenced the decision regarding what materials to test.

The materials were chosen based on four factors: cost, durability, ease of access, and workability. Given the narrow Gemstone budget, and the fact that the intention of the project was to create a cheap alternative to conventional solar power, cost was the main concern of the team. In addition, the ability to withstand the extremes of Maryland weather was particularly salient, as the collector would be spending the entirety of the testing phase (nearly two years) outside. While the small size of the panels would allow them to be moved inside during storms, the size of our reflector meant it would have to remain outside. To account for this concern, the materials chosen were materials typically used outdoors in the construction and agricultural industries.

Furthermore, all the materials used were locally available in hardware stores, ensuring that this technology could be easily and cheaply adapted to the rest of Maryland. Lastly, the material choices were limited to those that would be workable using the tools and equipment at the team's disposal, and equipment that would be readily available for a consumer of this technology. For example, some consideration was initially given to the potential to make the

collector out of metal but given limited metal fabrication experience, and the inability to access metal-working machinery on a consistent basis, the idea was discarded. Having given consideration to each of these concerns, a final list of materials, as seen in Table 1, was developed for use in the prototype.

Table 1: Reflector Material Summary

Material	Use	Justification
2 by 3 inch oak planks	Frame	Cheap, readily available, sturdy, able to stand up to the elements with water-proofing, easy to work
Particle board	Ribs of reflector	Cheap, readily available, sturdy, can be cut to the curve needed without splintering or warping.
Masonite	Reflector backing	Smooth, firm, flexible. Weathering less important because damage would be mitigated by Mylar
Mylar	Reflector surface	Cheap, highly reflective, easy to work with
Decking screws	Connecting the pieces of the frame	Cheap, corrosion resistant
Liquid water-proofing	Applied to the oak planks and back of Masonite to prevent water damage	Enable frame to withstand rain and snow better
Wallpaper glue	Adhesive used to attach the Mylar with Masonite	Easy to apply, did not distort the surface of the Mylar when applied

The above materials were tested through the use of the aforementioned scale model. A smaller version of the reflector was built and left outside for two weeks in October 2010, long enough to ensure that the collector would face a variety of weather conditions over the testing

period, including rain, sun, and moderate winds. The test reflector, seen in Figure 4, ensured that the Masonite would maintain its rigidity, while curved, even after getting wet. Additionally, it made sure that the Mylar surface would stay reflective and adhered even after harsh weather. Moreover, it confirmed that the structural integrity of the reflector itself was sufficient to withstand most typical weather conditions in the local area.

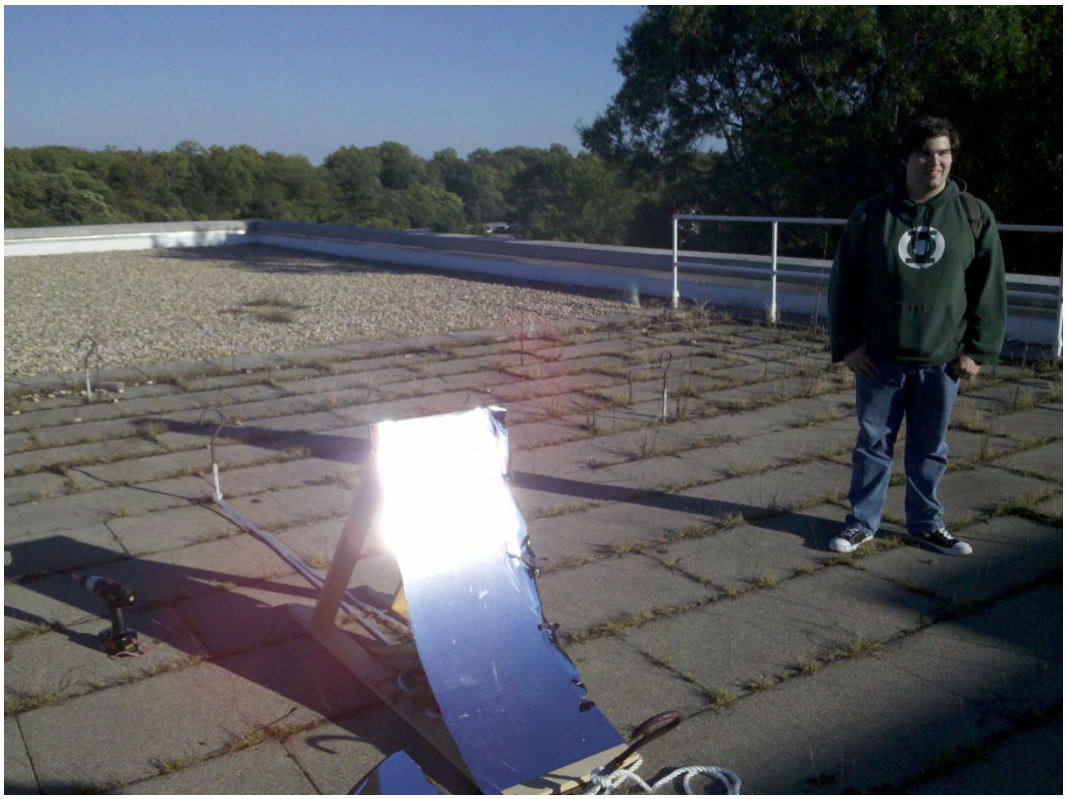

Figure 4: Weather Testing of the Test Reflector

The most helpful part of the testing process was the realization that the type of adhesive originally used to attach the Mylar to the Masonite severely diminished the concentrator's reflective properties. At first, a 3M adhesive spray was used to attach the Mylar to the Masonite, but after a few days on the roof, the Mylar had scrunched up, making the reflective surface rough and dispersing the reflected light. Next, wallpaper glue was tested and it was able to maintain a solid hold on the Mylar, without noticeably lessening its reflectivity. The test reflector was remade using the wallpaper glue and, even after being left outside in a storm, the overall

reflectivity of the Mylar immensely improved. The difference between the two glues can be seen in Figure 5, below.

Figure 5: Mylar Reflectivity with 3M Spray (top) and Wallpaper Glue (bottom)

Following the materials testing phase, was the final reflector construction. The first step in the construction was translating the coordinate output of the program into a set of dimensions.

The dimensions would then be used to fabricate the ribs for the collector. The ribs would eventually support the shape of the reflector itself, and therefore needed to be cut as closely to the actual design as possible. In order to get the dimensions, the program was modified by the team to output a set of points along the optimized reflector's curve, seen in Table 2, below. The section of the left reflector below the zero point was removed for the following two reasons. First removing that section of the reflector would lower the center of gravity of the system, thus making them less susceptible to getting knocked over by strong winds. Second, the section was removed in an attempt to equalize the flux on either side of the bifacial solar panel between the reflectors.

Table 2: Dimensional Output of Ray Tracing Program

Left reflector position (x) and height (y)			
x (m)	x (in)	y (m)	y (in)
-1.000	-39.37	1.000	39.37
-0.991	-39.03	0.972	38.28
-0.924	-36.39	0.778	30.63
-0.800	-31.51	0.493	19.40
-0.638	-25.14	0.219	8.61
-0.463	-18.24	0.007	0.27
Data Below is unused			
-0.301	-11.86	-0.132	-5.21
-0.177	-6.98	-0.210	-8.26
-0.110	-4.34	-0.243	-9.56

Right reflector position (x) and height (y)			
x (m)	x (in)	y (m)	y (in)
0.102	4.00	0.182	7.15
0.110	4.34	0.180	7.09
0.177	6.98	0.188	7.40
0.301	11.86	0.251	9.87
0.463	18.24	0.384	15.10
0.638	25.14	0.562	22.12
0.800	31.51	0.749	29.51
0.924	36.39	0.902	35.53
0.991	39.03	0.989	38.93

-0.102	-4.00	-0.247	-9.71	1.000	39.37	1.000	39.37

The points of each curve were plotted onto appropriately sized pieces of construction paper, which would then be used to trace the curves onto particle board, as seen below in Figure 6. This reduced the possibility of error in the construction of the ribs, as it was only a matter of re-tracing the points and curve along the cutout, instead of re-measuring the distances between each point for every cut. Three ribs were made for each reflector and, after tracing and cutting the ribs, the deviations from the intended shapes were sanded away.

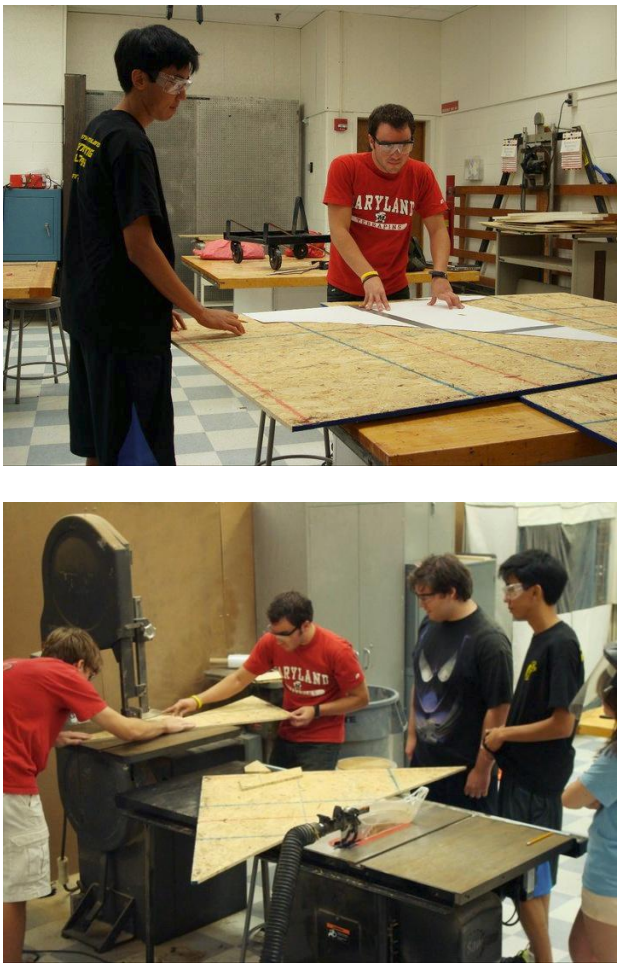

Figure 6: Rib Construction

After completing the ribs, the frame was built with two-by-three inch wooden planks. The planks were cut to the proper lengths and attached together to form six L-brackets, which were intended to structurally reinforce the ribs themselves, while also providing a means of connecting the ribs together. Each reflector consisted of three connected L-brackets, the lengths of which were determined by the length of the corresponding ribs. Therefore, the lengths of these sections differed between the left and right reflectors, but were the same within each side. For the right reflector, additional pieces of wood were affixed to the bottom of the L-brackets, so that the ribs would be able to reach the height specified by the program. The two frames with the L-brackets attached can be seen below in Figure 7.

Figure 7: Left and Right Reflector Frames under Construction

The three L-brackets of each side were connected by screwing two 6 foot planks along the back of each piece. Each L-bracket was evenly spread out along the length of the plank, so that one was at either end, and one was in the middle, as seen in Figure 8. More specifically, the

middle L-bracket was actually about an inch off from the exact middle of the reflector, which allowed the corresponding rib to lie exactly at the midpoint of the reflector once it had been attached. For the right reflector, an additional plank was used to connect the front of the L-brackets in order to further reinforce the larger frame.

Figure 8: Attaching Ribs to Frame

In order to add additional reinforcement to the reflector surface, wooden planks were attached between the ribs, as depicted in Figure 9. This served the dual purpose of providing a place for the Masonite to attach and supporting the Masonite in case it became saturated with water and began to warp. The planks thus ensured that there were no unintended dips along the face of the collector in addition to increasing the structural integrity to the frame itself. Note that when the reflectors were first constructed, the Masonite was screwed directly into the ribs which, over time, caused splintering leading to the reflectors having to be partially rebuilt. The method shown below is for the second and final reflector construction.

Figure 9: Masonite Supports being attached to the Ribs

To finish the reflector, the Masonite was attached to the supports, following the shape of the ribs, and then the Mylar was adhered. After having placed the sheet of Mylar, a smoothing tool was used to ensure the Mylar was firmly attached to the Masonite backing. This process removed any excess glue and spread the remaining glue out evenly beneath the Mylar, removing inconsistencies such as air bubbles. The application of Mylar was completed by using a pin to pop any remaining air bubbles, and cleaning any excess glue off the Mylar. One of the completed reflectors can be seen in Figure 10, below.

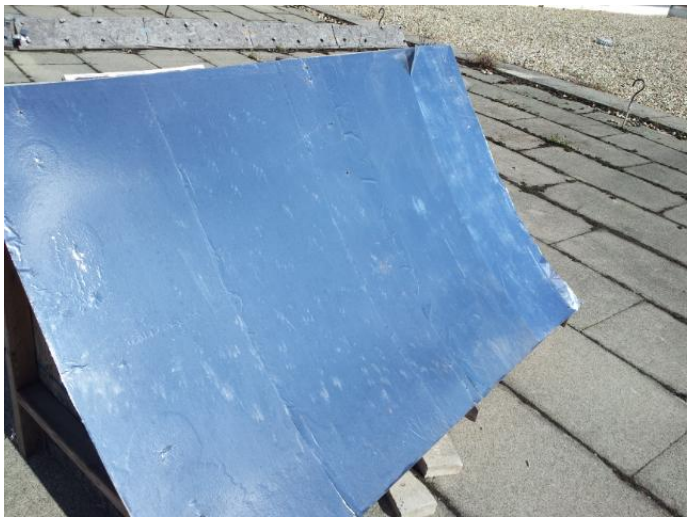

Figure 10: Completed Reflector

The last step was to build the supports for the solar cells themselves. This was done with the same technique used to make the frame; two-by-three inch wood planks were screwed together to create two separate but identical supports. Each side was made up of three planks of wood, one vertical piece to connect to the cells, one running along the ground perpendicular to the reflector, and a last plank running along the ground parallel to the reflector to add stability to the support. In the vertical piece of wood, several holes were drilled so that adjustments could be made to the height of the cells to account for the changing focal point of the reflector as the height of the sun changed throughout the year. The completed panel supports can be seen in Figure 11, below.

Figure 11: Solar Panel Supports

Solar Panel Construction and Testing: Generation 1

The original two solar panels built for the CPV system prototype each consisted of an array of 30 polycrystalline PV cells wired in series on a wooden backing. As explained in the literature review, polycrystalline cells were determined to be the optimum PV cell type for the prototype because they are the most commonly used type of PV cell on the market, are the cheapest, and are generally less efficient than monocrystalline cells, so would see a bigger impact from concentration.

Each solar panel was 8 feet long, the maximum length that would still enable them to be transportable from the storage location to the testing site mentioned in the introduction to the methodology. They were originally constructed to this length because it would maximize the hypothesized difference between the power outputs in and out of the reflector. Note that the difference discussed here is the raw value; the percent increase in power should remain the same

regardless of the length of the cells. Additionally, the longer panel would reduce the impact of imperfections in the reflector surface on the power output, thereby resulting in a more realistic power comparison between the two panels.

The individual cells were rated at 0.5V, so the open circuit voltage of the panels was 7.5V. Note the cells only produce this much voltage when they are exposed to strong radiation, namely sunlight. The top and bottom of the PV cells were determined to be negatively and positively charged, respectively. As explained in the literature review, this polarity arises from the cell construction—electrons sent across the p-n junction after being ionized by incoming radiation.

Due to the geometrical constraints of the backing of the two panels, the cells were wired together lengthwise, as seen in Figure 12. The dimensions of the cells, as discussed in the concentration modeling section were 3 by 6 inches and the panels were built to accommodate that. The flat panel—the panel that would generate energy without the aid of the reflector—was 8 inches wide and would support two side-by-side rows of 15 cells, wired in series to arrive at the previously stated total of 30 cells in series. The bifacial panel was 6 inches wide and consisted of two rows of 15 cells, each row on opposite sides of the panel. The bifacial construction was intended to use two reflectors, one on either side of the panel, to achieve maximum focus by concentrating on a small area. Additionally, the cells in each panel were wired into three "modules", allowing smaller subsets of the cells on each panel to be tested in case of a malfunction. This design would enable the team to pinpoint a problem mush faster.

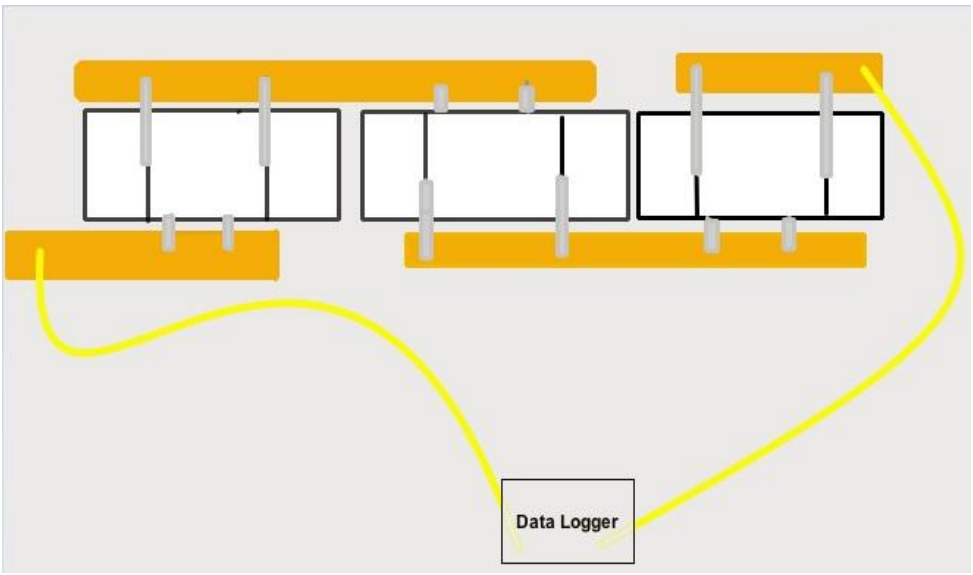

Figure 12: Solar Cells Wired in Series

After the cells were wired together, the panels were weatherized. Plexiglas was attached to the two panels, covering the PV cells, and silicone caulk was used to attach the Plexiglas to the wooden backing. This type of caulk was used to allow the Plexiglas to be removed in case of a disconnected wire. Furthermore, the exposed backside of the flat panel was coated with a waterproofing spray. The finished flat panel can be seen in Figure 13.

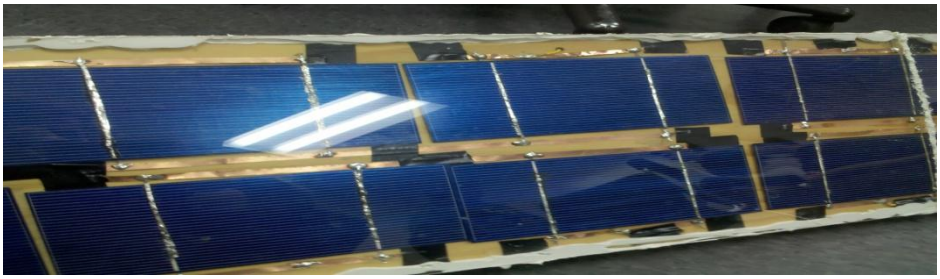

Figure 13: Weatherized Generation 1 Flat Panel

In addition to weatherizing the solar panels, the data loggers were also weatherized. A Tupperware container was attached to the underside of the flat panel and another one was hung off the side of the bifacial panel. The containers would enclose and protect the data loggers, along with the leads coming from the panels and the resistors wired into the circuit. The

container on the flat panel is pictured in Figure 14. Also depicted in Figure 14 are triangular angular adjustments on the flat panel. These were built to keep the flat plate at the ideal angle of 66° from horizontal. The ideal angle, derived previously in the concentration modeling section of the methodology, was built into the flat plate to ensure that it was perpendicular to the incoming light rays to achieve maximum flux. Acting as a control under the optimal conditions to collect sunlight, it would give more credence to the results of the experiment.

Figure 14: Adding Tupperware and Angle Supports to the Generation 1 Flat Panel

Following the completion of the weatherization, but prior to allowing the panels to remain outdoors for extended periods of time, the panels were tested to ensure that they were generating comparable amounts of power under direct sunlight. The results of this test can be seen Figures 15 and 16, below. A voltage measurement was taken every second and where the panels read out 0V at the beginning and end datasets is simply an indication of the time it took to connect the data logger after starting them or stop then after finishing the trials. The brief drop to 0V in the middle of the bifacial panel curve shows where the data logger was temporarily disconnected, to indicate that the side facing the sun was switched with the shaded side. This switch was made to ensure that both sides were generating comparable voltages, as only one side could face the sun at one time.

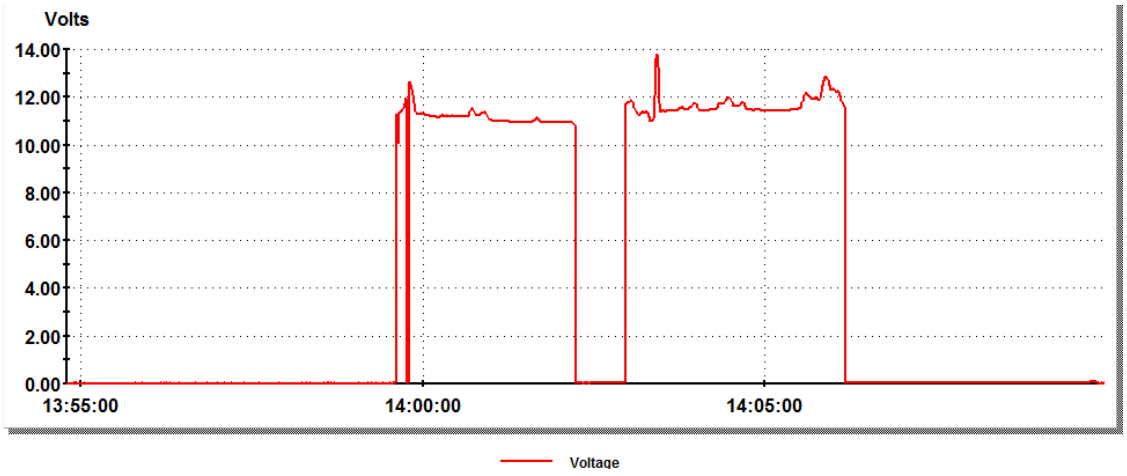

Figure 15: Generation 1 Bifacial Panel Voltage

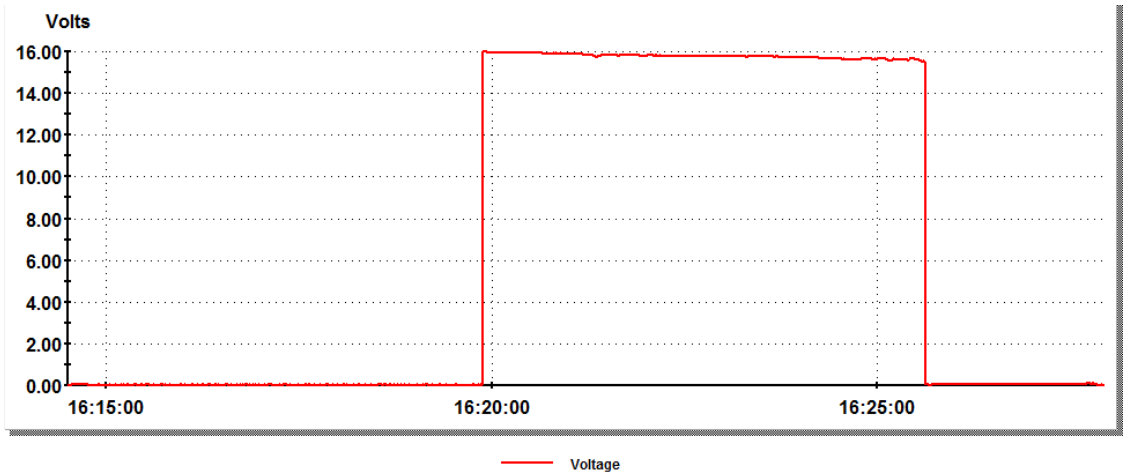

Figure 16: Generation 1 Flat Panel Voltage

There is a consistent difference of four volts between the two panels due to the limitation that only a single side of the bifacial panel could face the sun at a time. The bifacial panel produced more than half the voltage of the flat panel because of ambient light reaching the dark side. Note that for these tests, both panels were tested at the same angle, even though the bifacial panel did not have angle supports (it was manually supported at 66° for the duration of the tests). Additionally, the panels were tested at open circuit, i.e. zero resistance, because the purpose of the test was simply to determine if the panels were working properly. Due to the varying amounts of sunlight received by the two panels (all cells in direct sunlight versus half direct and

have indirect), the voltage would follow a nonlinear curve when at a nonzero resistance, thus making the data much more difficult to interpret.

Once comparability testing was completed, the panels were moved the roof of Glenn L. Martin Hall, our designated testing area discussed in the introduction to the methodology, for weatherizing tests. This particular round of testing was important because of the need to keep solar arrays outside semi-permanently and the propensity for rain in the Maryland area. Almost immediately moisture collected in the panels, fogging the Plexiglas and severely hampering the potential for power generation. Water was leaking through some small openings in the caulk as well as seeping through the wood backing, as seen in Figure 17.

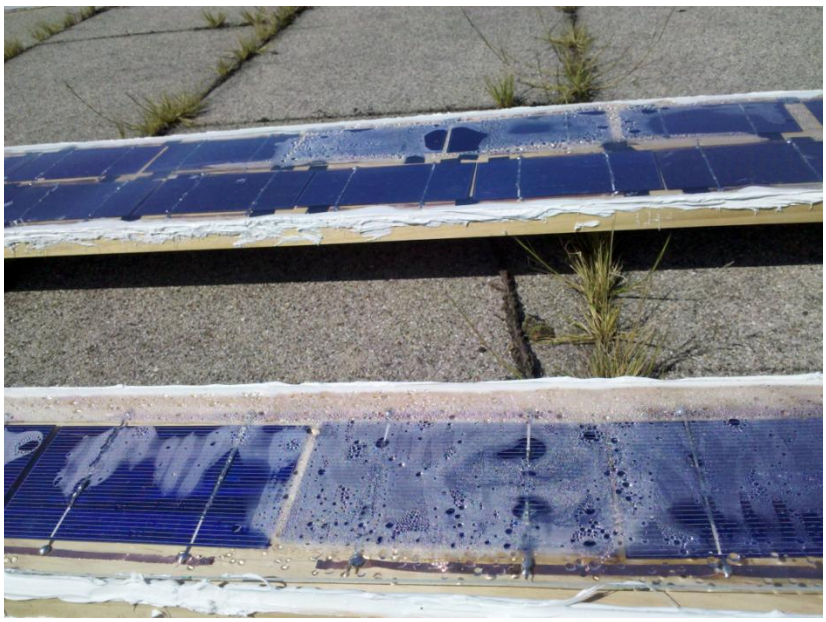

Figure 17: Water Infiltration and Warping in Generation 1 Panels

As the water seeped through the wood, it warped the panels. Unfortunately, due to the panels' low width to length ratio, the moments of inertia were large, so the warping was quite severe. Using the model in Figure 18, the panels' warping, or deflection δ, can be calculated. The deflection of the beam, or panel, can be calculated using equations 3 and 4. Note that a

summary of all the variables in Figure 18 and Equations 3 and 4 is included in Table 3. From equations 3 and 4, it is plain to see that a low width to length ratio will cause a large amount of deflection, or warping.

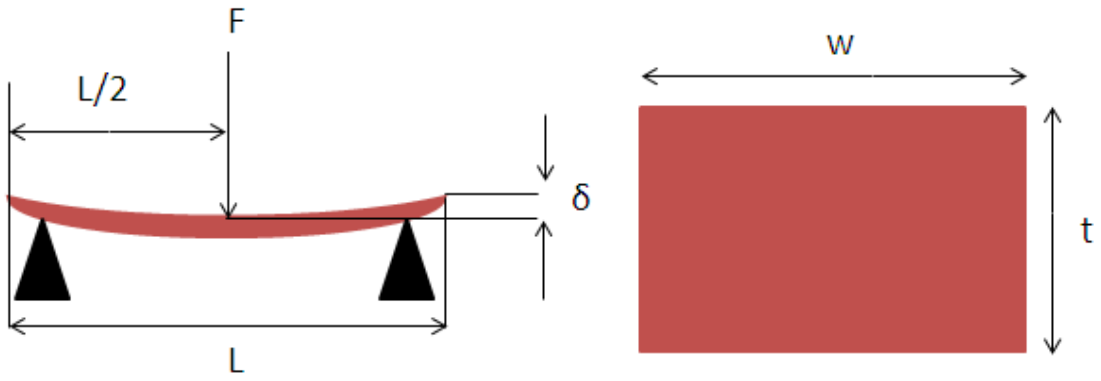

Figure 18: Solar Panel Deflection (left) and Cross-Sectional Area (right)

Variable	Meaning
F	Force on Panel (Weight)
δ	Panel Deflection (Warping)
L	Length
w	Width
t	Thickness
I	Moment of Inertia
E	Young's Modulus

Table 3: Summary of Variables Pertaining to Figure 18

$$\delta = \frac{FL^3}{48EI} \tag{3}$$

$$I = \frac{wt^3}{12} \tag{4}$$

In summary, the first generation of solar panels failed to survive the weather due primarily to material choice. The warping was mainly caused by water saturating the wooden panel backing. Water was able to enter the panels through two different means. First, water was able to condense through the wood, even though it had been protected with a water sealant. The sealant could only make the panel water resistant, thus, in heavy rain, water seeped through. Furthermore, water was able to leak through the silicone caulk sealant that was supposed to insulate the cells by sealing the Plexiglas cover to the wood backing. This sealant was degraded by the weather, resulting in some of the Plexiglas detaching and water leaking in. When hot, sunny weather returned, the water steamed out of the wood, warping it in the process. The dimensions of the solar panels exacerbated the warping because the length was roughly 8 times the width, which led to increased torque.

Solar Panel Construction and Testing: Generation 2

As discussed in the previous section, the initial photovoltaic panel system ran into several problems. The preliminary prototype not only taught the team about how photovoltaic cells work and how to wire solar panels, it uncovered several important facts about weatherization for us as well. To reiterate, the major problems with the first pair of solar panels were warping and leaking.

The goal of Generation 2 was to correct the problems encountered with the first panel and complete testing of the hypothesis. Thus, AZEK Trim, displayed in Figure 19, was chosen to replace the wood. This material is an imitation wood made of compressed PVC, which makes it impervious to moisture (AZEK Building Products, 2011). Moreover, the AZEK planks cost

around the same amount as the wood previously used in the first generation of panels, so did not interfere with the goal of keeping the product affordable. Two new panels, a flat plate and a bifacial panel, were constructed to be half as long as the original panels, only four feet in length.

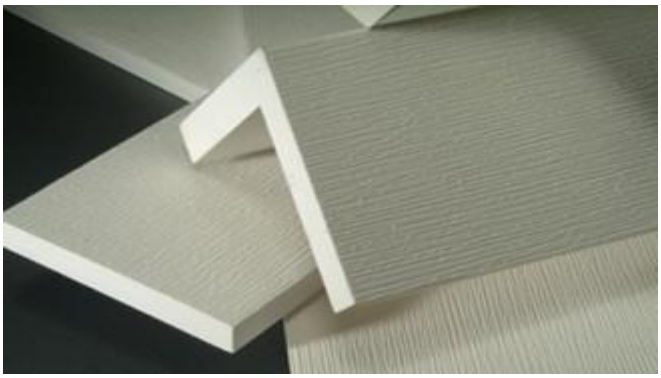

Figure 19: AZEK Trim **("AZEK Trim Styles & Sizes," n.d.) that was used in the second iteration of PV panel** construction

The reason for reducing the size of the panels was threefold. First, it reduced the potential warping by decreasing the moment of inertia of the panels; and second, it made the panels much easier to transport to and from the testing area. Third, the reduced size allowed for a smaller reflector setup, furthering the idea from the hypothesis that this technology can be used on a small scale. To ensure that the entire bifacial panel would be in reflected sunlight for the maximum amount of time throughout the day, the reflector had to be longer than the panel. Thus, shortening the solar panels meant that the reflector length could shrink to 6 feet. To reiterate, with the reflector 6 feet long and the panels 4 feet, there was a 1 foot buffer zone on each end which ensured that as the angle of the sun relative to the reflector shifted throughout the day, the entire solar panel would continue receiving concentrated light throughout the majority of the day. Additionally, the decreased length meant that fewer solar cells were needed—so cells salvaged from the Generation 1 panel could be reused—but also that the system's power output would be diminished.

Another faulty component of the Generation 1 panels was the sealant. The main problem with water leaking into the previous panels through the sealant was that it degraded the panels' power output. Water rusted some of the cell connections, increasing the internal resistance, and fogged the glass, blocking the cells from sunlight. In order to solve these problems, 3M 5200 Marine Adhesive Sealant was chosen to attach the AZEK and the Plexiglas for Generation 2. This caulk is commonly used to plug holes and seal joints in boats and is usable below the waterline ("3M Marine Adhesives and Sealants Product Application Guide and Coverage Charts," 2008). The reason it was not used in the previous generation is because it makes disassembly nearly impossible without destroying the materials that were bonded. Due to the reduced length, modules—as used in Generation 1—were not being used so access to the individual cells for rewiring was no longer necessary. Therefore, the stronger, waterproof sealant was the ideal solution to sealing the cells in between the compressed PVC wood and the Plexiglas.

Before constructing the new panels, the durability of the new materials was tested in new weatherization trial. The preliminary testing began with first creating a small test panel (dimensions: 1.75in x 6in x 12in) with a single PV cell sealed inside. The test panel was completely submerged in water for one week and, at the end of the week, the inside of the panel was completely dry and there was no evident warping. Thus, it was concluded that the new weatherization method worked extremely well, as the panel was able to survive a much harsher environment then it would encounter outside. Subsequently, the new panels were built from the new materials, reusing the PV cells from the original panels due to budget constraints.

This first solar panel was built with two parallel rows of 7 PV cells each (14 cells total) wired in series, as seen in Figure 20. This panel, another flat panel, was constructed in order to

act as a baseline, or control, for the experiment. It would be simply laid out facing the sun and reuse the same triangular supports and optimization (optimized for summer at an angle of 66°), as the original flat panel. This solar panel was necessary to definitively determine whether or not the reflector significantly impacted the power output capabilities of the test panel.

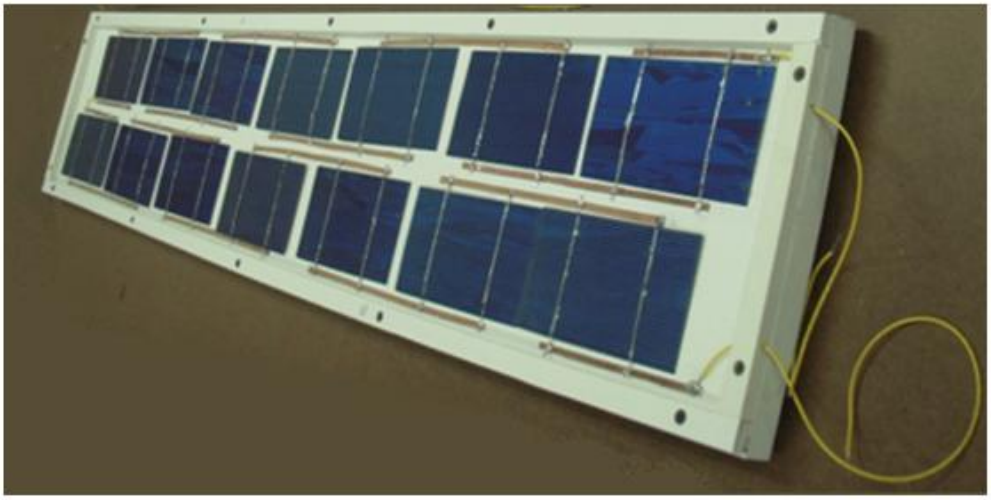

Figure 20: Completed Flat Panel

The flat panel was expected to produce a voltage of approximately 5.6V across a resistance of 3.5Ω around solar noon, for a maximum power of about 9W. The maximum power point of the panel was determined by testing different resistance across the panel and measuring the voltage at solar noon. A graph illustrating the maximum power point is displayed below in Figure 21, with the maximum power point indicated with a data cursor. Note that this data were based on the panel collecting sunlight with no aid from a reflector.

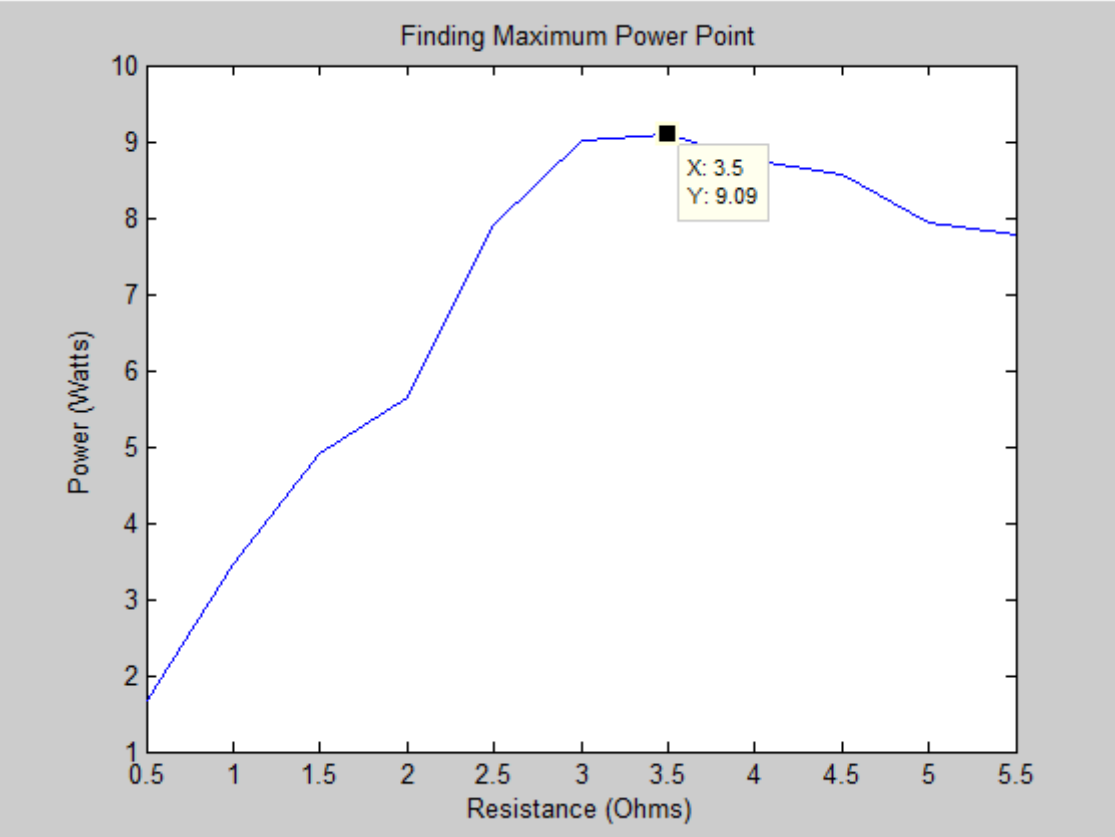

Figure 21: Max Power Test for 14-Cell Panel

The bifacial solar panel, which would be situated in the focal point of the concentrator, was built with two rows of 7 PV cells each (one row on each side) wired in series, for the same total of 14 cells. The panel can be seen under construction in Figure 22. It was not actually possible to test the baseline (no concentrator) power of the panel because one side would always be facing away from the sun This imbalance would lead to a smaller maximum power point than what the cells were actually capable of producing. Additionally, once the panel was sealed in the Plexiglas, it was no longer possible to test each face of the panel individually. However, all the component cells were tested prior to being installed and produced the same voltage and current as the flat panel's cells. Once the panel was complete, it was wired with the same resistance as the flat panel. The panels were wired the same because they had the same number of cells so, in theory, should have the same power output.

Figure 22: Constructing the bifacial solar panel

It should be noted that using the same resistance for the bifacial panel as for the flat panel does create some minor errors. The bifacial panel would actually have a slightly different maximum power point, corresponding to a different optimum resistance, because of the increased incident radiation from the reflectors. In fact, because the concentration ratio from the reflector magnifies any changes in sunlight throughout the day, the optimum resistance would also change, so a variable resistance would have to be used to account for this. However, for consistency, we wanted two identical panels, so we did disregarded this effect. Plus, accounting for it could only increase the power of the bifacial panel because the reflector only would increase the amount of incident radiation. Consequently, accounting for the change in the max power point could only strengthen the case of the reflector. If the bifacial panel still generated significantly more power than the flat panel with an equal resistance, there would be no need to account for a minor variation in the maximum power point. Of course, in a final product, this would need to be considered in order to achieve maximum efficiency and get the maximum power possible out of the system.

The panel would be supported between the two reflectors and get its light mainly from them. Based on the reflector program, with light concentrated on both sides of the panel, this panel was expected to get 11.8 times as much light as the flat panel, as predicted by Dr. Adomaitis's modeling program. This would generate a similar increase in power, but due to efficiency losses when PV cells heat up, we anticipated a lower—but still noticeable—increase in power output of the panel. The cells were on two sides of the panel in single-cell-width rows because the reflector was designed to focus the light across the panel with a width of 3 inches, the width of the cells.

A third panel, seen in Figure 23, was constructed, consisting of a single row of 7 PV cells wired in series. The purpose of this panel was to test the necessity and efficacy of a second concentrator. There was a need for this test because of the possibility that the reflectors would not focus equal amounts of light on the two sides of the bifacial panel. This disparity would lead to a "virtual shading effect", such that the power output of the panel would be limited by the cell with the least sunlight, and thus least current, in the series. Although none of the cells would be shaded, some would be getting markedly less radiation than others and would limit the total power output of the panel. This third panel would fix this potential problem because it would only face one reflector.

Figure 23: Single-sided concentrator panel

This solar panel was wired with half the resistance of the other two because it had half as many PV cells. This correspondence was predicted, but to be sure of its correctness, it was confirmed with another maximum power test at solar noon, the results of which can be seen below in Figure 24. In summary, there was an expected 4.5W from a voltage of 2.8V across a resistance of 1.75Ω. The power of this panel would be doubled in order to compare its efficiency to that of the flat panel and the bifacial panel, both of which had twice as many PV cells. Again, these measurements were based on the panel collecting sunlight with no aid from a reflector, so this does induce a small error as the max power point would change as more current runs through the panel. However, like before, this effect is neglected.

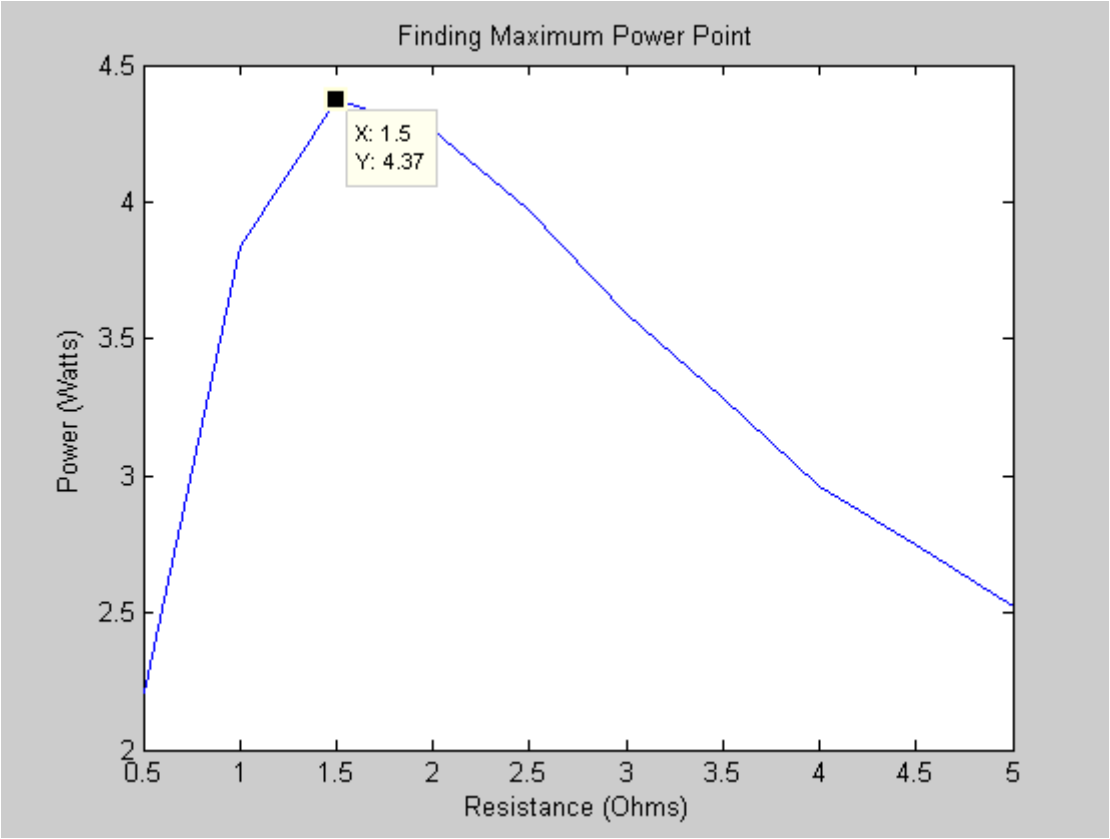

Figure 24: Max Power Test for 7-Cell Panel

Following the resistance testing, the 14-cell flat panel and the bifacial panel were set up on the roof of Glenn L. Martin Hall at solar noon on March 17th, 2011. It was an ideal day for collecting data because the weather was clear. Although the reflector was optimized for summer, it was still possible to collect relevant data with a small adjustment to the height of the bifacial panel to account for the different solar angle. The flat panel was also adjusted slightly to be angled perpendicular to the incident sunlight. The setup of the two panels can be seen in Figure 25, below.

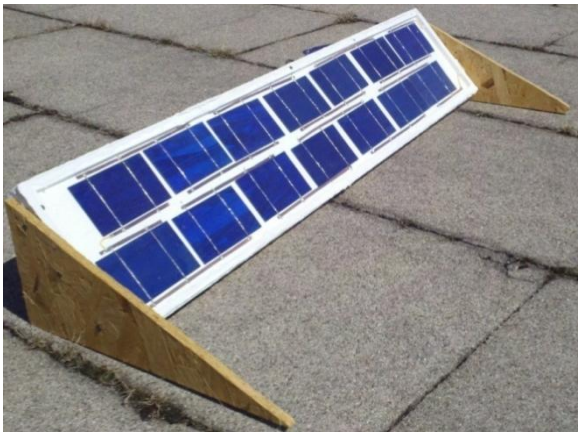

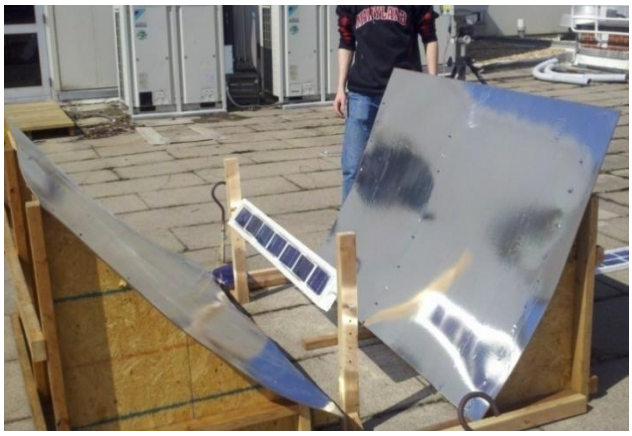

Figure 25: Flat and Bifacial Panel Setup

The flat panel was producing 7.1W of power (5V across 3.5Ω), slightly less than the expected output. However, the bifacial panel was producing even less. After setting up the bifacial panel between the two concentrators, it quickly became apparent that one of the reflectors was not concentrating nearly as much light as the other. This was the reflector with its back to the sun. After measuring the power output of the panels, it became clear that virtual shading was a real problem. The bifacial panel was only producing around 4.6W of power (4V across 3.5Ω), much lower than the expected 9W (5.6V across 3.5Ω)—and lower than the flat panel as well. The bifacial panel did not receive much direct sunlight because it was oriented perpendicular to the ground, not perpendicular to the incident ray of light from the sun. The reflectors were supposed to direct much more radiation at the bifacial panel then it would have

gotten from just directly facing the sun, due to their larger flux (more surface area angled at the sun), but this was not the case. The reflector facing away from the sun was actually directing less light onto the bifacial solar panel than it would have received had it been facing the sun directly. Hence, there was a virtual shading effect on the panel that limited its power output.

When solar cells are shaded, they actually absorb power, decreasing the total power output of the solar panel and releasing heat (Eicker, 2003). This problem, coupled with the increased radiation on the side of the bifacial panel with the reflector that was working properly, caused an unexpectedly high and rapid increase of heat in the circuit. This heat could not convect away because of the nearly airtight weatherization of the cells. The trapped heat built up over the course of a few hours and began to char the solar panel. The backing was not wood, so instead of burning, it melted. The AZEK, essentially compressed PVC, began to bubble out in the areas directly beneath the PV cells on the high concentration side. This pushed the cells outward, thereby breaking the circuit and cracking some cells, as seen in Figure 26. Following this incident, an extensive thermal analysis was completed and further testing using the 7-cell flat panel as a stand in with one reflector was decided against due to the likelihood of further overheating.

Figure 26: Broken circuit connection (left) and charred/melted AZEK (right)

From this unexpected—but nonetheless useful—data, the following conclusions could be made in order to advance to the third generation prototypes. First, use only one reflector: the second reflector did worse than nothing, it actually hurt the power output of the solar panel because of the substantial virtual shading problems it caused. To have a comparable concentration, it would have to be even larger, and it was already the larger of the two reflectors. This would be a waste of materials that could be used to make another single-reflector-single-sided-panel system. It would be only slightly larger than the double-concentrator-bifacial-panel system and use the same amount of materials. Additionally, a single-reflector system avoids the possibility of virtual shading, barring minor inconsistencies in the mirrored surface of the one reflector. Second, the system generates a significant amount of heat. It would be important in the future to get a quantitative measurement of the temperature disparity between the two panels. Also, as described in thermal analysis section, the lack of convection was the major reason for such a high temperature. Thus Generation 3 would be an open-air system (unweatherized for testing purposes) and a future system would need to use materials that can conduct heat away or, ideally, incorporate a thermal energy collection (solar thermal) system to get the maximum amount of energy out of the system as possible. The following section of thermal analysis will explain this in more detail.

Thermal Analysis

When the second generation of solar panels was first set up for data collection under concentrated light, the cells became extremely hot within a few hours. This caused the PVC substrate to melt and begin to bubble up in places, which cracked several of the cells and deformed the Plexiglas covering. In order to plan for future heating problems and avoid overheating on the third generation of cells, a thermal model simulation was created to predict

the maximum temperature reached by the cells under different environmental conditions. A representation of the heat transfer modes can be seen below in Figure 27.

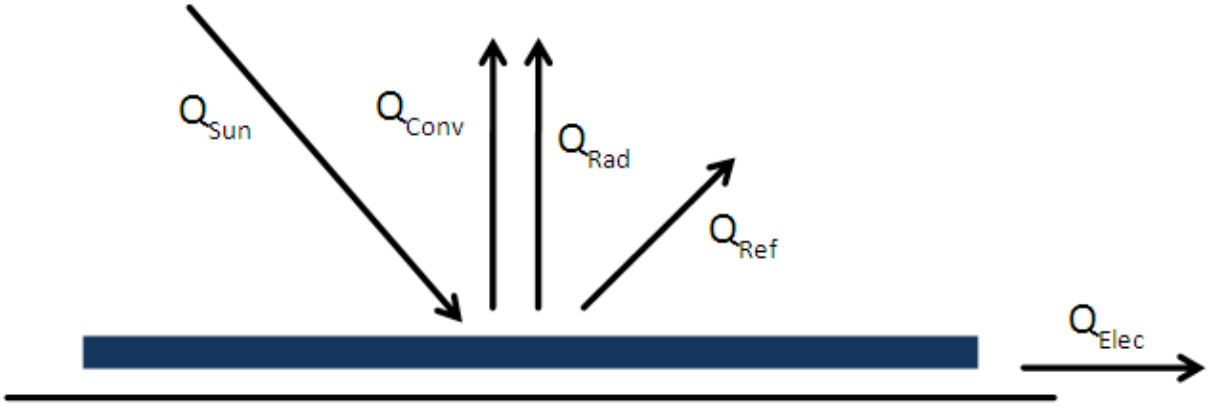

Figure 27: Blue solar cell with heat transfer modes shown by arrows

For the simulation, a lumped capacitance model was used to find the steady state temperature reached by the cells. An energy balance equation was used that included the incoming radiation from the sun, the emitted radiation from the cell, and the heat transfer through convection to the surrounding air. The cells only contacted the substrate at the solder points, so no conduction was assumed at this interface. This results with equation 5:

$$\frac{1}{2}\varepsilon\sigma T_C^4 + hT_C = (1-\eta)\dot{Q}_S + hT_A + \frac{1}{2}\varepsilon\sigma T_{sky}^4 \quad (5)$$

In the above equation, ε represents the emissivity of silicon (0.86) and σ is the Stefan-Boltzmann constant (5.67*10-8 W/m^2K^4). T_C is the temperature of a cell, T_A is the temperature of the surrounding air, and T_{sky} is the background temperature of the sky (assumed to be 273K). The efficiency of the cell, η, was conservatively estimated at 10% for this simulation. $\dot{Q}_S$ is the incoming power per square meter received by the cell from the sun. Although the terms for each mode of heat transfer include area, the area is the same for all components, so the value cancels out. The heat transfer coefficient, h, varies with the difference in temperature between and

object and its surrounding fluid, so its calculation was included in the iterations used to find the steady state temperature. In this case, h was found using equation 6:

$$h = \frac{Nu * k}{L} \tag{6}$$

In equation 2, k is the thermal conductivity of the fluid, which for air is 0.2624 W/mK. L is the height of the flat plate, which is 3 in or 0.0762 m. Nu is the Nusselt number, a dimensionless number that can be found for a flat plate oriented perpendicular to the ground by using equation 7 below:

$$Nu = 0.59 * Ra_L^{\frac{1}{4}} \tag{7}$$

Ra_L is the Rayleigh number, another dimensionless number that can be found using equation 8:

$$Ra_L = gL^3\left(\frac{\Delta T}{\nu \alpha T_A}\right) \tag{8}$$

The Rayleigh number is calculated where g is the acceleration of gravity (9.81 m/s^2), ΔT is the difference in temperature between the cell and the air, ν is the specific viscosity of air ($1.57*10^{-5}$ m^2/s), and α is the thermal diffusivity of air (2.22*10-5 m^2/s).

The solar irradiance at the Earth's surface was approximated as 1000 W/m^2. The concentration factor of the reflectors was estimated by observing the pattern of reflected light on a flat surface to be about 4.5, meaning that about 4500 W/m^2 of solar energy was hitting the cells. A worst case scenario for the ambient temperature of 40˚C (104˚F) was estimated, based on historical weather in Maryland. The simulation assumed only natural convection, though any wind would increase the rate of heat loss due to convection.

The second generation panels used a Plexiglas cover to protect the cells from the environment. However, this cover effectively insulated the cells by separating them from the outside environment. It added a small layer of enclosed, stagnant air between the cells and the

Plexiglas, which virtually eliminated any heat transfer due to convection. Thus, the simulation was run without convection, giving a theoretical maximum temperature of the cells of 370.1˚C. While achieving a temperature this high is unlikely, as there will always be some small amount of convective heat loss through the Plexiglas, it shows why the cells heated so rapidly on the second generation panels.

Next, the simulation was run with convection, removing the sheet of Plexiglas covering the cells. Using these equations to find the steady state temperature of the cells with these parameters returns a temperature of 89.4˚C. This is still above the recommended maximum operating temperature of most silicon cells (85˚C), which would indicate a potential problem. However, the conditions assumed in this simulation (40˚C, 4.5 concentration factor, and no wind) are very unlikely to occur simultaneously for a long period of time. A small reduction in temperature to 35˚C (95˚F), results in a drop of cell temperature to 84.5˚C, below the maximum operating temperature. The estimated concentration factor of 4.5 is also an ideal value. A reduction of concentration factor to 4.0 results in a drop in the temperature of the cell to 84.9˚C, just below the maximum operating temperature. Based on these results, it was determined that using exposed cells in a vertical orientation would be unlikely to cause any heat related issues with the cells. However, for Generation 3, a metal support structure was used to eliminate the chance of melting or significant deformation due to heating.

The final prototype would be open-air, or without the Plexiglas covering, so the cells would lack protection from rain or impact, but are able to be cooled by the outside air. A final product would be constructed in a similar manner as currently produced commercial solar panels with a metal support structure and a glass or Plexiglas cover. This would allow heat to convect away from both sides of the panel while maintaining protection from the elements.

An additional simulation was run to predict the effect of a conductive backing to the cells. With the cells bonded to a metal support structure and exposed to the environment, convection was able to occur on both sides of the panel, further improving its heat transfer properties. With this new parameter, the simulation was run with the concentration factor of 4.5 and an ambient temperature of 40˚C, and the maximum temperature reached by the cells was 73.9˚C. Since this is the worst case scenario, this result was very encouraging and indicated that data collection with this panel setup could proceed. Also, most of the final testing occurred during the Fall and Winter, so the chance of overheating was further reduced.

The thermal analysis revealed some of the problems that led to the overheating and destruction of the second generation panels and provided insights into design changes that would prevent similar problems from occurring on future panels. The results indicate that exposed solar cells in a vertical orientation will be unlikely to overheat under low concentrations such as the ones achieved in this project, especially if they are built into a conductive substrate that is allowed to interact with the outside air. To protect the cells from the elements while preventing overheating, a clear thin layer that contacts the cells will need to be used to allow heat to easily flow from the cells and convect into the outside environment. The other possible method is to use an active cooling system, although this can greatly add to the cost and complexity of a panel. Since the goal of this project is to reduce cost as much as possible, the thin covering would be a more practical long-term solution to the problem.

Solar Panel Construction and Testing: Generation 3

The focus of the project from Generation 2 to Generation 3 shifted from having a market-ready product to a proof-of-concept prototype. In essence, Generation 3 was the culmination of the knowledge gained in the first two sets of solar panels. Although it was somewhat of a

simplification of the first two generations, it did succeed in correcting all the problems of the previous generations, namely warping and heat tolerance, while still keeping costs low. Therefore, the new backing had to be a material that was much more tolerant of heat and resistant to warping then the previous panels.

The new backing for Generation 3 was decided to be galvanized steel beams. The metal would not warp, nor would it have any problems with melting or substantial swelling due to an excess of heat, making our new panels much more resistant to changes in environment than the previous two generations of panels. The backing of each panel was made from two four-foot by one inch metal L-beams. The L-beams were bolted together into two sets of two. Liquid Nails caulk was used to affix the solar cells to the metal backing. The finished product can be seen in Figure 28 below. Two identical solar panels were made in this manner. One panel would be used as the flat panel for the control and the other would be placed in the focal point of our reflector. They could be made with the same construction method because a bifacial panel was no longer being used due to the elimination of the second reflector. As before, the cells were wired in series.

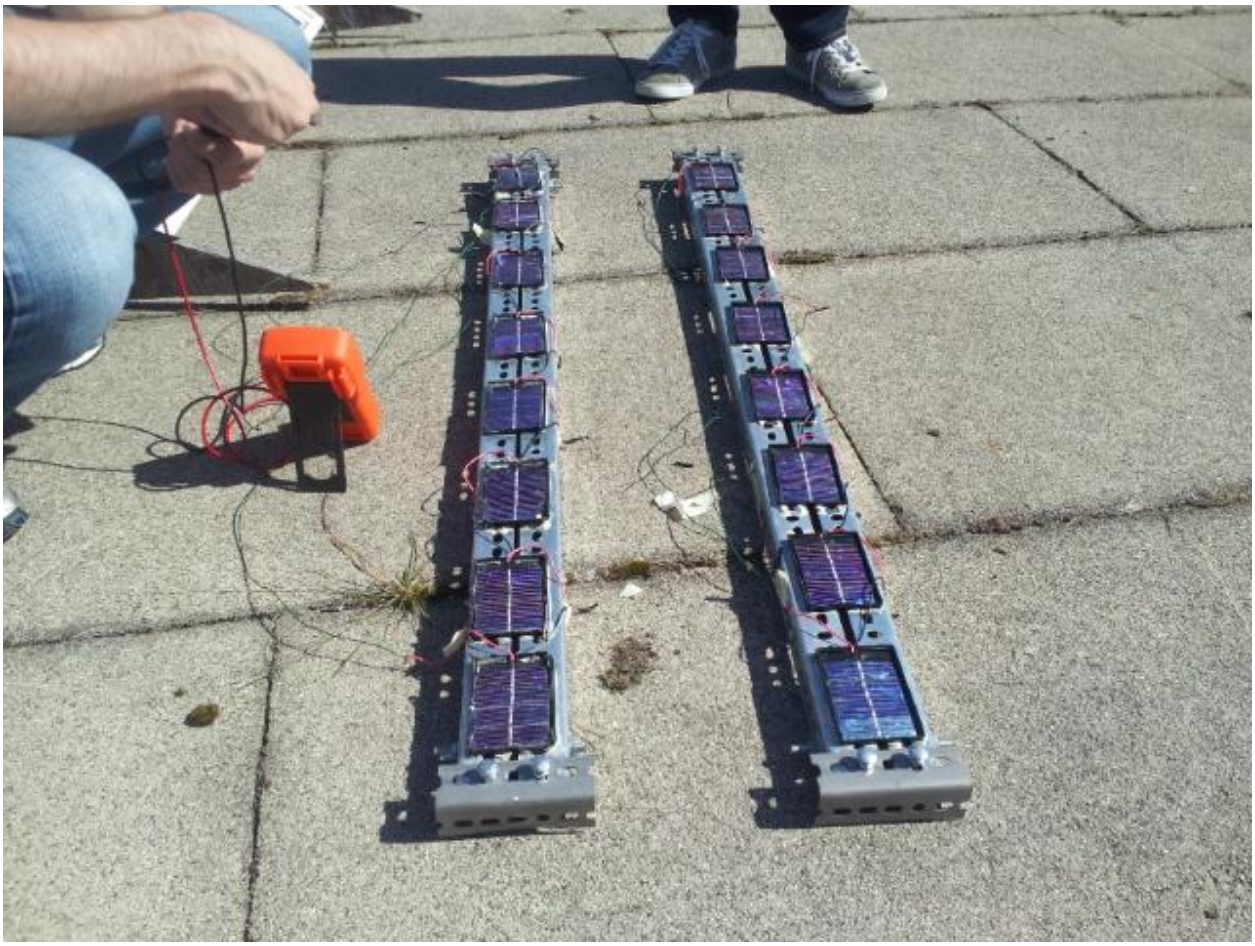

Figure 28: Completed Generation 3 Solar Panels

In addition to the backing, the individual solar cells that were used for Generation 2 had to be replaced as well, since the swelling of the AZEK caused many of them to break. Although the cells were from a different manufacturer than the original ones, they were still polycrystalline cells, for reasons stated previously and for consistency.

Data was collected from both the flat panel and the panel in front of the concentrator for most of the month of July and the first week of August. However, in August, the reflector became damaged during a storm as a result of strong wind. The Masonite backing of the reflector was completely detached from the frame and pieces of wood had been ripped off of the plywood ribs where the screws had failed to hold the hardwood against the plywood. The

reflector was rebuilt by replacing the plywood ribs and the reflective surface (Masonite covered with Mylar).

In addition to damage to the reflector, the solar cells on both the flat panel and the concentrator panel had begun to bulge from heat exposure. This ruined the plastic seal on the cells and allowed water to build up inside. Because of the water, some of the cardboard cell backings dried in a curve, breaking some of the cells and damaging some of them beyond use. To rectify the situation, the clear plastic covering of each individual cell was cut off.

Unfortunately, the damage to the PV cells had reduced the efficiency of some of the cells, making the measured open circuit voltage, and thus potential power output, of the two solar panels significantly different. Some of the severely damaged cells on each panel were limiting the maximum voltage that could be produced by the panel as a whole. After the damaged cells were excised from the panel, the open circuit voltages returned to being almost exactly equal. However, the internal resistance had changed in the cells, so when tested over a resistance, the panels were producing different amounts of power. Further discussion of the results of Generation 3 is included in the Data Analysis section, next.

Data Analysis

Data Collection Overview

Although setbacks in testing prevented the gathering of a large amount of useable data, analysis was still performed on each panel to gain a deeper knowledge of each system. This knowledge can be used to make suggestions on how to analyze future experiments of this nature in addition to drawing conclusions on the potential usefulness of low concentrating systems. This section will detail statistical models used to describe the behavior of the panels, an analysis of how the power output of the panels changes with resistance and with concentration, and a brief thermal analysis to better explain the various obstacles faced during the testing process due to the heat absorbed by the concentrated systems.

The point of these experiments and analyses is to show that a photovoltaic system of this low concentrating scale would be a viable replacement for a flat panel system. In order to support this argument it is necessary to measure the power output of two identical systems where the only variable is the presence, or lack thereof, of the concentrating element. The final iterations of the tested systems are described in the methodology section. Physically, the systems are very similar: the same backing material was used to support each circuit of cells, and the same number of cells was connected on each panel in the same manner. Thus, the only factor to take into account would theoretically be the presence of a concentrating element, and the control system would be set at an angle normal to the sun's rays without concentration.

However, before the systems can be assumed to be identical, there are differences in the electrical properties of each cell that must be taken into account. In order to adjust for these differences, two tests must be done. These will be described as "baseline tests" from here

forward since they provide a basis from which to accurately compare each system. First, voltage must be measured across various resistances for each panel to calculate the current flowing through each system at those voltages. These tests are used to create plots of current vs. voltage that can be compared to theoretical models produced by the diode equation. Analyzing the similarity of the data produced by the systems to these theoretical models provides a solid knowledge of the behavior of the cells without concentration.

The second test compares the voltage output across various resistances with and without a concentrating element. In order to generate these data, the load resistance must be chosen in order to maximize the power each panel produces when it is under concentration. This value will most likely be different than the value that maximizes power output for a flat panel. With both of these tests completed, sufficient knowledge will be known about the systems to make substantial claims about their performance under concentration.

The primary data collection method, after completion of the baseline tests, was measuring the voltage of the optimized systems. This was done through the use of data loggers connected in series with the circuit. The loggers would be set to take voltage measurements at specified time intervals over a desired number of days. The voltage data collected then would be converted to power using Ohm's law

$$V = IR \tag{9}$$

and after the knowledge gained from the baseline data analysis was applied, significant claims could finally be made about the efficacy a low concentrating PV array.

Preliminary Data Gathered

While several attempts were made to gather data, the various setbacks encountered prevented the collection of enough useable data to support our primary hypothesis. The results of

the four main data collection periods are summarized in Table 4 below. Over the first two data collection periods, the lack of baseline tests resulted in an inability to discern the significance of the results. The results of the latter two data collection periods did not provide support in favor of the hypothesis. However, through each of these setbacks, a more refined approach has been created to account for and move past the obstacles described as follows.

Table 4: Primary Data Collection Problems

Dates	Resistance Used	Baseline Tests?	Quality	Useable to prove our hypothesis?
July 2011 (13 days) 7/13-7/17 7/19-7/27	60 Ω each	No	Good: Significant power difference in favor of hypothesis.	Weakly
August 2011 (3 days)	60 Ω each	No	Bad: Hurricane ruined setup.	No
November 2011 (4 days) 11/17-11/21	150 Ω each	Yes	Bad: Very little power difference.	No
Winter 2011-2012 (9 days) 12/10-12/14 1/12-1/17	150 Ω each	Yes	Bad: Very little power difference.	No

Summer Setbacks

Without the presence of baseline tests, any analysis of voltage data that is gathered is not sufficient to support low concentrating CPV. If the basic properties of the systems being tested are not understood, it is impossible to say with 100% certainty that the difference in power output of the two systems is due solely to concentration. As a result, no matter how promising the data looks, it is not enough to prove our hypothesis by itself.

That being said, data collected over the summer certainly encouraged further research into this area of low concentrating PV. Although the data collected in August was unusable due to weather destroying the reflectors, the results from the tests done during July show a significant increase in power of the system under concentration compared to the flat system. Although detailed analysis is not worthwhile without baseline information, viewing the power disparity leads to some interesting conclusions. The summarized data is shown in Figure 29 below. Examples of the output of the data logger's voltage data from this experiment can be found in the appendix.

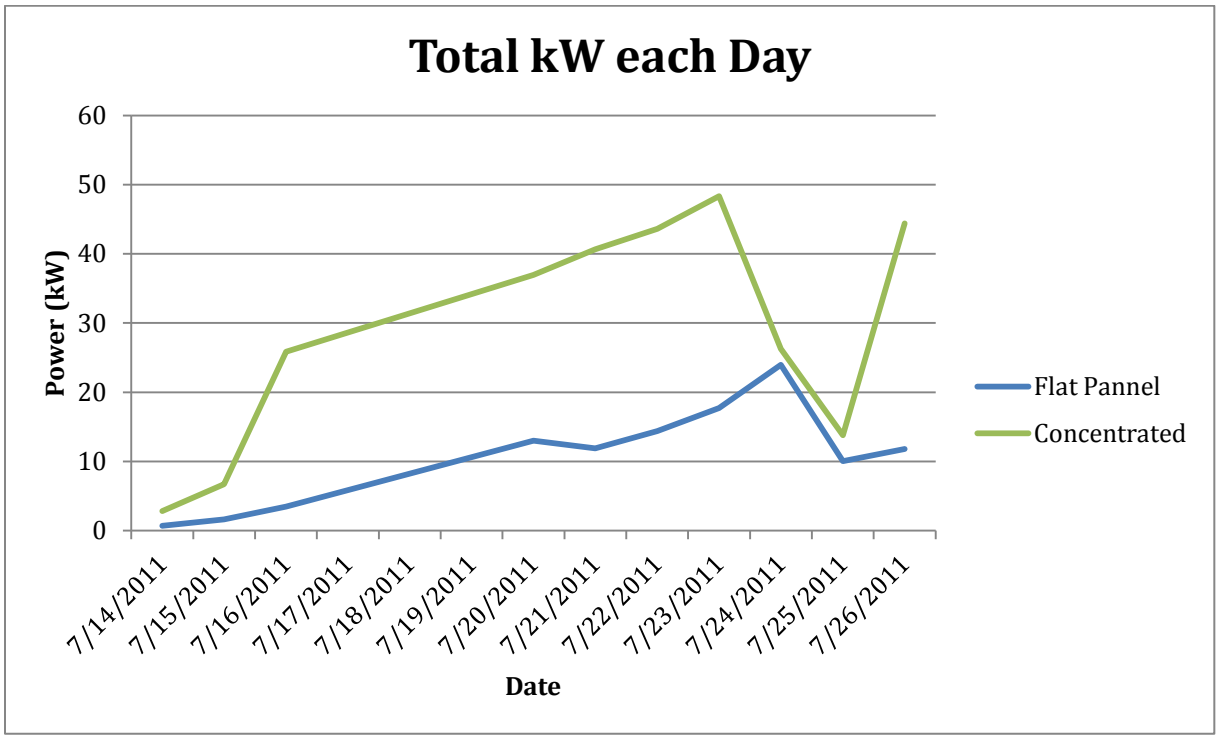

Figure 29: Summer 2011 Data

The data are intriguing for two main reasons. First, it can be seen that the concentrated panel consistently produces more power than the flat panel. As stated above, although no baseline data can confirm exactly how much is due to concentration, this provides reason enough to continue collecting more data. However, it is worth noting that the concentrated panel on average

produced more than three times the power output of the flat panel and even maxed out at seven times the power output on July 16, 2012.

The second part of this analysis is to note that the power difference between the concentrating and non-concentrating systems is not constant. This can be explained by looking back at the weather on different days. A full list of the weather conditions on this day can be found in Appedix 3. For the majority of these days, the sky was completely clear. However, between 7/24 and 7/25, there was a large amount of cloud coverage which significantly decreases the direct insolation from the sun. Without direct insolation, the concentrator is mostly ineffective, so the panels are essentially exposed to the same amount of indirect sunlight, hence yielding very similar power outputs. This is a problem that solar technology faces in general, but it is consistent with the systems that have been set up for this testing, thus adding some validity to the legitimacy of the data.

Winter Setbacks

After the weather complications in August 2011, it was decided that the status of the panels needed to be analyzed in greater detail then had been done in the past. Thus rudimentary baseline tests were done for each panel to quantify their power performance at various resistances. The results of this are shown in Figure 30.

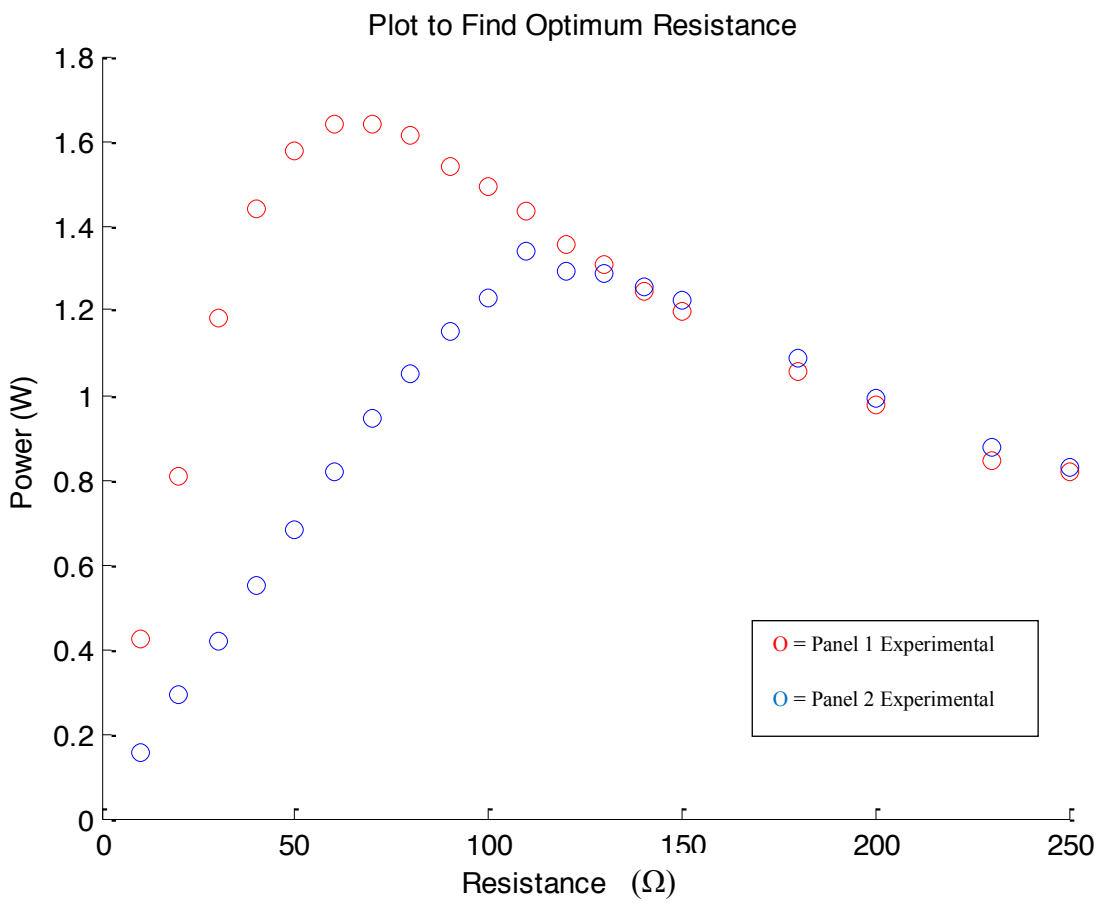

Figure 30: Power vs. Resistance without Concentration

It was seen that the panels behaved very differently at lower resistances. Although it was uncertain whether this was a result of weathering issues or simply differences between the properties of the cells themselves, it was clear that the knowledge gained from these baseline tests would need to be applied in later analysis of data. In order to avoid having to scale the data significantly later, a resistance was chosen where the systems provided the same voltage output (150 Ω as listed in Table 4 above).

This resistance was then used to take more experimental data comparing the concentrated panel to the flat panel. Unfortunately, the data gathered during the winter is not worth illustrating graphically since the outputs between the concentrating and flat panels were nearly identical.

This was initially disheartening, but it did give new light to a better approach to data collection in the future. The only difference between tests from the summer to these rounds of testing was the change in the resistance applied to each panel. However, when choosing the supposed ideal resistance for the comparison, while the panels behaved similarly at higher resistances, the panels' performance under concentration was not taken into account. Tests were done on a single panel to see if perhaps at higher resistances, the effect of concentration decreased. These results are shown in Figure 31.

These data gave new light to the physical behavior of the systems under concentration. The logical reasoning behind the nearly identical voltage outputs of each system is that at higher resistances, the panel will go towards open circuit conditions as seen by the data in Figure 32. Ohm's law shows that as voltage increases at a constant resistance, current will decrease. At a high resistance, the systems start off close to open circuit voltage and under concentration, the will reach open circuit voltage quickly. This means that after a certain amount of concentration, the voltage will reach a maximum. Because it is at the same resistance as the concentrated panel, when the flat panel reaches open circuit voltage, then there is no difference between maximum power values. This was found to be the case during the winter. It became evident from the data found in Figure 31 that in order to optimize power output of the concentrated system, a lower resistance needs to be used than the non-concentrated system. For new panels and future tests, these new optimal values would have to be calculated.

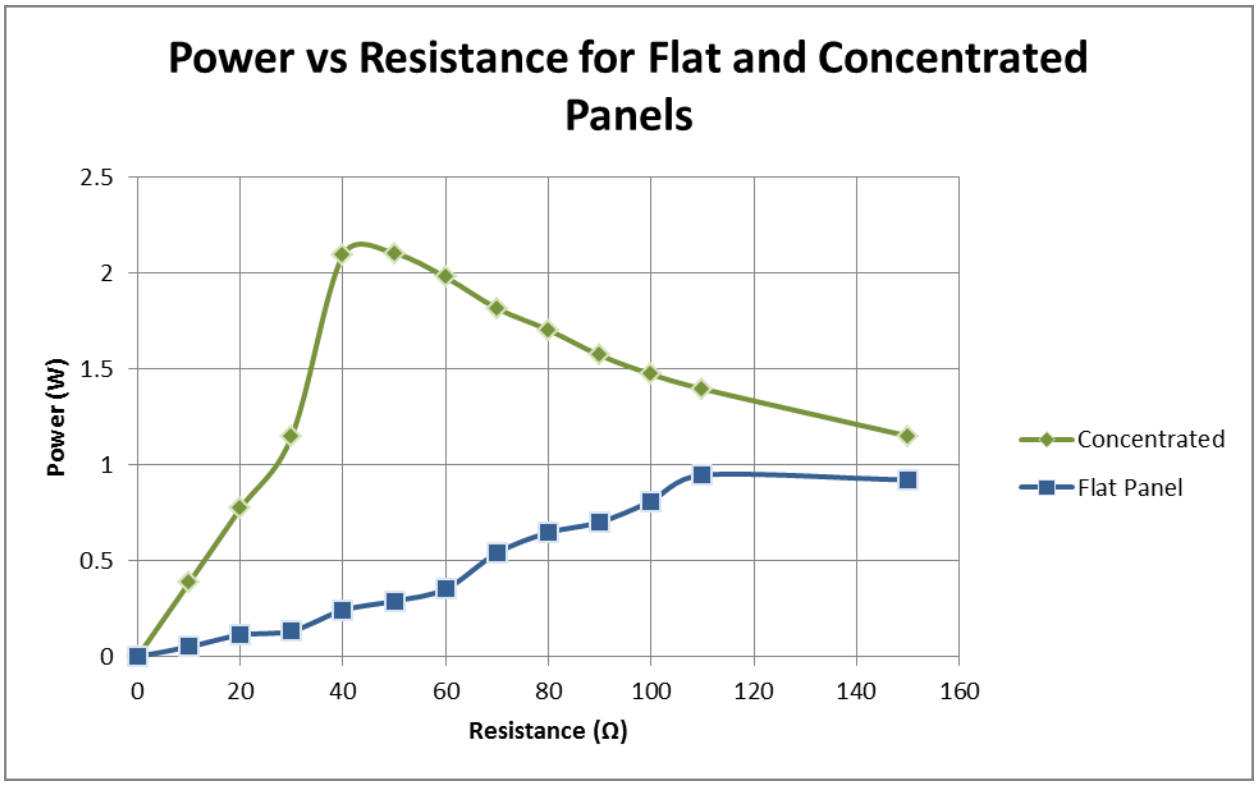

Figure 31: Panel Behavior With and Without Concentration

Conclusion

After all of the setbacks that the team faced with the cells that made up the experimental setup, reliable panels were finally fabricated to be analyzed in the beginning of February 2012. The complications with previous attempts at data collection laid out a rigorous method for analyzing the data that would be obtained from these panels. In this section, various elements have been discussed that are essentially rudimentary baseline data analysis, but when analyzing the systems that provided the primary data supporting low CPV, the following sections will describe all analysis in detail.

Baseline Test Data Analysis

Basic Behavior of Cells.

The key to understanding the basic properties of each panel is to treat each panel wired in series as an individual cell and to analyze that cell using the diode equation.

$$I_{ex} = I_{ph} + I_o\left(1 - \exp\left(\frac{qV_{ex}/N}{k\beta T}\right)\right) \quad (10)$$

I_{ph} is the current produced when the cell is exposed to light, or the photocurrent, I_o is a constant that describes the behavior of the cell without light, or the dark current, q is the elementary charge constant, V_{ex} is the external voltage drop, N is the number of cells wired in series, k is Boltzmann's constant, and T is the ambient temperature. β is a constant that takes into account deviations from ideality. To compare the data gathered to the 'ideal' system, it is initially defined as $\beta = 1$.

An example of the graph plotting the voltage measured over an external resistance during the baseline tests is shown in Figure 32. Again, it can be seen that there is disparity between the behaviors of the two panels at lower resistances. The main reason for the difference is most likely the wiring between the cells. If imperfect, the soldering and connections could provide an increased resistance, thus causing a voltage spike. However, choosing a higher resistance will decrease the efficacy of concentration, as discussed earlier. Thus when analyzing the relative performances of one of the panels when concentrated, the voltage and power measurements will have to be compared relative to its respective non-concentrated experimental data.

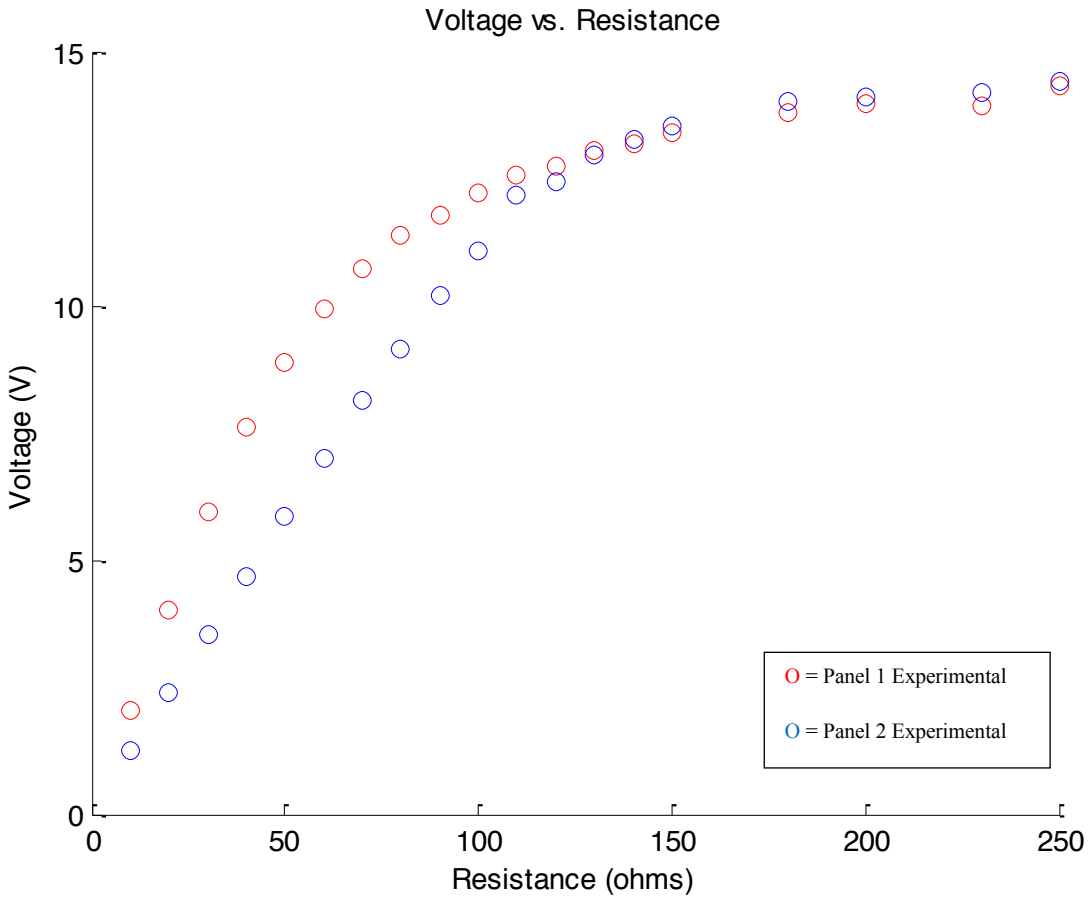

Figure 32: Voltage vs. Resistance Data

From here, the voltage and resistance data can be converted to current by Ohm's law.

$$V = IR \quad \rightarrow \quad I = \frac{V}{R} \tag{3}$$

The calculated current can then be plotted against voltage, as displayed by the data of Figure 33.

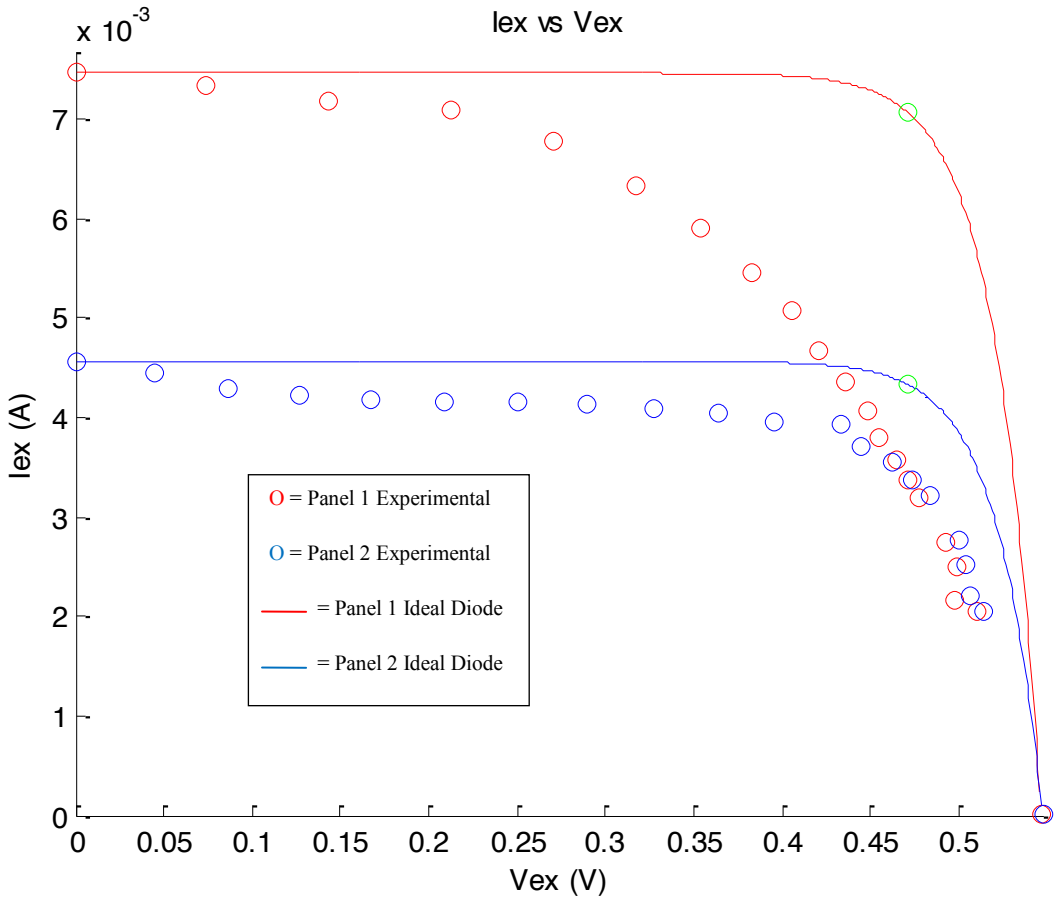

Figure 33: Current vs. Voltage – Experimental and Ideal

Now to see how the panels compare to the ideal circuit described by the diode equation, the variables I_{ph} and I_o must be determined.

When $V_{ex} = 0$, it is seen that I_{ex} is at a maximum. This is the short circuit current (I_{sc}). Because the current measured is the external current, it can be assumed that in an ideal system where the entire panel is treated as a single cell, this would be graphed by the diode equation. Thus, both for the experimental data and for the ideal diode equation, when V_{ex} goes to zero,

$$I_{ex} = I_{ph} = I_{sc} \tag{11}$$

So for the purposes of this analysis, the diode equation can be written as

$$I_{ex} = I_{sc} + I_o\left(1 - \exp\left(\frac{qV_{ex}/N}{k\beta T}\right)\right) \quad (12)$$

For each of the system, I_{sc} can be estimated by extending the experimental data to V_{ex}=0. When this is done, each panel is seen to have I_{sc} values of

$$I^1_{sc} = .0075 \text{ A}$$

$$I^2_{sc} = .0046 \text{ A}$$

where the superscripts 1 and 2 correspond to panel one and panel two respectively.

The dark saturation current (I_o) for each panel can easily be calculated by setting the diode equation equal to $I_{ex} = 0$. At this value, $V_{ex} = V_{open\ circuit} = V_{oc}$. Knowing that the open circuit voltages for panel one and panel two are 15.25 and 15.29 V respectively and the number of cells N = 28 for each, I_o can be calculated for each panel as

$$I^1_o = 4.23 \times 10^{-12} \text{ A}$$

$$I^2_o = 2.50 \times 10^{-12} \text{ A}$$

Because q, k, and T are known, the diode equation can finally be plotted against the experimental data as shown by the solid lines in Figure 33.

Series and Shunt Resistances. Resulting plots from above show that experimental data are far from the ideal curves. In general the most likely reason for the inconsistency with ideal behavior is series and shunt resistances, R_s and R_{sh}, respectively within the panel. The diode equation for panels with series and shunt resistances becomes

$$I_{ex} = I_{sc} + I_o\left(1 - \exp\left(q\frac{V_{ex}/N + I_{ex}R_s}{k\beta T}\right)\right) - \frac{V_{ex}/N + I_{ex}R_s}{R_{sh}} \quad (13)$$

Rigorously finding the values of the series and shunt resistances for each panel involves a fairly complex nonlinear regression procedure that is beyond the scope of this thesis. Instead the values will be determined by estimating different values of each term and defining a new diode equation that incorporates these internal resistances, a curve can be defined that is a very close fit to the data.

For each panel, values of beta, R_s, and R_{sh} were estimated to find a curve with the best fit. The values that yielded graphs closest to the curves with this procedure were the following.

$Beta^1 = 2$	$R^1_s = .0001\ \Omega$	$R^1_{sh} = 220\ \Omega$
$Beta^2 = 1$	$R^2_s = 1.9\ \Omega$	$R^2_{sh} = 650\ \Omega$

The improved diode equation including these new values for panel one and panel two are shown in magenta and cyan respectively below.

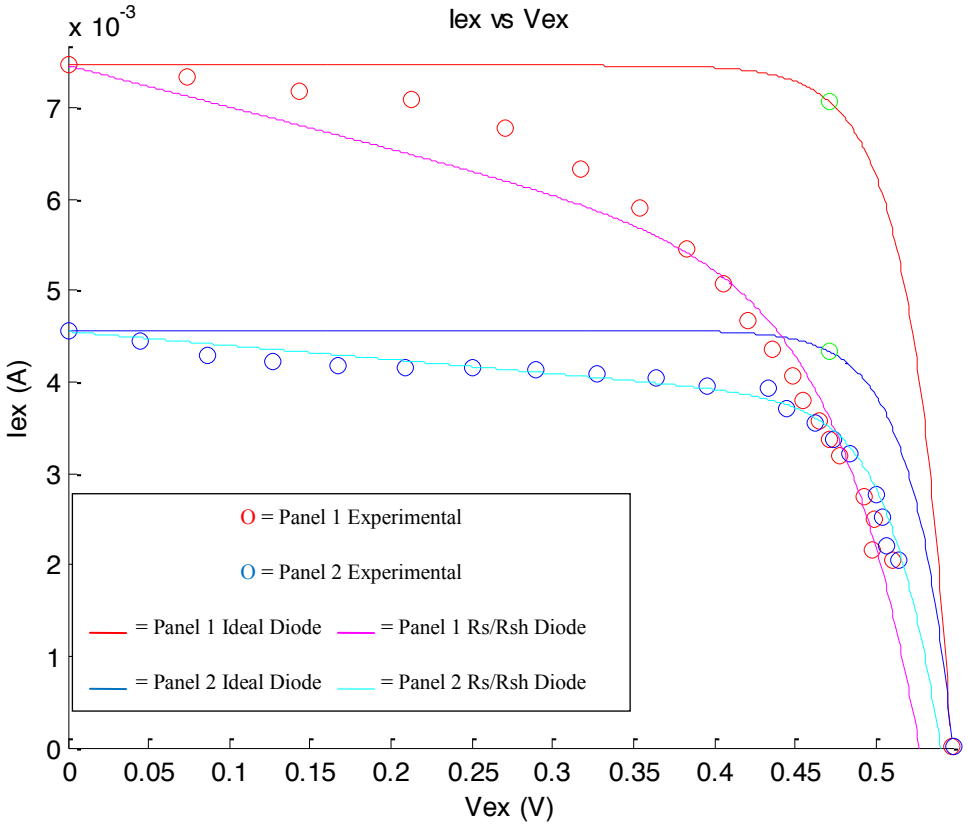

Figure 34: Diode Equation with Series and Shunt Resistances – Current vs. Voltage

Further analysis using Ohms law can provide the graph of power versus voltage since

$$P = IV \tag{14}$$

This graph is shown below, with panel one shown in magenta and panel two shown in cyan.

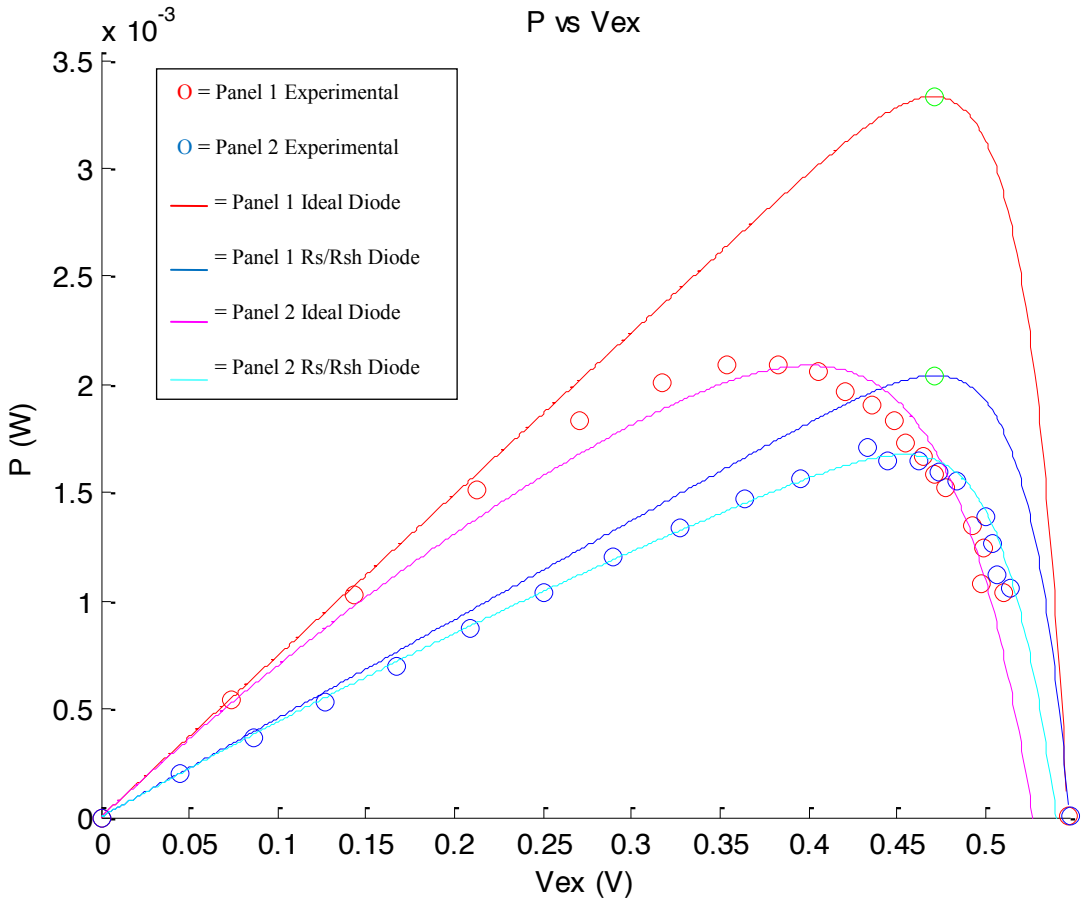

Figure 35: Diode Equation with Series and Shunt Resistances – Power vs. Voltage

This analysis is neither ideal nor precise enough to create a perfectly fitting curve for panel one, but luckily panel two can be quantified a little more precisely. Nonetheless, by doing this analysis for each panel, a more thorough understanding of the properties of each system and the reasons for the deviation from ideality has been gained. With this knowledge, data gathered from whichever panel is concentrated can be compared to these curves to see how much of an effect concentration has on the systems.

Flat Panel vs. Concentrated Panel Data Analysis

The data loggers record the amount of voltage produced by each system over a given amount of time. In order to take that data and draw useful conclusions from it, the voltage data must be converted to a measure of power by the relationship in the equation below.

$$P = IV = \frac{V}{R}V = \frac{V^2}{R}P = IV \tag{15}$$

Where P is power and I is the current running through the system which, according to Ohm's law is equivalent to voltage (V) divided by resistance. Thus, the voltage output measured by the system can easily be converted to power output by simple integration and unit conversion techniques.

The data from the data logger was recorded and analyzed in a manner shown in the chart below showing data taken during the summer.

Table 5: Sample Data Analysis from Summer 2011

Time	Voltage (V)	V^2	Integration
13/07/2011 14:22:06	1.3	1.69	16.9
13/07/2011 14:22:16	1.55	2.4025	20.4625
13/07/2011 14:22:26	1.6	2.56	24.8125
13/07/2011 14:22:36	1.6	2.56	25.6
13/07/2011 14:22:46	1.65	2.7225	26.4125
13/07/2011 14:22:56	1.55	2.4025	25.625
13/07/2011 14:23:06	1.5	2.25	23.2625
13/07/2011 14:23:16	1.45	2.1025	21.7625
13/07/2011 14:23:26	1.5	2.25	21.7625

The units of the integral are V^2s because the heights of the trapezoid have the units of V^2 and the length is measured in time. It is calculated by using numerical integration through a simple trapezoidal rule given by the following formula.

$$Area\ under\ curve = \frac{V^2(t1) + V^2(t2)}{2} * (t2 - t1) \tag{16}$$

To convert this to power, it must be divided by the known resistance of each system as seen in equation 1. Doing this yields the units W·s which can then be divided by 3600 s/hr to yield the desired units W·hr.

All of the data for both systems will be analyzed using the trapezoidal rule (equation 16) and the subsequent methods listed above. As data comes in that is useable, it will be analyzed in this way to produce a graph comparable to Figure 31.

Concentrating Diode Equation. The last element of analysis needed for full understanding of the efficacy of concentration is to create a model to analyze the effect of concentration. The only part of the diode equation that is affected by light being present is the value of the photocurrent (I_{ph}). When concentration is taken into account, it is possible to quantify exactly how much extra sunlight is being focused onto the cells by multiplying the photocurrent by a concentration constant "X."

$$I_{ex} = \boldsymbol{X} * I_{ph} + I_o\left(1 - \exp\left(q\frac{V_{ex}/_N + I_{ex}R_s}{k\beta T}\right)\right) - \frac{V_{ex}/_N + I_{ex}R_s}{R_{sh}} \quad (17)$$

When data are collected, a graph of power versus time can be created. Because of the baseline analysis done previously, a model can be developed for any theoretical concentration constant "X." When the model matches the experimental data gathered, X can be calculated and a solid estimate on just how effective low concentrating systems can be. This combined with the comparative power outputs between concentrated and flat systems will hopefully give a solid foundation to build a framework for future research in the low scale CPV field.

Final Testing Problems

Ultimately, when data was collected in an attempt to compare the concentrated system to the flat panel, complications arose due to the cells overheating. Specifically, during the final weeks of resistance testing, a severe drop in voltage output was viewed when the panels were placed in the concentrated region in front of the reflector. Thermocouples were used to see if this was a result of heating issues and sure enough the concentrated cells were reaching temperatures upwards of 210 °F. Because of the inability of the backing of the system to dissipate heat sufficiently quickly, a more active cooling system would need to be implemented. This would require a more expensive and complicated design than the project originally intended. Ultimately, the data collection was stopped, and it was necessary to perform a thermal and concentration analysis on the system.

Concentration Ratio. Concentration ratio is a value inherent to the system that represents the amount of sunlight that is reflected onto the cells given a specific certain reflector. It is calculated in units of "suns," a unit that represents the amount of ambient sunlight that naturally falls on a surface. Put simply, a flat panel can only have a concentration ratio of one sun because it is only exposed to the ambient light it is exposed to. If a reflector was used in combination with this panel and concentrated twice as much light onto the cells, the system would have a concentration ratio of two suns. This ratio is equivalent to the variable "X" in the concentrated diode equation and can be estimated by a simple experiment on any day of the year at solar noon.

The ratio for the system tested for this thesis was calculated in the Fall of 2010 as a simple experiment to estimate how well the reflector was performing. The ratio is calculated by equation 18

$$Concentration\ Ratio\ (CR) = \frac{Optical\ Length\ (L)}{Solar\ Cell\ Length\ (L_c).} \quad (18)$$

The length of the solar cells is more accurately the length of the most concentrated band of light that results when the reflector is used. The optical length is essentially the 'length' of sunlight that is being concentrated onto this solar cell length. To help simplify the visualization of the optical length and the physical significance behind this calculation, see Figure 36 below.

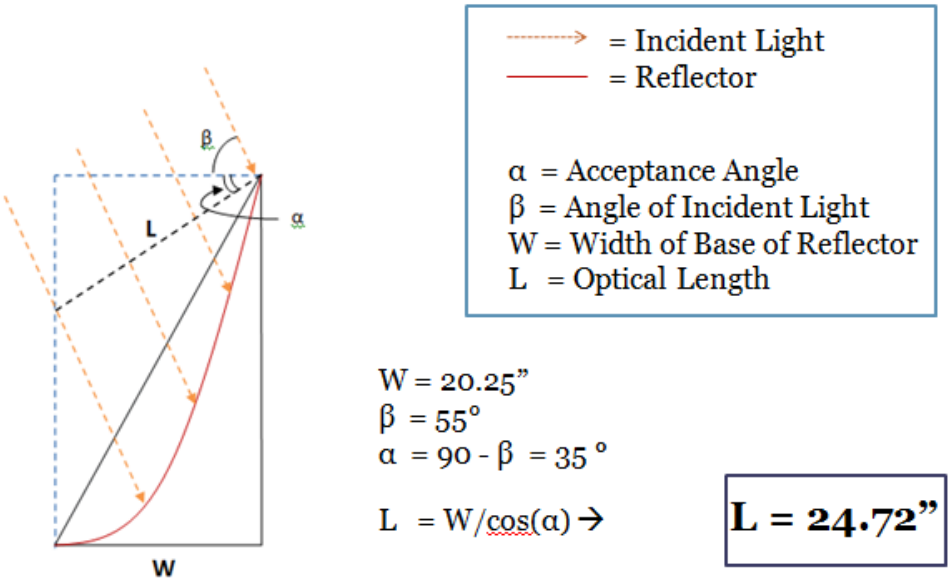

Figure 36: Calculation of Optical Length

Thus, since the dimensions of the reflector are known, calculating the ratio is just a matter of trigonometry, but first it is necessary to define two final terms – the angle of incident light and the acceptance angle. The angle of incident light is the angle at which the sun shines down on the system, and it is measured from the horizontal. It is calculated by equation 19 (Wenham, et al., 2006, p. 23).

$$\beta\ (angle\ of\ incident\ light) = 90 - (\theta_E(t) + \theta_{Lat}) \quad 19$$

where θ_{Lat} is the latitude of College Park, Maryland (38.88°), and $\theta_E(t)$ is the tilt of the equator on a given day. This value is calculated by equation 20.

$$\theta_E(t) = 23.44° \cos\left(\frac{2\pi t}{365}\right) \quad (20)$$

The variable 't' is the number of the days from the winter solstice. Thus, β can be calculated for any given day of the year. For the day this calculation was made, it was calculated as β = 55° as seen in Figure 36.

Physically speaking, the acceptance angle is the angle that light must hit a reflector in order for it to effectively concentrate light onto a point. Theoretically, anything higher or lower than that angle would cause the light to miss the point of concentration entirely. The acceptance angle for the system tested in these experiments was technically a range of angles since the reflector was designed to concentrate light over an area. For the purpose of this analysis though, this value, as can be seen in Figure 36, is geometrically the complement of the angle of incident light and can easily be calculated by trigonometric relationships. Consequently, the optical length was calculated to be

$$\text{Optical Length} = 24.72"$$

The other value needed to calculate the concentration ratio is the 'solar cell length' or the length of the concentrated region of light resulting from the use of the reflector. This is much easier to obtain and is found by holding a board perpendicular to the reflector and measuring the region with a ruler as displayed in Figure 37.

Figure 37: Measurement of Theoretical "Solar Cell Length"

Because varying the position of such a large board greatly affected the concentration band in addition to where it was located horizontally along the panel, only a rough estimate of this region could be obtained. After several measurements were collected, the theoretical 'solar cell length' was found to be

$$\text{Solar Cell Length} = 5.5".$$

Thus, given equation 18, the concentration ratio for this system was calculated to be

$$\text{Concentration Ratio} = 4.5 \text{ suns}$$

Figure 2 shows that the theoretical maximum concentration ratio for a reflector designed exactly with the intended dimensions was 11.8 suns. Although 4.5 suns is obviously less than ideality, for an imperfect reflector, this was an exciting number to calculate and certainly adds validity to future research into low-scale concentrated photovoltaics. It is important to note that given the computer program developed to retrospectively analyze any reflector given its dimensions, a more accurate theoretical solar cell length could be achieved for the system, and a more rigorous concentration ratio could be defined.

Thermal Analysis. As discussed earlier, heat absorbed by the concentrated systems caused some complications in the design of the experimental panels and ultimately proved the system incapable of operating efficiently under certain seasonal conditions. At high temperatures, the open circuit voltage of the system and consequently the power output of the panels (Wenham, et al., 2006, p. 50). Although a full thermal analysis is not necessary for the purpose of proving low concentrating PV system, the obvious heat that resulted from concentration on the panels warranted some further investigation. A simple temperature comparison was done by connecting thermocouples across a cell on each panel. This thermocouple took temperature measurements in Fahrenheit over specified time intervals from December 10 to December 14. The result of this test is displayed in Figure 38 below. Examples of the output of the thermocouple's temperature data from this experiment can be found in the appendix.

The implications of this data are very intriguing. At points, the concentrated panel is twice the temperature of the flat. This speaks even further to the efficacy of the concentrated solar power. Although the systems being tested were only set to utilize the light from the sun through photovoltaic energy conversion, the heat radiating from the sun could theoretically be harnessed through the use of a water tube or some other method. This leads to future applications of low concentrating systems that could include a PV and solar thermal hybrid energy collecting system.

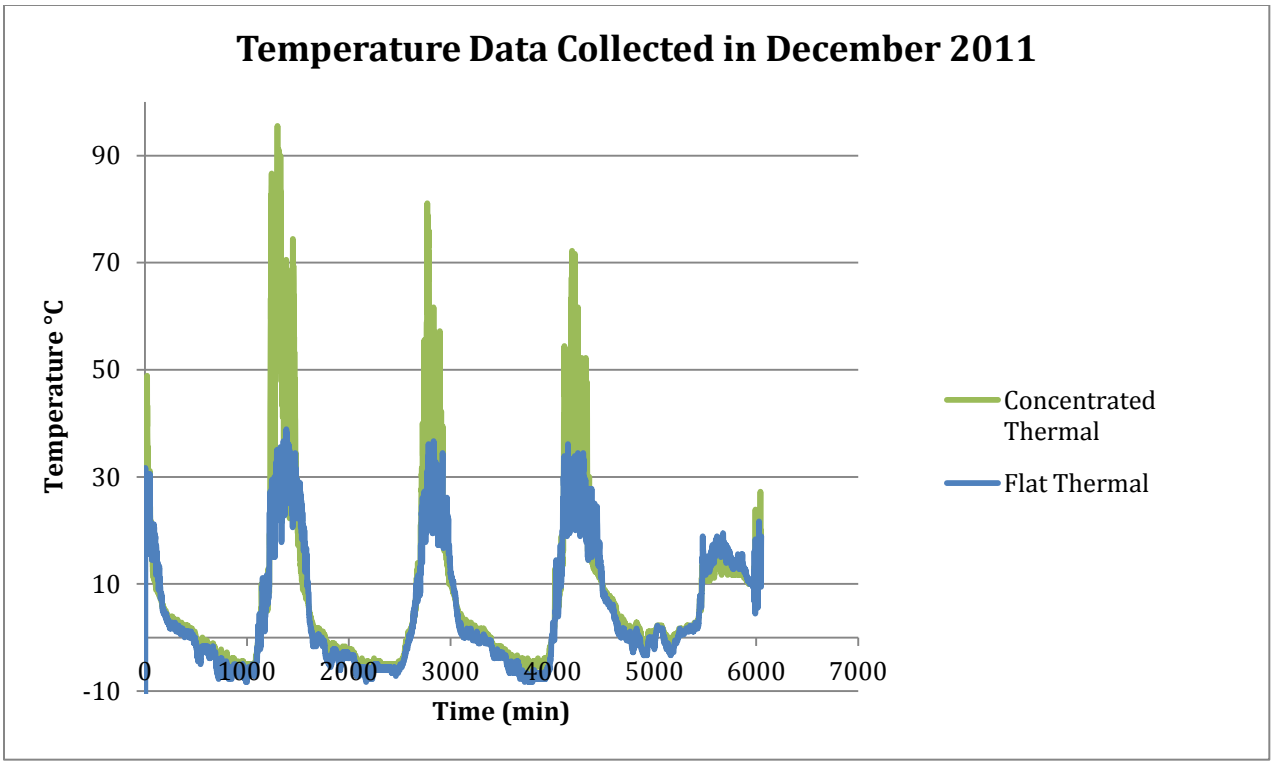

Figure 38: Temperature Data from 12/10/11 - 13:31 to 12/14/11 - 18:16

Error Analysis

Because of the setbacks previously discussed, there was insufficient data gathered to do a meticulous error analysis. This is not a major setback since the conclusions drawn from the data are in no way rigorous in their claims. As such, since the thrust of the paper is simply to encourage further research in the field of low concentrating photovoltaic technology, a simple error analysis was done to ensure that the experimental data taken was statistically significant. For the long term data collection gathered by the data loggers, the error was listed in the manuals as ± 1% for the voltage logger and ± 1°C for the thermocouple (DataQ Instruments, 2011). For the purposes of this paper, these values are not large enough to be of concern in the analysis of the data.

For data gathered in the baseline tests, an analysis of the error resulting from the use of Ohm's law to calculate the current and power output of each system was done. This is found through the use of Equation 21 and 22 derived from techniques found in (Taylor, 1997).

$$\Delta I = I\sqrt{(\frac{\Delta R}{R})^2 + (\frac{\Delta V}{V})^2} \tag{21}$$

$$\Delta P = P\sqrt{(\frac{\Delta I}{I})^2 + (\frac{\Delta V}{V})^2} \tag{22}$$

In equation 21, the values of ΔR and ΔV are the values of the intrinsic error from the resistor and the measuring error from the multimeter respectively. The resistance error was experimentally measured to be about ±0.005 ohms using the multimeter to compare the true resistance to the ideal resistance. The multimeter has specifications claiming it to be accurate to 0.3%.

Thus a sample calculation using data collected for panel 1 can be done using equation 21 to find the range of the accuracy of the current calculations.

$$\Delta I = I\sqrt{(\frac{\Delta R}{R})^2 + (\frac{\Delta V}{V})^2} = (0.206\ A)\sqrt{(\frac{\Delta(0.005\ ohm)}{10\ ohms})^2 + (\frac{0.3\% * 2.06\ V}{2.06\ V})^2}$$

$$\Delta I = 6.3 * 10^{-4}\ A$$

A similar analysis can be done with equation 22 to find the error in power.

$$\Delta P = P\sqrt{(\frac{\Delta I}{I})^2 + (\frac{\Delta V}{V})^2} = (0.423\ W)\sqrt{(\frac{.00063\ A}{.206\ A})^2 + (\frac{0.3\% * 2.06\ V}{2.06\ V})^2}$$

$$\Delta P = 1.8 * 10^{-3}\ W$$

Thus, since this error is over an order of magnitude smaller than the measurements made, it is not significant enough to reduce the legitimacy of the very general claims made in the proceeding sections.

When calculating the concentration ratio, the only error present results from measuring the "solar cell length" (L_C) and from calculating W in Figure 36, the width of the reflector. Error from W is calculated by equation 23.

$$\Delta L = \frac{1}{\cos(\alpha)} \Delta W \tag{23}$$

In this equation, α can be assumed to be exact since it is calculated from a formula given in Wehnam. Sinc W was measured with a yard stick exact to the tenths decimal place, the error can be estimated to be $\Delta W = 0.005$". Thus, the error in L becomes $\Delta L = 0.005$". Since the measurement of L_C was done with the same measuring stick, it too has an error of $\Delta L_C = 0.005$". The error in the concentration ratio, by using equation 18 can then be represented by equation 24 (Taylor, 1997).

$$\Delta CR = CR \sqrt{(\frac{\Delta L}{L})^2 + (\frac{\Delta L_C}{L_C})^2} \tag{24}$$

$$\Delta CR = 4.5\ suns \sqrt{(\frac{0.005\ in}{24.72\ in})^2 + (\frac{0.005\ in}{5.5\ in})^2}$$

$$\Delta CR = 0.004\ suns$$

Again, it is clear that the error of this calculation does not affect the claims made of the efficacy of the reflector. For the purposes of this study, simply ensuring that the numbers calculated are reasonable enough to draw general conclusions from is sufficient. Since the errors in the long term experimental data, the baseline data, and the concentration ratio are all over an order of magnitude less than the values being discussed, this is all the error analysis needed.

Cost Analysis

Comparing the cost effectiveness of the two photovoltaic system required answering a simple question: Does the concentrating system's output compensate for the increased cost of the reflector? It was decided that the simplest possible method should be used to analyze the cost of the flat plate and concentrator. Given that the photovoltaic module (the cells and backing) were the same between each system, the difference in cost would be entirely due to the cost of reflector. The cost effectiveness of the systems could therefore be determined by comparing to the concentrating system to a flat plate of comparable cost – one in which the cost of the reflector had been invested in additional solar cells of the same type. Although such a system was not tested, it could be modeled by using the flat-plate's power output per a cell in the experimental data.

This section provides the details of this analysis. First, the cost of the reflector is calculated. Second, the comparable power output of an equally priced flat-plate system is determined. Next, the out-put level at which is reflector would be more cost-effective than a equally priced flat-plate is determined. Lastly, conclusions are made on whether such an output is realistic given the experimental data, and whether certain assumptions inherent in the analysis are realistic.

While more complicated methods might be able to take into account a greater number of factors that affect costs, these models would inevitably require an undue amount assumptions and inferences. This method of directly comparing the material cost of each photovoltaic system against their output was preferred given the minimal number of assumptions.

Costs of the Reflector

While the team maintained a budget throughout the project, further calculations are necessary to determine the precise costs of each system. While the budget reflects the total cost of the materials purchased, only the costs of the materials used should be considered for a proper cost analysis. Also, while different prices may be available for these same materials, only the purchasing cost received by the team is considered for simplicity's sake. Shipping costs are also excluded.

Items used in Reflector	**Quantity**	**Unit Price**	**Total Cost**
8' 2x3 Boards	7	$2.60	$18.20
3/16" 4x8' Hardboard (Masonite)	1	$12.60	$12.60
7/16" 4x8 OSB	1	$10.50	$10.50
41 Deck Screws	1	$2.50	$2.50
Mylar (per square foot)	32	$0.36	$11.52
Total Cost of Reflector			**$55.32**

The figure above shows the costs of all the materials included in the reflector. Since the unit price of the boards, Masonite, and OSB, was known, these costs were simple to include. Things were slightly different for the Deck screws and the Mylar. The reflector required the use of 41 deck screws total: 12 to hold the ribs to the Masonite, nine to hold the ribs to the Frame, 12 to hold the frame together, and eight to build the panel supports. The box of deck screws was purchased for $25.00 and included 400 screws. That comes down to around six cents a screw, and 2.50 for 41 (given the small fraction of the overall cost the screws constitute this simple math was considered sufficient). As for the Mylar, 166 square feet was purchased (it came in a roll 40 inches by 50 feet) at a price of $59.95. This comes down to around 36 cents per a square foot of Mylar. Having used 32 square feet of Mylar were used to cover reflector face (the surface was four feet by eight feet), this comes to a total of $11.52 spent on Mylar.

Adding all these costs results in a total cost of the reflector of $55.32. While this number should be taken as an estimate, it's difficult to determine how conservative it is. While not buying the materials in bulk may have made them slightly more expensive, it is just as likely that they could have been purchased at lower prices with a little more shopping around (the team simply purchased them from the nearby hardware store).

The Solar Cells

The next step is to determine the output that could be expected if the $55.32 spent on the reflector was instead used to buy additional solar cells. The cells used in both systems cost $9.95 each. This means that instead of buying the materials for the collector, five additional solar cells could be purchased ($55.32/$9.95 = 5.56). Now, assuming that that there's a linear relationship between the number of solar cells and the power output, (assumptions that are warranted due to data collected during the testing phase) the corresponding power output should be easily extrapolated from our experimental data. The flat plate tested included eight solar panels, so including an additional five solar panels should have increased the power output by 1.625 times. Therefore, in order to be more cost effective than a normal flat-plate design, the reflector must increase the power output by more than 1.625 times.

Analysis and Conclusions

Although it is difficult to determine the precise difference in output that might be expected over an extended period of time, the data supports the conclusion that the concentrating system is a more cost effective design. The difficulty in determining the extent of this difference in output results from the fact that different circumstances (including levels of resistance, luminosity, and heat) impact the two systems in different ways. As a result, a wide difference in

comparative outputs was observed. At the high end, the concentrating system outperformed the flat-plate system's power output by as much as six times. Yet at other times, the outputs of the two systems were nearly equivalent. Based on all the data collected, a conservative estimate would be that the concentrating system outperformed the flat-plate system by about two times. The data presented in Figure 29, and Figure 31 makeup the strongest data for this conclusion.

Resistance Variance, and Figure 31

As noted in our data-analysis, the load attached to the concentrated system exerted a large influence on the output of the collector. However, the different systems were by no means affected in the same way, as evidenced by Figure 31. As shown in Figure 31, The maximum power output of the concentrating system was two watts, occurring at a resistance around 40 ohms, whereas the maximum power output of the flat-plate system was 1 watt, occurring at a resistance 110 ohms. This data was taken at nearly the same time, with the same level of luminosity. Therefore, this data suggests that the maximum power output of the concentrating system is roughly twice that of flat-plate, when the systems are unaffected by any other factors related to differences in luminosity.

Luminosity Variance and Figure 29

Figure 29 demonstrates comparative power output of the two systems at different luminosities. This data was taken over the course of a number of days, leaving the resistances constant. For the majority of the data-set, the concentrating system outperforms the power output of the flat-plate by well over two times, reaching a high of around 6 times on 7/16/2011. Equally importantly, the comparative power output of the concentrating system only falls below the level of cost effectiveness (1.6 times that of the flat-plate) for only two of the 13 days of the sample

(7/24/11 and 7/25/11). Even at these low points, the concentrating system still managed to match the absolute power output of the flat plate.

Conclusion

The data therefore suggests that the power output of the concentrating system was well over 1.6 times the power-output of a flat plate of the same cost, rendering the concentrating system as a whole a more cost-effective option. It is worth acknowledging that this analysis does come with it's own set of assumptions, mainly that the two systems would be maintainable over the same time-span, that the level of thermal degradation of the cells would be equivalent between the two systems, and that the reflector would be the only difference in cost between the two systems. Unfortunately, our data wasn't collected for a sufficient duration to take these into account. It is suspected that modern manufacturing techniques for the cells would overcome these types of issues in the concentrated system, in the same way that they have overcome these issues in a flat-plate system. Nonetheless, the extent of the difference in power-output between the two systems offers strong support that a concentrating photovoltaic system of this design could offer greater cost effectiveness than the traditional flat-plate design.

Conclusions and Future Works

Introduction

As explained in the methodology the team went through a number of iterations of designs and faced several hardships and setbacks in both hardware and data analysis realms. These setbacks, in and of themselves were instructional in many ways though not always directly helpful in answering the ultimate question of whether low scale CPV could outperform a traditional flat-plated design in terms of power output (given solar and weather conditions in the geographical location of testing).

Regardless of these difficulties, the data suggests that future research into concentrated photovoltaic research is warranted. First, the evidence suggests that a reflector such as the one used in this project could be a viable design for cheap, temporary photovoltaic systems. Second, thermal issues are likely to exist with any time of concentrating system, regardless of the types of cells used. Third, an algorithm was developed to calculate how efficiently a given reflector could concentrate light onto a specified area of cells. Fourth, the systems were proven to cohere to theoretical models, and a rigorous approach to analysis of future projects in this field should be modeled after these methods of modeling. Fifth, a rough concentration ratio was calculated to prove that the reflector design that was tested created a low-scale concentration system, thus supporting a fixed reflector design as opposed to the more commonly used high end tracking systems implemented in larger photovoltaic systems. Sixth, the evidence suggests that a concentrating photovoltaic system could work even in areas of substantial diffuse light, such as Maryland. Finally, this project poses several future applications for this technology, such as in the creation of photovoltaic thermal hybrid solar systems.

The Reflector

A defining characteristic of this project was the team's ability to create a workable concentrated photovoltaic system using cheap, readily available materials. Furthermore, ignoring design, the construction of the system requires little technical expertise, and could be accomplished with relatively simple tools that require minimal training. Yet, given these less than demanding characteristics, the reflector was still able to stand up to the elements for over two years with little degradation. This demonstrated durability suggests that the design may be a viable option for future low-concentrating systems.

The reflector design holds certain advantages that make it ideal for powering temporary structures and systems. In particular, this type of system may be particularly suited for addressing the need for cheap electricity in developing countries, where basic materials used for the reflector are often available but technical experience and PV cells are in short supply.

The reflector was composed of only four parts: a wooden frame, three particle board ribs, a curved Masonite backing, and the Mylar surface. The particle board ribs supported the shape of the reflector and were in turn supported by the wooden frame. The Masonite backing was attached to the ribs, taking the shape of the reflector, and the Mylar was attached to the Masonite using wall-paper glue to give it a reflective surface. The finishing touches consisted of spraying the wooden frame with a waterproofing spray.

These materials are inexpensive and robust enough for long distance transport. Moreover, other materials may be substituted for them without impacting the efficacy of the reflector. For example, most readily available woods may be used in place of the oak planks or the particle board. Also, a piece of sheet metal may replace the Masonite/Mylar combination. Additionally,

most of the construction was done with hand-held tools (hammers, screwdrivers, brushes). The only exception to this was our need to use jig-saws to cut the ribs for the collector, yet even this could be done with a handheld saw if necessary.

Although the CPV system did not perform as expected, the reflector was nonetheless a huge success, given its ability to reflect light effectively through two years of weathering. Examples of the reflector's success in reflecting light are evident from our findings. The temperature readings are perhaps the most direct empirical evidence in support of how much light was being reflected by our reflector. The cells receiving light from the concentrator would heat up to roughly twice the temperature of the control panel within one minute. It is important to note that these levels of reflection were achieved over the entire two year course of our testing, with little maintenance. The reflector was exposed to everything from sunshine, to tropical storm winds, and even stood strong against a small earthquake.

Of course some minor maintenance was required. About halfway through our testing, it was necessary to replace the Mylar, which had degraded slightly due to weathering. This was a fairly simple process though – the old Mylar was stripped off and a new sheet of Mylar was applied in the same fashion as the original. Given the cheapness of the Mylar, and the short time required for the new layer of Mylar to be applied, this minor level of maintenance is more or less negligible in determining the reflector’s durability.

Nonetheless, the Mylar covering was effective at preventing damage from weathering on the side of the reflector that it covered. The part of the reflector that was not covered accumulated significantly more damage over the two years it remained on the roof despite the waterproof sealant. Water damage and loss of integrity at the joints seemed to be the primary

problems. The large temperature fluctuation throughout the day on an exposed roof contributed as well, especially given the added heat from concentration.

For any future reflector design, it would be important to keep in mind that the stresses it must endure are greater than the normal wear-and-tear that any material stored outside will undergo. In our design the constant heating and cooling caused a lot of expansion and contraction, which put a lot of stress on the joints. For instance, the nails holding the reflector to the frame came out several times. This was most likely due to heat expansion. Using more flexible fasteners than nails or screws, or fastening things together somewhat loosely with longer nails, could help reduce this stress.

The heat and water damage to the reflector could be fixed in one of two ways. The first and most obvious way to prevent it would be to select more durable materials, such as ceramics. However, this could increase the cost of the reflector considerably. A cheaper and more convenient solution would be to find a more heat and water-resistant coating to use on the wood from the reflector than we did in our project, as we did not realize how much additional stress the heat would place on it. It is also important to remember that the reflector might not be intended to last for many years in some applications, such as at a construction site. The use of inexpensive materials and the flexibility of the program that determines the ideal reflector shape lend themselves well to uses that do not require a particularly long-term installation.

In summation, despite a few limitations, the reflector 1) used cheap materials, 2) used readily available materials, 3) could be constructed with little technical training, 4) could be constructed with simple tools, 5) reflected light effectively, and 6) could weather the elements

for over two years with little maintenance. The only technically demanding part of the design process was in generating the curve of the reflector.

The Cells

When the various types of PV cells were investigated during the initial experimental design of the CPV system, polycrystalline silicon cells were ultimately chosen because they were the cheapest and most readily available type of photovoltaic cell. Polycrystalline silicon cells have the disadvantage of being inefficient relative to some of the newer types of PV cells (Cheng et al., 2009) but, because the power output was to be compared between two identical panels varying only in concentration, it was expected that this would not have a large impact on results. More specifically, the main thrust of this project was to design a reflector that could increase the power output of any solar system—the cells were just used to show how effective the system would be. The design was not limited in intended application to only polycrystalline cells, but they were used to test it because they are the most common.

There was some initial concern about the increased temperature of the concentrated cells as a result of greater insolation. Insolation, measured as irradiation, is the sunlight that any region receives. The performance of a PV system has been directly related to the ambient temperature of the PV module (Makrides et al., 2012). The referenced study shows that an increase in module temperature is a very important performance loss factor, and studies show that the performance of crystalline silicon PV cells reduce with an increased temperature (Makrides et al., 2012). It was expected then, within this experimentation, to find that the increased performance of the

concentrated system over the control would be somewhat diminished by the coinciding increase in module temperature.

What was found, however, surpassed temperature expectations and quickly limited the output of the concentrated cells. During testing the concentrated module reached temperatures in excess of 90◦ C. As a result of this, measured power output from the concentrated system was very low. This suggests the question of whether this tremendous decrease in performance could be avoided if a different type of solar cell was chosen.

Research by Makrides et al. shows that the highest thermal losses are, in fact, recorded for polycrystalline and monocrystalline silicon cells. Thin film and amorphous silicon technologies experienced a lower loss of power and would thus theoretically perform better under higher temperatures. The difference between the two losses in efficiency, however, was relatively small: 5% for thin films vs. 8% for crystalline silicon. This research was also performed at relatively low module temperatures (T<70◦ C). At higher temperatures, it is predicted that performance would continue to decline (Makrides et al., 2012). At high temperatures, such as those found within this experiment, the difference between these efficiencies would likely be negligible, as both efficiency losses would be high.

This suggests that the way to compensate for higher panel temperatures under concentration is not to change the type of panel suggested, but instead to seek out a method to better cool a concentrated system. There are a number of options that could be pursued along this avenue. First, a cooling system, either passive or active, could be incorporated into the concentrated solar panels. The panels used within the testing were well insulated by their own plastic backing. With this backing removed it is possible that a heat sink or water cooling system

could be incorporated to reduce the temperature of the panels to such a degree as to minimize losses. Second, infrared light could be filtered out before concentrated solar radiation reached the PV modules. The reduction in infrared radiation would drastically reduce heat received by the panels without majorly impacting received usable radiation, which exists primarily within the visible portion of the spectrum. The high measured panel temperature also suggests that there may be a strong potential for the coupling of solar thermal and photovoltaic systems within one concentrated solar energy system.

The Program

Two different programs were used in support of the overall project. The first, written in MATLAB, optimizes a reflector for certain angle of the sun. The second, written in Python, simulates the reflection process for an existing reflector.

Before collecting any data, it was necessary to know what shape the reflector would take. A roughly parabolic shape was assumed for the reflector, but the exact shape was yet to be determined. The MATLAB program helped out in this regard. In exchange for three parameters, the angle of the sun, and the height and length of the PV element, it numerically estimated, with minimal error, the twenty Cartesian coordinates that would constitute the left and right elements of the reflector.

Having built the reflector off of the model computed by the MATLAB program, a mechanism was needed to model the operation of the constructed reflector. Variations from the original program were expected, mainly resulting from construction imperfections and movement of the sun. This gave rise to the Python program, which took in three groups of

parameters, the coordinates of the reflector, the coordinates of the PV element, and the position of the sun. This program uses basic physical principles to model the reflection of light off of a reflective surface. It uses these inputs to simulate the reflection of the sun's rays with respect to the actual layout of the reflector. As a result, the program can be used to model the reflective behavior of any desired reflective surface.

Gathered Data and Methodology

The calculation for the solar concentration ratio done in the data analysis section shows that the system tested during this project reflected 4.5 suns onto the cells in the design. This characterizes the setup as a 'low concentrated system.' With this degree of concentration, it was not anticipated that there would be a significant amount of heat absorption, especially not to a degree that would substantially impact the efficiency of the cells. However, as discussed in the data analysis and methodology section, there was a substantial amount of heat retained by the cells, so much so that the concentration had an adverse effect on the conversion efficiency of the cells without the presence of a cooling system. Rather than view this as a design failure, it is beneficial to look into ways to implement solar thermal collecting elements in future iterations of this design.

It is also worthwhile to note that the models discussed in the data analysis section match the experimental data fairly well. This shows that a deep physical understanding as to how and why the cells were behaving the way they were was obtained, and adds legitimacy to the experimental processes that developed from them. For example, during the winter testing months when the systems were achieving the same voltage output, the basic knowledge obtained by the

models allowed for conclusions to be made about the physical behavior of the panels and ultimately led to the revision of the test procedure to account for the concentrated system reaching open circuit too quickly at higher resistance values. These models are essential for any subsequent projects in this field as they quantify the differences between two seemingly identical panels. When a variable is changed for one of the panels (i.e. concentration), the knowledge obtained by these models enable comparisons to be made with 100% certainty that differences in system behavior are due to the change in the variable factor.

Weather and Location

Concentrating was effective in Maryland, despite the medium levels of insolation. This suggests that places with similar insolation and irradiation could have similar levels of success. While the overall sunlight that any region of the earth receives over the course of a year is equal, the concentration each season varies by a region's latitude, longitude, and air mass (AM). On average, Maryland receives a solar irradiation of 5.5 kWh/m2 per day over the summer, and 3.5 kWh/m2 over winter (Messenger, Ventre, 1999). As the concentrating system is optimized for the summer, regions that receive around 5.5 kWh/m2 of irradiation will have results comparable to those in Maryland (Messenger, Ventre, 1999). Some of these regions include areas just west of the Great Lakes in North America, across southern Canada, parts of Central America, and northeast regions of South America, northern Spain, southern France, Italy, parts of Eastern Europe, southern Russia, central China, and north central Australia. The climates of these regions vary vastly and so the weather will make a big difference on whether a similar system will truly work in the regions listed above. Furthermore, irradiance varies based on minor

differences in the areas observed, including the shadows produced by objects in the vicinity, buildings, trees, etc (Messenger, Ventre, 1999).

Regions that receive higher solar irradiation would have fared better in terms of concentration and performance. Within the United States, in the summer, these regions include California (most specifically the Mojave Desert region), the northwest (Oregon and Washington), Arizona, Texas, and Florida, as well as southern states (Messenger, Ventre, 1999). Globally, this includes sub-Saharan and northern Africa, as well as large regions of the northwest and southeast coasts of Africa such as The Gambia, Senegal, and Mozambique (Messenger, Ventre, 1999). During summer in the southern hemisphere, south and central Australia, south and western India, South Africa and surrounding countries, as well as New Zealand receive irradiation comparable to or higher than the summer values in Maryland (Messenger, Ventre, 1999). Low and medium concentration, at the same rates as this project accomplished, could be successful in all of above listed regions. From these regions, those with weather comparable to or drier than Maryland can successfully implement a CPV system comparable to this project using the same materials. Maryland climate is humid subtropical and subtropical highland. Mid-Atlantic and south-eastern US states have humid subtropical climate and comparable or higher irradiance. Regions of New Zealand are comparable in irradiance and climate to parts of Maryland.

Future Directions

The design specifications of this concentrated photovoltaic system may not satisfy the demands of many solar energy applications. Confirmation of the short-term survivability in

Maryland weather of a reflector over a period of two years means little when the economics of solar technology often require the systems to be usable for 20 years in order to reach profitability (Messenger, Ventre, 1999). Nonetheless, the precise characteristics that lead to the system's short life-cycle, also make it a viable, if not preferable, design under certain conditions.

Solar energy has been widely employed to power systems where access to existing energy infrastructure is either cost-prohibitive or simply not available. This occurs abroad in underdeveloped countries and lowly populated areas. The low concentrating reflector developed in this project would ideally be used in one of these areas, when a temporary increase in power is needed. Examples of situations in which the low concentration reflector would prove useful include powering temporary medical centers set up in remote areas of the world, or setting up temporary shelters after natural disasters. As long as the reflector is needed for a short span of time and is relatively cheap, this low concentrating reflector would be a viable energy solution. The data collected in this project suggests that a comparable, potentially superior energy output can be reached using concentrated photovoltaic technology, when compared to a flat plate installation with an equivalent number of cells. However, a cooling system—such as an integrated solar thermal component—would be necessary to ensure the increased output. Alternatively, the reflector could be used as only a solar thermal installation, providing hot water.

As discussed in previous sections, the PV cells became very hot when subjected to concentrated sunlight. This heat reduced the effectiveness of the cells, and, in some cases, damaged the substrate supporting them. Therefore, in order to implement a concentrating PV system, the excess heat from the cells must be dissipated or removed. One way to improve the

efficiency of the system is to collect the waste heat generated by the PV cells to use for thermal energy generation.

Solar thermal energy collection is used in many applications, from residential water heating to large scale electricity generation. Adding a channel of fluid behind the existing panels will help alleviate the current overheating problem by carrying away excess heat from the cells. For small scale applications, the system could be used to generate hot water and reduce the total electricity usage of the home or business. On a larger scale, power generating plants could be built to harvest energy using a combination of a steam turbine and the PV cells. Both of these ideas are based on widely used solar thermal systems and would be relatively simple to implement. However, combining the concentrating PV system with commonly used solar thermal technology has the potential to yield a greater power output than a comparable CPV system operating alone.

Creating a combined solar thermal and PV system is the best option to maximizing energy collection in a solar concentration system. However, it may prove ineffective or unnecessarily complicated to use the solar thermal system to cool the PV panels. Instead, another possibility is to incorporate a standard PV system into a concentrated solar thermal system.

The idea behind this combined approach stems from two main facts. First, even at small (<10 suns) concentration ratios, CPV systems heat PV cells to the point when their internal resistance makes them less efficient than a conventional PV system. As discussed extensively in the proceeding sections, the CPV solar panels will reach temperatures more than two times the temperature of the standard PV panels. This causes a significant increase in the internal resistance of the panels, thus dramatically cutting the power output. The second fact that leads to

this idea is that PV cells absorb a large portion of the spectrum, while solar thermal systems need only the infrared. Therefore, this idea proposes that the infrared portion, which heats up the cells, is reflected off the cells onto the thermal absorption component.

The hybrid system suggested would be based off a standard solar thermal system. The PV portion of the system would be incorporated by attaching a layer of thin-film PV cells directly onto the reflector. These cells are flexible, so would be able to conform to the shape of the concentrator. The thin-film cells that would be used are transparent to the infrared—and much of the visible—portion of the spectrum. Thus, the cells could generate energy, while avoiding the excessive heating of a concentrated system and without hampering the collection capabilities of the solar thermal system. Moreover, the cells would not be heated by conduction because the cells would be removed from the thermal collection part of the system (a tube of water or salt, depending on scale of concentration).

Conclusion

After extensive construction and testing of a prototype parabolic reflector/photovoltaic panel system, the team's conclusion is that concentrated photovoltaic systems are a subject that warrants further research in the state of Maryland. The results obtained in testing indicate that, despite the many replacements and different iterations of solar panels, there seems to be potential in the fundamental concept being tested.

The ability of the parabolic reflector design to stand up to the elements for over a year, despite being constructed with inexpensive materials, is a notable success. This result indicates that the technology could have potential uses in low-income areas, including developing nations,

as a replacement for expensive solar tracking systems. In addition to the success of the reflector, the program that was developed during testing also has potential applications for future concentration systems. Although numerous setbacks occurred during the course of testing, it was determined that many of the problems that were encountered, such as overheating, would be problematic for any solar panel system, not just a concentrating system. Despite the setbacks, the overall conclusion reached is that although further testing is needed, preliminary results show that photovoltaic concentration systems have the potential to work even in parts of the world with low incident solar flux, like Maryland. Future applications for this technology could even attempt to integrate photovoltaic cells with a thermal energy system. The potential for future experimentation in this field is limitless.

Appendices

Appendix 1: Data Samples & Format

The following is a sample selection of our data in the text file format in which it is collected by our data loggers. The data loggers keep track of the date and time of each recording increment, as well as the voltage being produced across the resistors. The text files keep the data categories in separate columns, so the data can be easily uploaded into Microsoft Excel or other spreadsheet programs for analysis. Below is a screenshot of a selection of data in text file format.

```
TeamLeaf1,Time,Voltage(Volts),Serial Number
1,19/07/2011 15:50:05,0.85,000018157
2,19/07/2011 15:51:05,5.60
3,19/07/2011 15:52:05,4.95
4,19/07/2011 15:53:05,4.80
5,19/07/2011 15:54:05,4.90
6,19/07/2011 15:55:05,4.65
7,19/07/2011 15:56:05,4.60
8,19/07/2011 15:57:05,4.45
9,19/07/2011 15:58:05,3.65
10,19/07/2011 15:59:05,3.75
11,19/07/2011 16:00:05,4.00
12,19/07/2011 16:01:05,3.60
13,19/07/2011 16:02:05,3.70
14,19/07/2011 16:03:05,3.25
15,19/07/2011 16:04:05,2.85
16,19/07/2011 16:05:05,3.90
17,19/07/2011 16:06:05,4.10
18,19/07/2011 16:07:05,4.30
19,19/07/2011 16:08:05,4.30
20,19/07/2011 16:09:05,4.50
21,19/07/2011 16:10:05,4.95
22,19/07/2011 16:11:05,4.60
23,19/07/2011 16:12:05,4.00
24,19/07/2011 16:13:05,3.70
25,19/07/2011 16:14:05,3.75
26,19/07/2011 16:15:05,3.80
27,19/07/2011 16:16:05,3.55
28,19/07/2011 16:17:05,3.90
29,19/07/2011 16:18:05,4.10
30,19/07/2011 16:19:05,3.50
31,19/07/2011 16:20:05,2.95
32,19/07/2011 16:21:05,2.50
33,19/07/2011 16:22:05,2.15
34,19/07/2011 16:23:05,2.00
35,19/07/2011 16:24:05,2.10
```

Of course, this format is not very useful for analysis. We were able to upload our data from a text file into a spreadsheet program, which allowed for much better data analysis. Below is a screenshot of the same data in a spreadsheet program.

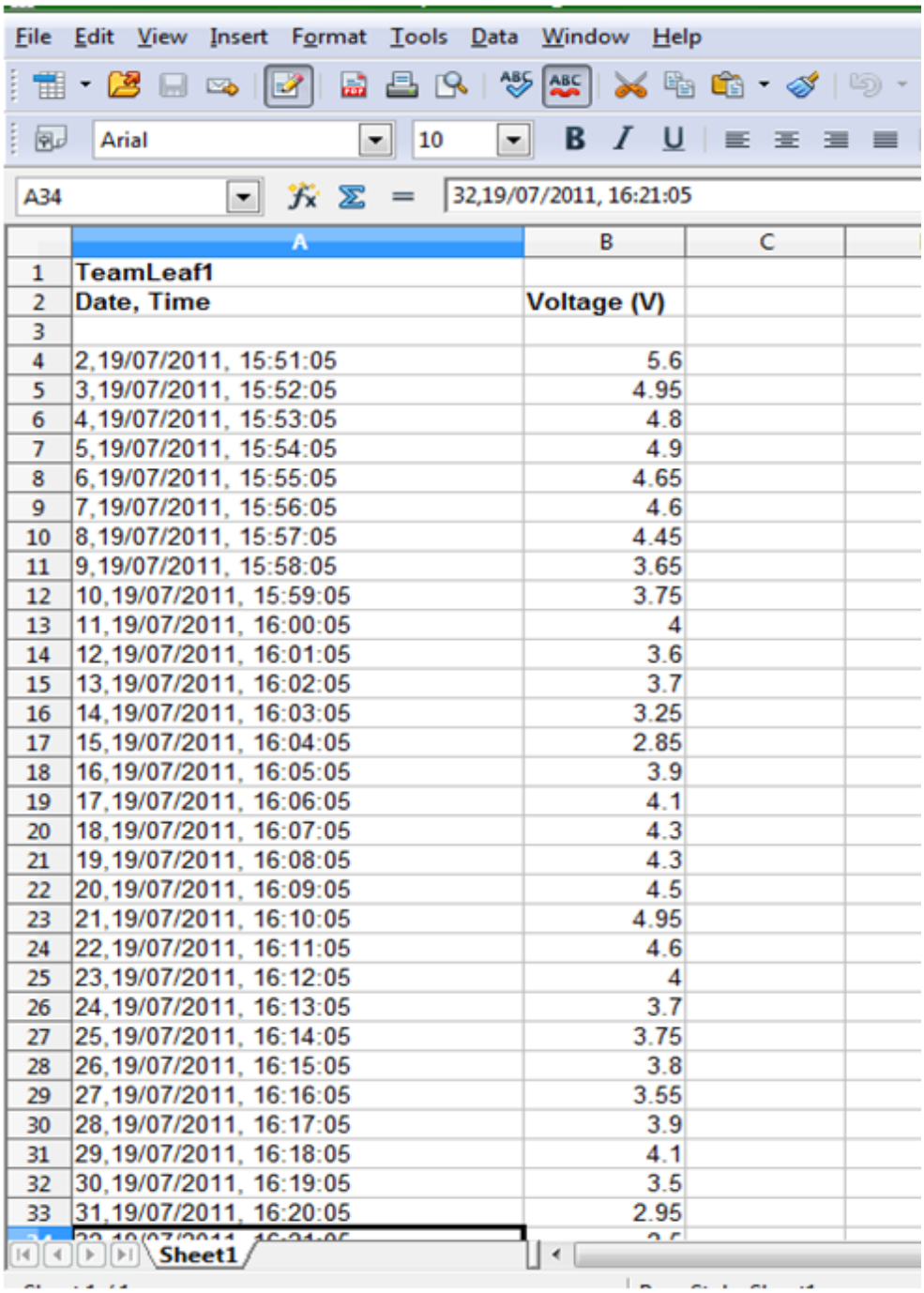

	A	B	C
1	TeamLeaf1		
2	Date, Time	Voltage (V)	
3			
4	2,19/07/2011, 15:51:05	5.6	
5	3,19/07/2011, 15:52:05	4.95	
6	4,19/07/2011, 15:53:05	4.8	
7	5,19/07/2011, 15:54:05	4.9	
8	6,19/07/2011, 15:55:05	4.65	
9	7,19/07/2011, 15:56:05	4.6	
10	8,19/07/2011, 15:57:05	4.45	
11	9,19/07/2011, 15:58:05	3.65	
12	10,19/07/2011, 15:59:05	3.75	
13	11,19/07/2011, 16:00:05	4	
14	12,19/07/2011, 16:01:05	3.6	
15	13,19/07/2011, 16:02:05	3.7	
16	14,19/07/2011, 16:03:05	3.25	
17	15,19/07/2011, 16:04:05	2.85	
18	16,19/07/2011, 16:05:05	3.9	
19	17,19/07/2011, 16:06:05	4.1	
20	18,19/07/2011, 16:07:05	4.3	
21	19,19/07/2011, 16:08:05	4.3	
22	20,19/07/2011, 16:09:05	4.5	
23	21,19/07/2011, 16:10:05	4.95	
24	22,19/07/2011, 16:11:05	4.6	
25	23,19/07/2011, 16:12:05	4	
26	24,19/07/2011, 16:13:05	3.7	
27	25,19/07/2011, 16:14:05	3.75	
28	26,19/07/2011, 16:15:05	3.8	
29	27,19/07/2011, 16:16:05	3.55	
30	28,19/07/2011, 16:17:05	3.9	
31	29,19/07/2011, 16:18:05	4.1	
32	30,19/07/2011, 16:19:05	3.5	
33	31,19/07/2011, 16:20:05	2.95	

In order to avoid pages of data, a graph of all of the voltage measurements from July 13- July 17, and July 19- July 27 (shown in the "summer setbacks" section of the Data Analysis) is depicted below.

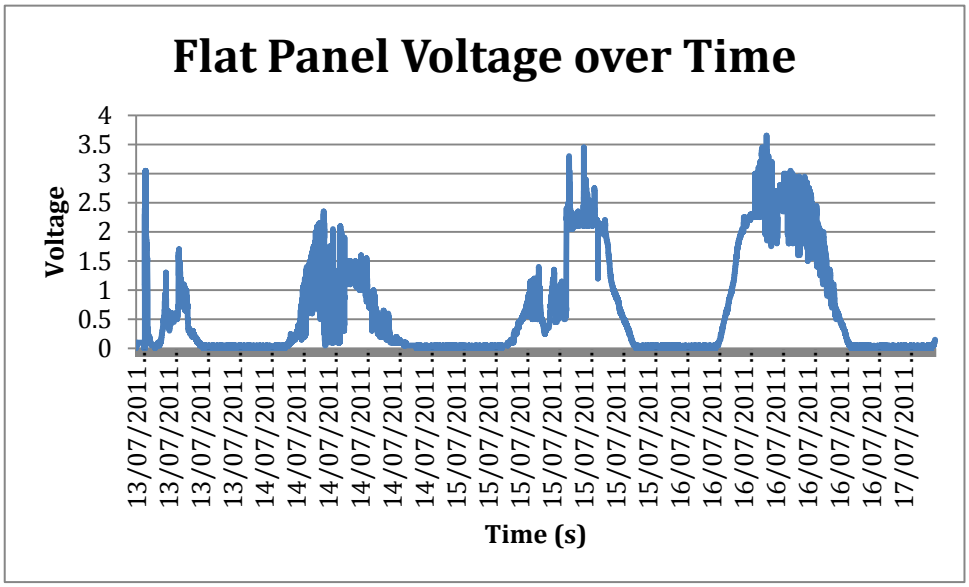

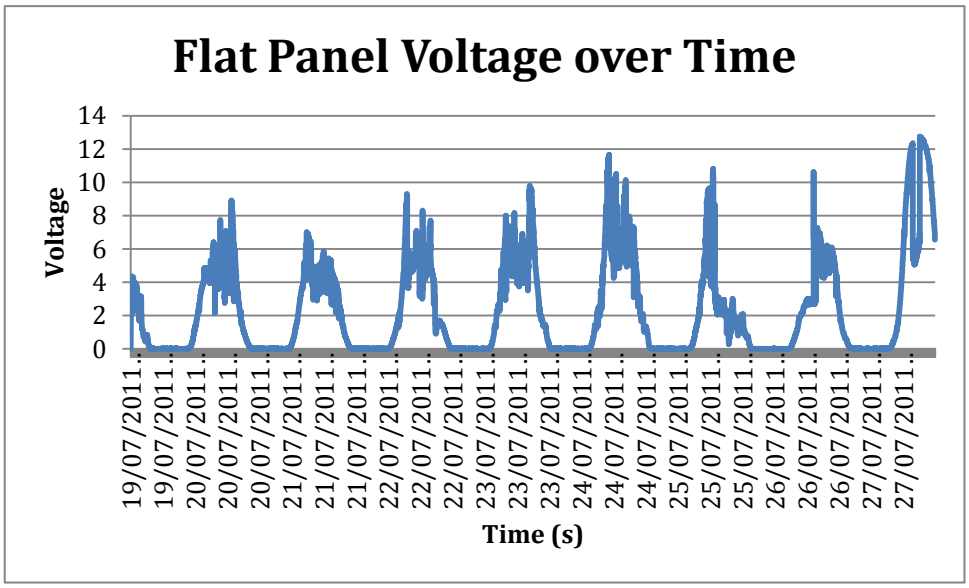

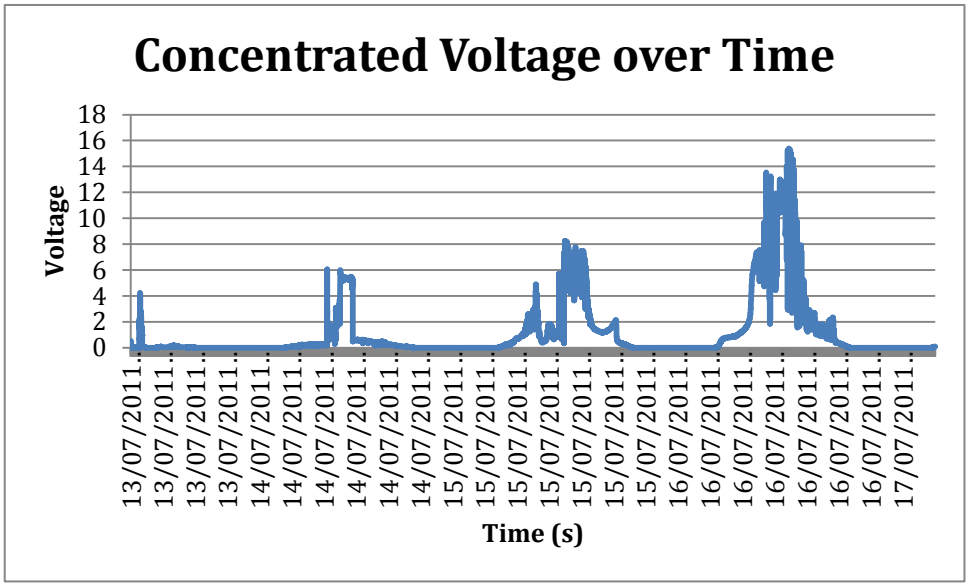
Concentrated Voltage over Time
Voltage
18
16
14
12
10
8
6
4
2
0
13/07/2011..
13/07/2011..
13/07/2011..
13/07/2011..
14/07/2011..
14/07/2011..
14/07/2011..
14/07/2011..
14/07/2011..
15/07/2011..
15/07/2011..
15/07/2011..
15/07/2011..
15/07/2011..
15/07/2011..
16/07/2011..
16/07/2011..
16/07/2011..
16/07/2011..
16/07/2011..
16/07/2011..
17/07/2011..
Time (s)

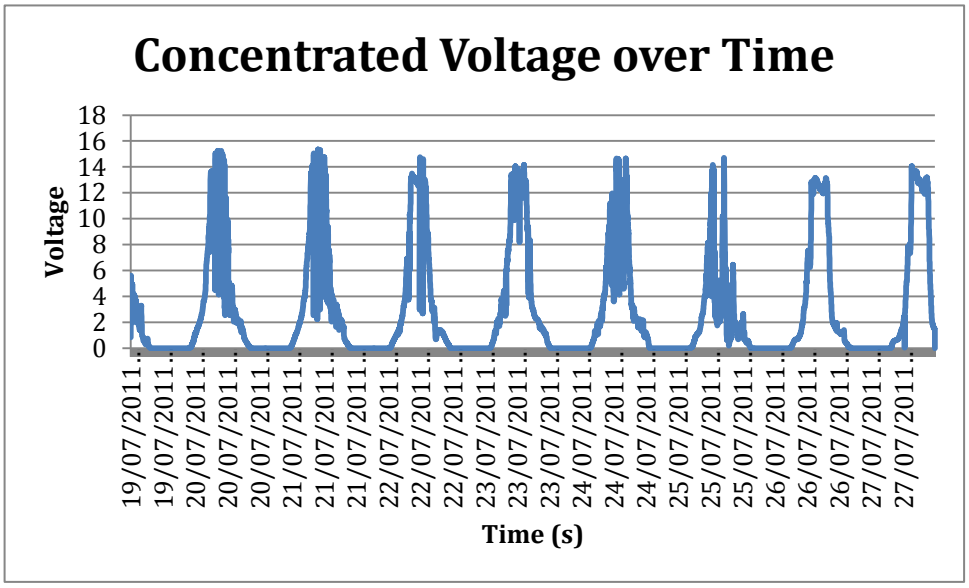
Concentrated Voltage over Time
Voltage
18
16
14
12
10
8
6
4
2
0
19/07/2011..
19/07/2011..
20/07/2011..
20/07/2011..
20/07/2011..
21/07/2011..
21/07/2011..
21/07/2011..
22/07/2011..
22/07/2011..
22/07/2011..
23/07/2011..
23/07/2011..
23/07/2011..
24/07/2011..
24/07/2011..
24/07/2011..
25/07/2011..
25/07/2011..
25/07/2011..
26/07/2011..
26/07/2011..
26/07/2011..
27/07/2011..
27/07/2011..
27/07/2011..
Time (s)

When doing the thermal analysis, thermocouples were connected to the panels to measure the temperature over a specified time interval during testing in late December. The data from the thermocouple was recorded by the data loggers and the output was recovered in the following format.

```
EasyLog USB,Time,Fahrenheit(°F),Serial Number
1,10/12/2011 13:31:16,67,000017115
2,10/12/2011 13:32:16,105
3,10/12/2011 13:33:16,90
4,10/12/2011 13:34:16,87
5,10/12/2011 13:35:16,94
6,10/12/2011 13:36:16,83
7,10/12/2011 13:37:16,92
8,10/12/2011 13:38:16,99
9,10/12/2011 13:39:16,100
10,10/12/2011 13:40:16,103
11,10/12/2011 13:41:16,110
12,10/12/2011 13:42:16,119
13,10/12/2011 13:43:16,93
14,10/12/2011 13:44:16,94
15,10/12/2011 13:45:16,108
16,10/12/2011 13:46:16,102
17,10/12/2011 13:47:16,113
18,10/12/2011 13:48:16,103
19,10/12/2011 13:49:16,120
20,10/12/2011 13:50:16,103
21,10/12/2011 13:51:16,110
22,10/12/2011 13:52:16,101
23,10/12/2011 13:53:16,98
24,10/12/2011 13:54:16,96
25,10/12/2011 13:55:16,82
26,10/12/2011 13:56:16,91
27,10/12/2011 13:57:16,96
28,10/12/2011 13:58:16,86
29,10/12/2011 13:59:16,83
30,10/12/2011 14:00:16,78
31,10/12/2011 14:01:16,83
32,10/12/2011 14:02:16,81
33,10/12/2011 14:03:16,81
```

To make this data easier to manipulate, again, excel was used to import the text file. The plots of the data are shown in the thermal analysis section of the data analysis.

Appendix 2: Computer Code

The following is the Python code used to simulate the path of sun rays as they are reflected and absorbed by various portions of our setup.

```
from pylab import *

#Box

x = 10

y = 10


#Element

xls = [7, 9, 1, 3, 5, 7]

xlnr = [7, 9, 1, 3, 5, 7]

yls = [2, 4, 7, 4, 2, 4]

ylnr = [1.5, 3.5, 6.5, 3.5, 1.5, 3.5]

for k in range(0, len(xls)/2):

xl = xls[2*k:2*k+2]

yl = yls[2*k:2*k+2]

plot(xl, yl)

xl = xlnr[2*k:2*k+2]

yl = ylnr[2*k:2*k+2]

plot(xl, yl)


plot([0, x, x, 0, 0], [0, 0, y, y, 0])


#Sunlight
```

```
angle_of_sun = -66

angle_of_sun = angle_of_sun*pi/180

m_fix = tan(angle_of_sun) #slope of sunlight

#bs = array([-10, -5, 0, 5, 10, 15, 20]) #array of y-intercepts for sunlight, number of elements denotes number of rays of sun

bs = array([15])


#Reflect

for i in bs[:]:

flag = True

counter = 0

index = -1

xs = array([-20, 20]) #x-coordinates for sunlight

ys = m_fix*xs + i #y-coordinates for sunlight

while flag:

intersections_ray = zeros(len(xls)/2)+5

intersections_panel = zeros(len(xls)/2)+5

intersections_nonref = zeros(len(xls)/2)+5

intersections_raynf = zeros(len(xls)/2)+5

for k in range(0, len(xls)/2):

xl = xls[2*k:2*k+2]

yl = yls[2*k:2*k+2]

xla = xlnr[2*k:2*k+2]

yla = xlnr[2*k:2*k+2]
```

```
#solve for intersection
matrix_A = matrix([[xl[1] - xl[0], xs[0] - xs[1],0,0], [yl[1] - yl[0], ys[0] - ys[1],0,0], [0,0,xla[1] -
        xla[0], xs[0] - xs[1]], [0,0,yla[1] - yla[0], ys[0] - ys[1]]])
matrix_b = matrix([[xs[0] - xl[0]], [ys[0] - yl[0]], [xs[0] - xla[0]], [ys[0] - yla[0]]])
if(round(linalg.det(matrix_A), 10)!=0):
matrix_sol = linalg.solve(matrix_A, matrix_b)
t1 = round(matrix_sol[0], 10)
t2 = round(matrix_sol[1], 10)
t3 = round(matrix_sol[2], 10)
t4 = round(matrix_sol[3], 10)
if(0<=t1<=1 and 0<=t2<=1):
intersections_panel[k] = t1
intersections_ray[k] = t2

if(0<=t3<=1 and 0<=t4<=1):
intersections_nonref[k] = t3
intersections_raynf[k] = t4



if(index!=-1):
intersections_panel[index] = 5
intersections_ray[index] = 5
intersections_nonref[index] = 5
```

```
intersections_raynf[index] = 5


t_ray1 = min(intersections_ray)
t_ray2 = min(intersections_raynf)
if(t_ray1<t_ray2):
index = intersections_ray.argmin()

else:
index = intersections_raynf.argmin()

t_panel = intersections_panel[index]
t_nf = intersections_nonref[index]
if(0<=t_panel<=1 and t_panel<t_nf):
xl = xls[2*index:2*index+2]
yl = yls[2*index:2*index+2]
x_crit = xl[0] + t_panel*(xl[1] - xl[0])
y_crit = yl[0] + t_panel*(yl[1] - yl[0])
if(xl[0] == xl[1]):
vo = array([0, 15 - y_crit])

elif(yl[0] == yl[1]):
vo = array([15 - x_crit, 0])

else:
#generation of vector to reflect over; i.e. the panel's perpendicular
```

```
m_panel = (yl[1] - yl[0])/float(xl[1] - xl[0]) #panel slope
m_vo = -1/m_panel # slope of normal to panel
b_vo = y_crit - m_vo*x_crit # y intercept of panel normal originating at reflection point
vo = array([x_crit - 10, y_crit - (10*m_vo + b_vo)]) # changes normal to a vector

#generation of vector to reflect: i.e. the sunlight
vr = array([xs[1] - xs[0], ys[1] - ys[0]]) # changes incident ray to vector
ordinality = abs(angle_of_sun)/angle_of_sun

#reflection
result = 2*dot(vo, vr)/dot(vo, vo)*vo - vr # dot is dot product function
xr = [x_crit, x_crit+ordinality*result[0]]
yr = [y_crit, y_crit+ordinality*result[1]]
plot([xs[0], x_crit], [ys[0], y_crit]) # incident ray
xs = xr
ys = yr

elif(0<=t_nf<=1 and t_nf<t_panel):
flag = False
xl = xlnr[2*index:2*index+2]
yl = ylnr[2*index:2*index+2]
x_crit = xl[0] + t_nf*(xl[1] - xl[0])
y_crit = yl[0] + t_nf*(yl[1] - yl[0])
plot([xs[0], x_crit], [ys[0], y_crit]) # incident ray
```

```
else:
plot(xs, ys) # plots all the way thru (no reflection)
flag = False




axis([-11, 11, -11, 11])
axvline()
axhline()
show()
```

Appendix 3: Weather Data for July 2011 Testing

Temperature					Conditions				
Month	Day	Min	Max	Mean	Length of Day	0000-0800	0800-1600	1600-2400	Precipitation
July	14	60	75	68	14h 39m	Clear	Clear	Scattered Clouds	0.00
July	15	68	75	70	14h 38m	Clear	Clear	Clear	0.00
July	16	60	73	66	14h 37m	Clear	Scattered Clouds	Clear	0.00
July	17	69	78	73	14h 35m	Cloudy	Scattered Clouds	Clear	0.00
July	18	71	87	78	14h 34m	Clear	Scattered Clouds	Clear	0.00
July	19	77	88	82	14h 33m	Clear	Mostly Cloudy	Scattered Clouds	0.00
July	20	76	89	81	14h 31m	Clear	Clear	Scattered Clouds	0.00
July	21	78	95	86	14h 30m	Clear	Scattered Clouds	Scattered Clouds	0.00
July	22	80	89	84	14h 28m	Clear	Scattered Clouds	Clear	0.00
July	23	78	91	84	14h 26m	Clear	Clear	Clear	0.00
July	24	80	89	84	14h 25m	Clear	Clear	Clear	0.00
July	25	78	91	84	14h 23m	Clear	Cloudy	Cloudy	0.00

Appendix 4: Materials Spec Sheet and CAD Drawings

ENCAPSULATED SOLAR CELL (2V/200MA)

Jameco Part no. 200221	
Manufacturer	VELLEMAN INC.
Manufacturer no.	SOL4

Catalog 121 , page 182

velleman

Overview

Mini Solar Panel

Ready to use, no Soldering! These encapsulated mini-panels utilize solar cells similar to those that power our satellites in space, yet they are safe and simple to use. Mini-panels allow for handling without the normal breakage and cell damage associated with fragile solar cells. They come with 6 inch red and black lead wires. The panels can also be connected in series or parallel to create different outputs.

Features:

- Solar panel material: polycrystalline
- Voltage: 2V
- Current: 200mA
- Connections: leads
- Dimensions: 3.0" x 3.7" x 0.2"

Mylar®
polyester film

Optical Properties

Transmission of Radiation

Type D Mylar® polyester film transmits light very similar to window glass throughout the absorption spectrum at low wavelengths as shown in **Figure 1**. **Figure 2** illustrates substantial difference at high wavelengths. Type A Mylar® transmits much less radiation due to its light-scattering characteristic (as shown in **Figure 1** for a film having a 54% haze).

Refractive Index

The refractive index of Mylar® polyester films is between 1.640 and 1.670.

Figure 1. Absorption Spectrum for Mylar® (Low Range)

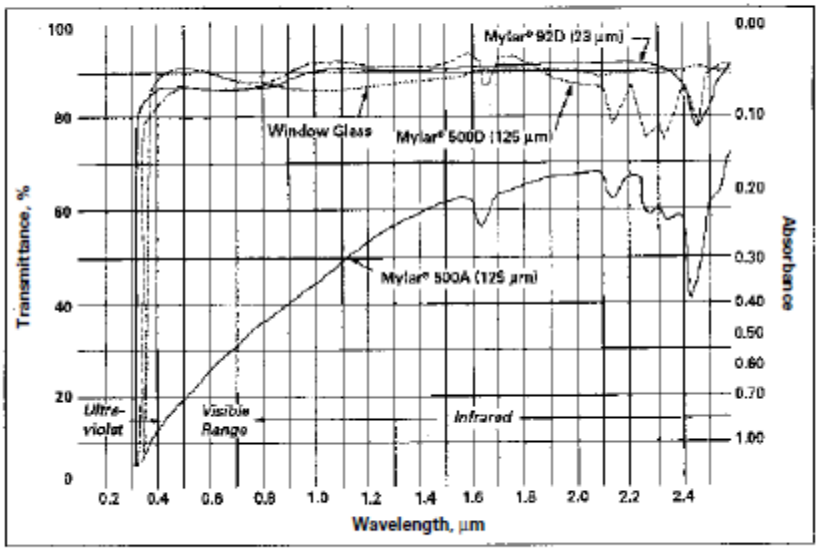

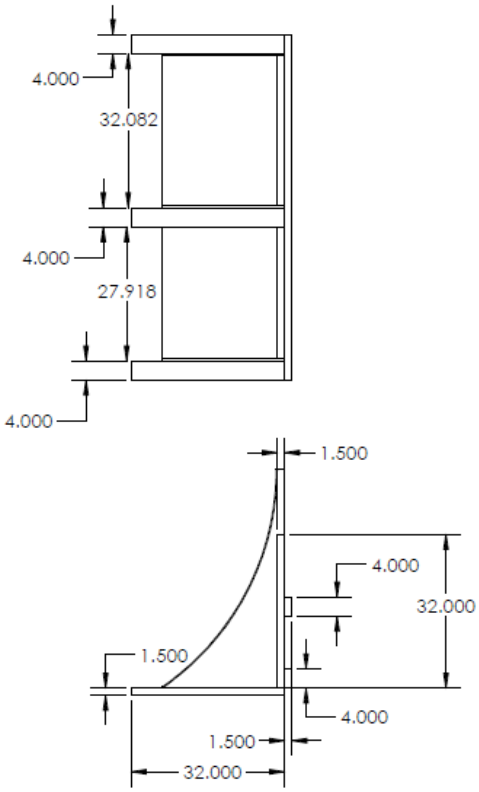

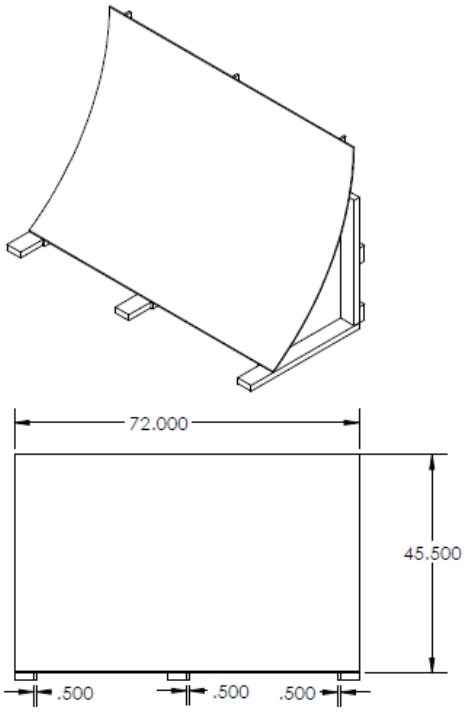

Units: Inches

Team Leaf	Gemstone
Reflector Assembly	2011

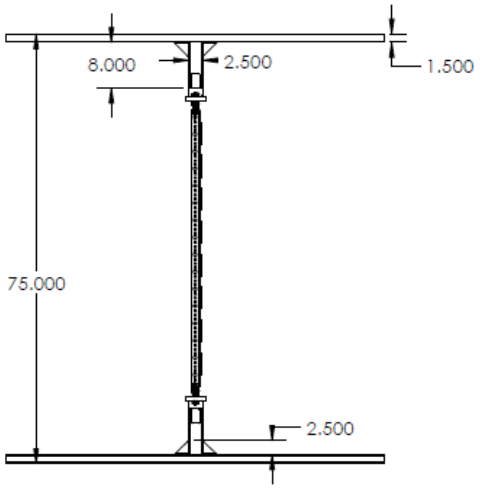

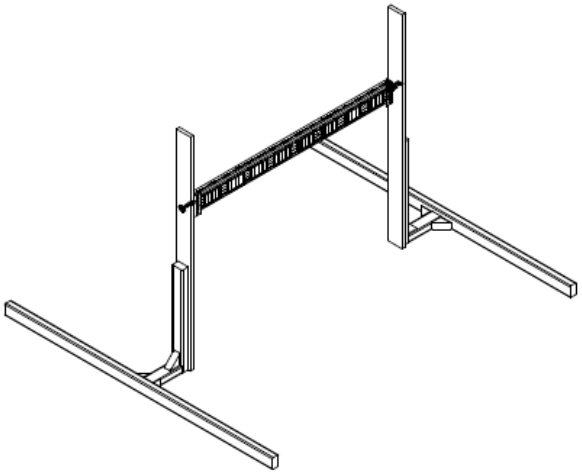

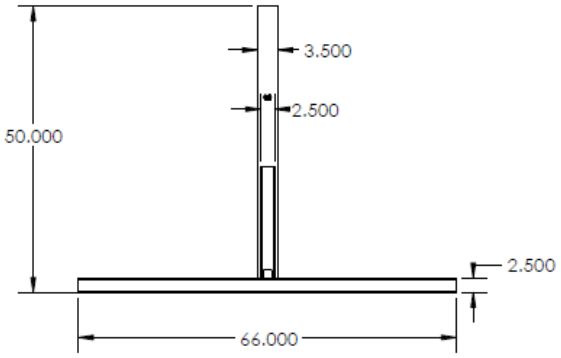

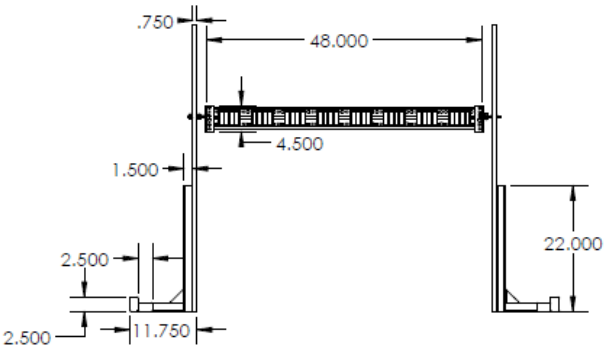

Units: Inches

Team LEAF	Gemstone
Panel Support Assembly	2012

References

Al-Hasan, Ahmad Y.; Ghoneim, Adel A (2005). "A new correlation between photovoltaic panel's efficiency and amount of sand dust accumulated on their surface", 24, pp. 187-197.

Antony, F., Dürschner, C., & Remmers, K. H. (2007). *Photovoltaics for professionals: Solar electric systems marketing, design and installation*. Berlin: Solarpraxis AG.

Aristizábal, A. J., & Gordillo, G. (2008). Performance monitoring results of the first grid-connected BIPV system in Colombia. *Renewable Energy, 33*(11), 2475-2484. doi: 10.1016/j.renene.2008.01.018

AZEK Building Products (2011). *Trim & Moulding.* [Brochure]. Scranton, PA: Author.

AZEK Trim Styles & Sizes - Profiles for AZEK Trim. *PVC Decking, Trim, Porch & Railings | Best Composite & Wood Alternative | AZEK*. Retrieved from http://www.azek.com/azek-trim/styles/

Azzopardi, B., Mutale, J., & Kirschen, D. (2008, November 24-27). Cost boundaries for future PV solar cell modules. *Sustainable Energy Technologies, IEEE International Conference on ICSET*, pp. 589-594. doi:10.1109/ICSET.2008.4747076.

BIPV: Solar-friendly versus architectural aesthetic. (2003). *Photovoltaics Bulletin, 2003*(9), 7-9. doi: 10.1016/S1473-8325(03)00925-8

3M Marine Adhesives and Sealants Product Application Guide and Coverage Charts. (2008). *Boatbuilding.net: An Online Resource for Boat Repair, Restoration and Building*. Retrieved from http://www.boatbuilding.net/article.pl?sid=08/09/22/1259202&mode=thread

Bradford, T. (2006). *Solar revolution: The economic transformation of the global energy industry*. Cambridge, MA: MIT Press.

Bradsher, K. (2011, January 14). Solar panel maker moves work to China. *The New York Times*. Retrieved from http://www.nytimes.com/2011/01/15/business/energy-environment/15solar.html

Brakmann, G., Aringhoff, R., Geyer, M., & Teske, S. (2005, September). *Concentrated solar thermal power - Now!* Retrieved from http://www.solarpaces.org/Library/CSP_Documents/Concentrated-Solar-Thermal-Power-Plants-2005.pdf

Brogren, M. (2004). *Optical efficiency of low-concentrating solar energy systems with parabolic reflectors.* (Dissertation/Thesis, Publication/Order No. C818253, Uppsala Universitet, Sweden). Available from ProQuest Dissertations and Theses.

Chen, Y. C., & Su, C. H. (2010). *Concentrator design of a Fresnel lens and a secondary optical element. AIP Conference Proceedings*, 1277. doi:109-112. 10.1063/1.3509166.

Cheng, C. L., Sanchez-Jimenez, C. S., & Lee, M. C. (2009). Research of BIPV optimal tilted angle, use of latitude concept for south orientated plans. *Renewable Energy, 34*(6), 1644-1650. doi:10.1016/j.renene.2008.10.025

Concentrating photovoltaic installations in the USA set to grow at a CAGR of 75% in the next five years. (2010). *Concentrated Photovoltaics Industry Report*. Retrieved from http://www.renewableenergyworld.com/rea/partner/first-conferences/news/article/2010/05/cpv-installations-in-the-usa-set-to-grow-at-a-cagr-of-75-in-the-next-five-years

DataQ Instruments (2011). *EasyLog Data Logger Series* [Fact Sheet]. Retrieved fromwww.dataq.com/products/hardware/easylog-data-logger.html

Dusonchet, L., & Telaretti, E. (2010). Economic analysis of different supporting policies for the production of electrical energy by solar photovoltaics in eastern European Union countries. *Energy Policy, 38*(8), 4011-4020. doi: 10.1016/j.enpol.2010.03.025

Eicker, U. (2003). *Solar technologies for buildings*. Chichester: Wiley.

Garris, L. B. (Ed.) (2009, August 1). BIPV and your building. *Buildings*. Retrieved from http://www.buildings.com/ArticleDetails/tabid/3334/Default.aspx?ArticleID=8695#top

Hegazy, A.A. (2001), "Effect of dust accumulation on solar transmittance through glass covers of plate type collectors", Renewable Energy 22, pp. 525–540.

Henemann, A. (2008). BIPV: Built-in solar energy. *Renewable Energy Focus, 9*(6), 14-19. doi: 10.1016/S1471-0846(08)70179-3

Henson, J. (2005). Integrating BIPV: How the market for building integrated photovoltaics is being created in the USA. *Refocus, 6*(3), 28-30. doi: 10.1016/S1471-0846(05)70396-6

Holmes, John K., & Papay, Larry (2011). Prospects for electricity from renewable resources in the United States. *Journal of Renewable and Sustainable Energy, 3,* 042701. doi:10.1063/1.3613947

James, P. A. B., Jentsch, M. F., & Bahaj, A. S. (2009). Quantifying the added value of BiPV as a shading solution in atria. *Solar Energy, 83*(2), 220-231. doi: 10.1016/j.solener.2008.07.016

Englander, D & Kann, S. (2009, December 23). United States PV market becomes a global demand leader by 2012. *Solar Magazine*. Retrieved from http://www.solarserver.com/solarmagazin/solar-report_1209_e.html

Keoleian, G. A., & Lewis, G. M. D. (2003). Modeling the life cycle energy and environmental performance of amorphous silicon BIPV roofing in the US. *Renewable Energy, 28*(2), 271-293. doi: 10.1016/S0960-1481(02)00022-8

Lorenzo, E., & Labed, S. (2005). The battery voltage distribution: a possible tool for surveying the state of health of stand-alone PV systems. *Progress in Photovoltaics: Research and Applications, 13*(3), 251-260. doi: 10.1002/pip.578

Lu, L., & Yang, H. X. (2010). Environmental payback time analysis of a roof-mounted building-integrated photovoltaic (BIPV) system in Hong Kong. *Applied Energy, 87*(12), 3625-3631. doi: 10.1016/j.apenergy.2010.06.011

Makrides, G., Zinsser, B., Phinikarides, A., Schubert, M., & Georghiou,G.E. (2012), "Temperature and thermal annealing effects on different photovoltaic technologies", *Renewable Energy*, *43*, 407-417. doi:10.1016/j.renene.2011.11.046.

Mapako, M. (2005), "Provision of long-term maintenance support for solar photovoltaic systems", Lessons from a Zimbabwean NGO", Journal of Energy 16.

Marsh, G. (2008). BIPV: innovation puts spotlight on solar. *Renewable Energy Focus, 9*(3), 62-67. doi: 10.1016/S1471-0846(08)70096-9

Matthews, H. S., Cicas, G., & Aguirre, J. L. (2004). Economic and environmental evaluation of residential fixed solar photovoltaic systems in the United States. *Journal of infrastructure systems, 10*(3), 105-105. doi:10.1061/(ASCE)1076-0342(2004)10:3(105)

Muller, M., Rodriguez, J., & Marion, B. (2009). *Performance comparison of a BIPV roofing tile system in two mounting configurations*. Poster session presented at the 34th IEEE Photovoltaic Specialists Conference, 7-12 June 2009, Philadelphia, Pennsylvania.

Golden, CO: National Renewable Energy Laboratory. (NREL/PO-520-46073). Retrieved from http://www.nrel.gov/docs/fy09osti/46073.pdf

Müller-Steinhagen, H. (2004, February/March). Concentrating solar power. *Quarterly of the Royal Academy of Engineering, Ingenia, 18*, 43-50. Retrieved from http://www.trec-uk.org.uk/resources/ingenia_18_Feb_March_2004.pdf

N.C. Solar Center & the Interstate Renewable Energy Council. (2009). DSIRE: Database of state initiatives for renewables and electricity. Retrieved from http://www.dsireusa.org/

Nieuwenhout, F., de Villers, T., Mate, N., & Aguilera, M. (2004). Reliability of PV stand-alone systems for rural electrification. Universidad Politecnica de Madrid, Energy Research Centre of the Netherlands, Innovation Energie Development, Itpower India.

Parida, B., Iniyan, S., & Goic, R. (2011). A review of solar photovoltaic technologies. *Renewable and Sustainable Energy Reviews, 15*(3), 1625-1636. doi: 10.1016/j.rser.2010.11.032

Price, H., Lüpfert, E., Kearney, D., Zarza, E., Cohen, G., Gee, R., et al. (2002). Advances in parabolic trough solar power technology. *Journal of Solar Energy Engineering, 124*(2), 109-109. doi: 10.1115/1.1467922

Ridlington, E., & Heavner, B. (2005). *Power plants and global warming: Impacts on Maryland and strategies for reducing emissions*. Baltimore, MD: MaryPIRG.

Milborro, David (2009). *Managing Variability*. Retrieved February 24, 2012, from http://assets.wwf.org.uk/downloads/managing__variability_report.pdf

Nieuwenhout, F. (2004), "Detailed Evaluation of Renewable Energy Power System Operation: A Summary of the European Union Hybrid Power System Component Benchmarking Project", Renewable Energy 27.

Roselund, C. (2010, May 3). Concentrated solar power: Versatile technology with huge potential for clean and affordable energy. *Solar Magazine*. Retrieved from http://www.solarserver.com/solarmagazin/solar-report_0410_e.html

Sandia National Laboratories. (2001). The photovoltaic effect - introduction. Photovoltaic Systems Research & Development. Retrieved from http://photovoltaics.sandia.gov/docs/PVFEffIntroduction.htm

Sawin, J. L., & Martinot, E. (2011, September 29). Renewables bounced back in 2010, finds REN21 global report. *RenewableEnergyWorld.com.* Retrieved from http://www.renewableenergyworld.com/rea/news/article/2011/09/renewables-bounced-back-in-2010-finds-ren21-global-report

Sivanandan, A. (2009). BIPV hotspots in the EU. *Renewable Energy Focus, 10*(2), 54-55. doi:10.1016/S1755-0084(09)70089-4. Also available at http://www.renewableenergyfocus.com/view/1708/bipv-hotspots-in-the-eu-/

Snieckus, D. (2012, January 31). Semprius claims record 33.9% efficiency for HCPV module.*Recharge*. Retrieved from http://www.rechargenews.com/business_area/innovation/article300969.ece

Swanson, Richard M.(2000). The Promise of Concentrators. *Progress in Photovoltaics: Research and Applications, 8,* 93-111. Retrieved from http://www.oilcrisis.com/apollo2/concentrators/promise.pdf

Taylor, J. (1997). *An Introduction to Error Analysis*. Sausalito: University Science Books.

Tsujikawa, T (2009). "Estimation of the lifetimes of valve-regulated lead-acid batteries", Power Sources 187, pp. 613-619.

Union of Concerned Scientists (2002, October). *Environmental Impacts of Renewable Energy Technologies*. Retrieved February 24, 2012, from http://www.ucsusa.org/clean_energy/technology_and_impacts/impacts/environmental-impacts-of.html

U.S. Department of Energy. (2003).Parabolic trough solar thermal electric power plants.(DOE/GO-102003-174). Retrieved from http://www.nrel.gov/docs/fy03osti/34186.pdf

Walker, G. (1980). *Stirling engines*. New York City, NY: Oxford University Press.

Wenham, S. R., Green, M. A., Watt, M. E., & Corkish, R. (2006). *Applied Photovoltaics*. Sterling, VA : Earthscan.

Wiser, R., Barbose, G., Peterman, C., & Darghouth, N. (2009). *Tracking the sun II: The installed cost of photovoltaics in the U.S. from 1998-2008*. (Report No LBNL-2674E) Berkeley, CA: Lawrence Berkeley National Lab.

World Wind Energy Association (2011). *World Wind Energy Report 2010*. Retrieved February 24, 2012, from http://www.wwindea.org/home/images/stories/pdfs/worldwindenergyreport2010_s.pdf

Xie, W. T., Dai, Y. J., Wang, R. Z., & Sumathy, K. (2011). Concentrated solar energy applications using Fresnel lenses: A review. *Renewable and Sustainable Energy Reviews, 15*(6), 2588-2606. doi:10.1016/j.rser.2011.03.031

Yoon, J. H., Song, J., & Lee, S. J. (2011). Practical application of building integrated photovoltaic (BIPV) system using transparent amorphous silicon thin-film PV module. *Solar Energy, 85*(5), 723-733. doi: 10.1016/j.solener.2010.12.026